

Seismic mapping of the Draupne
Formation:
a heterogeneous CO Storage complex

Lada Navratilova



Master Thesis in Geosciences
Sedimentology and Stratigraphy
60 credits

Department of Geosciences
Faculty of Mathematics and Natural Sciences

UNIVERSITY OF OSLO

May 2023

© Lada Navratilova 2023

NCCS Draupne Master Thesis: Seismic mapping of the Draupne Formation - a heterogeneous CO₂ Storage seal

Supervisors:

Assoc. Prof. Ingrid Anell,

Dr Sian Lianne Evans

Prof. Alvar Braathen

Sr. Specialist Elin Skurtveit, NGI

This work is published digitally through DUO – Digitale Utgivelser ved UiO

<http://www.duo.uio.no/>

Printed: Universitetet i Oslo

Abstract

The Draupne Formation is dominated by deep marine shales and forms an important sealing unit for future CCS operation in the North Sea. Meanwhile, seismic mapping has clearly shown the unit to be heterogeneous in lithology, showing variation in thickness and composition.

The aim of this thesis is to map the depositional heterogeneity and assess depositional environments and from this ascertain regional variation in sealing capacity within the Stord Basin and across the Horda Platform. The primary target will be a prograding clinoform succession in the Stord Basin with lateral analysis of the inter-fingering successions towards the deeper marine deposits towards the North. Geometric analysis of the clinoforms, which are covered by 2D seismic data, will allow for assessment of scale, dip and dimensions of these units which will lead to some tentative inferences on composition, classification, and depositional processes. Such insight can be linked to the successive prograding units above and provide important information on the spatio-temporal influx into the North Sea.

Our comprehensive study of the clinoforms within the Draupne Formation, particularly its calculated and measured parameters, has revealed crucial insights about the feasibility and risks associated with CO₂ storage and potential migration within this geological framework. The Draupne Formation benefits from a consistent sediment supply from the Hardangerfjord deltaic system, contributing to its dimensions and potential volume for CO₂ storage. Compared to other formations, the larger size of clinoforms in the Draupne Formation enhances its capacity to withstand CO₂ injection pressures, improving storage prospects. The surface map data suggests an eastward migration of CO₂ along the steepest surface gradient, with the Øygarden Fault Complex potentially acting as a barrier against CO₂ leakage. The heterogeneous deposition of the Draupne Formation indicates the presence of diverse potential storage sites for CCS, cyclical patterns and regional variations in thickness and lithology warrant further investigation with integrity assessment of overlying Cromer Knoll Group playing role as a thick caprock.

Acknowledgements

The Master thesis was conducted and the Geosciences Department at University of Oslo.

First, I would like to express gratitude and deepest thanks to my supervisors Assoc. Prof. Ingrid Anell and Dr Sian Evans for encouragement, interesting discussion, and guidance. For sharing knowledge, keeping me on the right track together with important feedback. Also, for comforting attitude and patience towards me, during hard times in forming the thesis.

Secondly, I am grateful for all well and 2D seismic data from NPD repository for possible to use them, and without it the thesis would not be possible.

Special thanks to my close ones, particularly my family, and dear friends, who despite the distance between countries, were present by strongly believing in me, and giving me an encouragement, which kept me going, and therefore helped to contribute to this work. Also, endless gratitude belongs to my flat mate for numerous discussions helping me to understand crucial principles and relation in a study. Other important grateful thank to my formal mentor, prof. Juraj Francu, RnDr., at my alma mater back in Czech Republic, without none of this would happen. The phone call on based on I have applied to master program at University of Oslo and being admitted.

A last thankful thought belongs to a trick of fate, that happened my beloved twin sister appear at the same state in a life and completing her master thesis, as well. Sharing concerns and fears helped me to deal with a deadline and finish this study.

Lada Navratilova

Norway. June 30th, 2023

Table of Contents

Abstract	iv
Acknowledgements	vi
Table of Contents	ix
1. Introduction	1
2. Geological Setting	3
2.1. Location of study Area	3
2.2. Geological evolution.....	5
2.3. Stratigraphy.....	10
3. Theory, data, and methodology	21
3.1. Theory.....	21
3.1.1. Reflection seismology.....	21
3.1.2. Seismic resolution.....	24
3.1.2.1. Horizontal and vertical resolution.....	25
3.1.2.2. Reflection configuration.....	25
3.1.3. Sedimentary principles.....	26
3.1.3.1. Seismic sequence stratigraphy	26
3.1.3.2. Seismic Reflection Patterns of clinoforms.....	37
3.1.4. Carbon Capture and Storage (CCS).....	40
3.2. Data	46
3.2.1. Software	46
3.2.2. Data set.....	46
3.2.2.1. Wellbores.....	46
3.2.2.2. Seismic reflection data	48
3.3. Methods	51
3.3.1. Viking Group and Sognefjord correlation.....	52
3.3.2. Clinoform analysing and measurement.....	53
4. Results	56
4.1. Architecture of a prograding deltaic sequence	56
4.2. Clinoform geometry	63
4.3. Trajectory of Shelf-edge scale clinoform.....	66
4.4. Calculation of Shelf-edge parameters.....	70
5. Discussion	73
5.1. Evolution of depositional environment.....	73

5.2.	Clinoform analysis.....	76
5.2.1.	Limitations and clinoform changing seismic facie pattern.....	76
5.2.2.	Geometry and facies	77
5.2.3.	Controls.....	78
5.3.	Similarities to Sognefjord and Johansen clinoform delta development.....	79
5.4.	Implication for CO ₂	81
5.5.	Recommendation for further work	83
6.	Conclusion	85
	Reference list	87

1. Introduction

The Stord Basin is an underexplored basin in the northern North Sea. CO₂ storage sites are under development in the northern Horda Platform (e.g. Northern Lights project), but the potential of the Stord Basin has so far been overlooked.

The NPD CO₂ Storage Atlas study modelled CO₂ injection and migration within a saline aquifer in the Stord Basin, which generally dips one degree from the Norwegian coast towards the basinal areas. A simulation model for a potential Upper Jurassic sand deposit ("Sandy delta") was built, based on seismic interpretation data, to simulate CO₂ injection (fig. 1.1). The model utilized varying injection rates over 50 years with different well numbers, continuing until CO₂ migration reached the east side, infiltrating the overlying Quaternary formations. However, the simplified models overlooked the importance of sedimentological heterogeneity within the aquifer, which has a significant impact on the storage potential. In this study we will examine the sedimentological heterogeneity of the Draupne Formation in the Stord Basin, and its implications for Carbon Capture and Storage (CCS).

This thesis aims to investigate the geological setting and clinoform architecture of a prograding deltaic sequence in the Stord Basin, with a specific focus on the Draupne Formation. The primary objectives are to create surface and thickness maps, analyze the clinoforms, and evaluate their trajectory and geometry. The research is structured to provide an introduction to the topic, discuss the geological setting, present the theory, data, and methodology used, showcase the results including surface and thickness maps as well as clinoform analysis, engage in a discussion about the findings and their implications, and provide recommendations for further work. The thesis seeks to contribute to the understanding of the depositional environment, clinoform development, and potential implications for CCS in the studied area. The structure of the thesis includes chapters on the introduction, geological setting, theory, data, and methodology, results, discussion, and recommendation for further work.

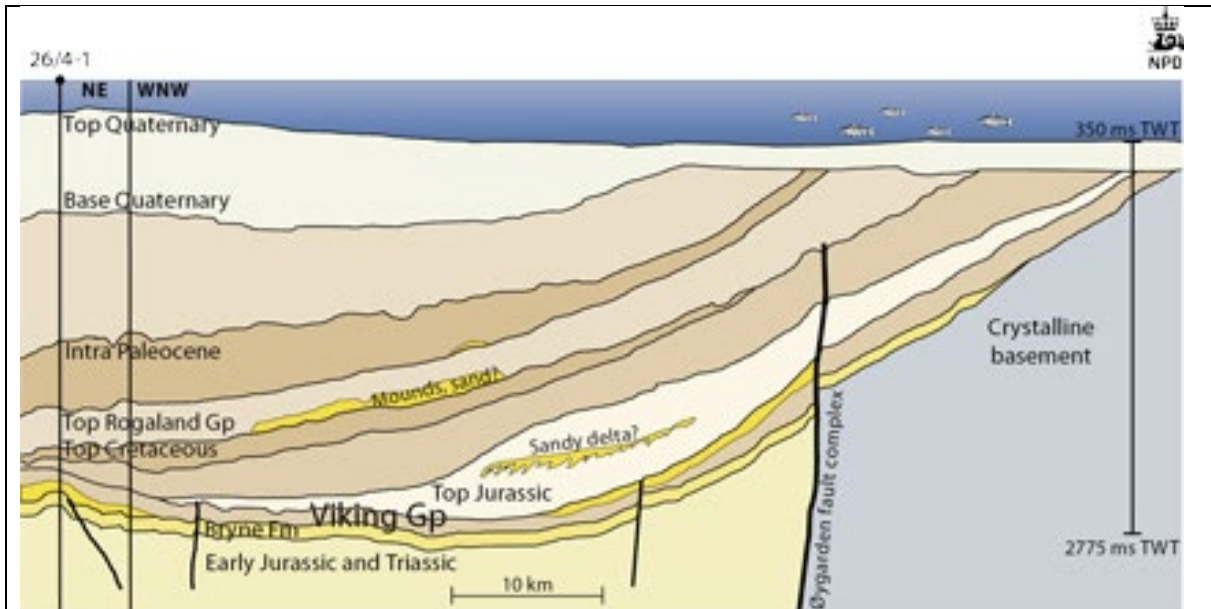


Fig. 1.1: Seismic cross section sediment succession with well 26/4-1, Stord basin's prograding delta of late Jurassic, Draupne Formation.

2. Geological Setting

The Stord Basin, located in the North Sea, is the focus of this study, specifically targeting the Draupne Formation. The Draupne Formation is a clastic unit that was deposited during the Late Jurassic to Early Cretaceous period. This formation is found directly above a sequence boundary associated with a middle Jurassic hiatus (Surlyk, 2003). Understanding the stratigraphy of the Stord Basin can be challenging, particularly in areas where the strata remain intact. Therefore, various methods are employed to predict the development of these strata, such as tracing reflection horizons from nearby boreholes (Jarsve, 2014).

Previous studies have utilized data reported from nearby wells situated predominantly in elevated areas, as well as seismic 2D and 3D surveys, to construct a lithostratigraphic chart for the Stord Basin (Zanella & Coward, 2003). However, relying solely on reflection seismic profiles and a limited amount of well data poses challenges when establishing regional-scale correlations of sequence boundaries (Jarsve, 2014). Despite these limitations, previous studies have provided a decent understanding of the structural and stratigraphic characteristics of the Stord Basin (Underhill & Partington, 1993).

2.1. Location of study Area

The research is centered in the northern section of the epicontinental North Sea (Fig. 2.1.1), situated on the European continental shelf, encompassing regions of Norway, Great Britain, Denmark, and Germany. The North Sea represents one of the three dominant geological provinces, along with the Mid-Norwegian Continental Margin and the Western Barents Sea (Faleide et al., 2015). The petroleum play, primarily dominated by the Viking Graben and the Horda Platform, provides a defining characteristic for the Northern North Sea (Zanella & Coward, 2003). The geology of the Northern North Sea is complex, bounded on the west by the East Shetland Platform and on the east by the Øy garden Fault Zone proximal to the Norwegian mainland (Faleide et al., 2015, 2021). The southern edge coincides with the tectonic boundary delineating the Sele High and Ling Depression, drawing a distinctive line along the Hardangerfjord Shear Zone (Phillips et al., 2019). To the north, the Møre-Trøndelag Fault Complex (MTFC) joins with the Tampen Spur to demarcate the Northern North Sea (Fazlikhani et al., 2017; Fossen et al., 2005, 2016; Osagiede et al., 2020; Phillips et al., 2019). The MTFC,

a substantial fault system, serves as a geological division between the continental crust of the Norwegian mainland and the oceanic crust of the Norwegian Sea. This system is integral to the geological evolution and hydrocarbon potential of the region.

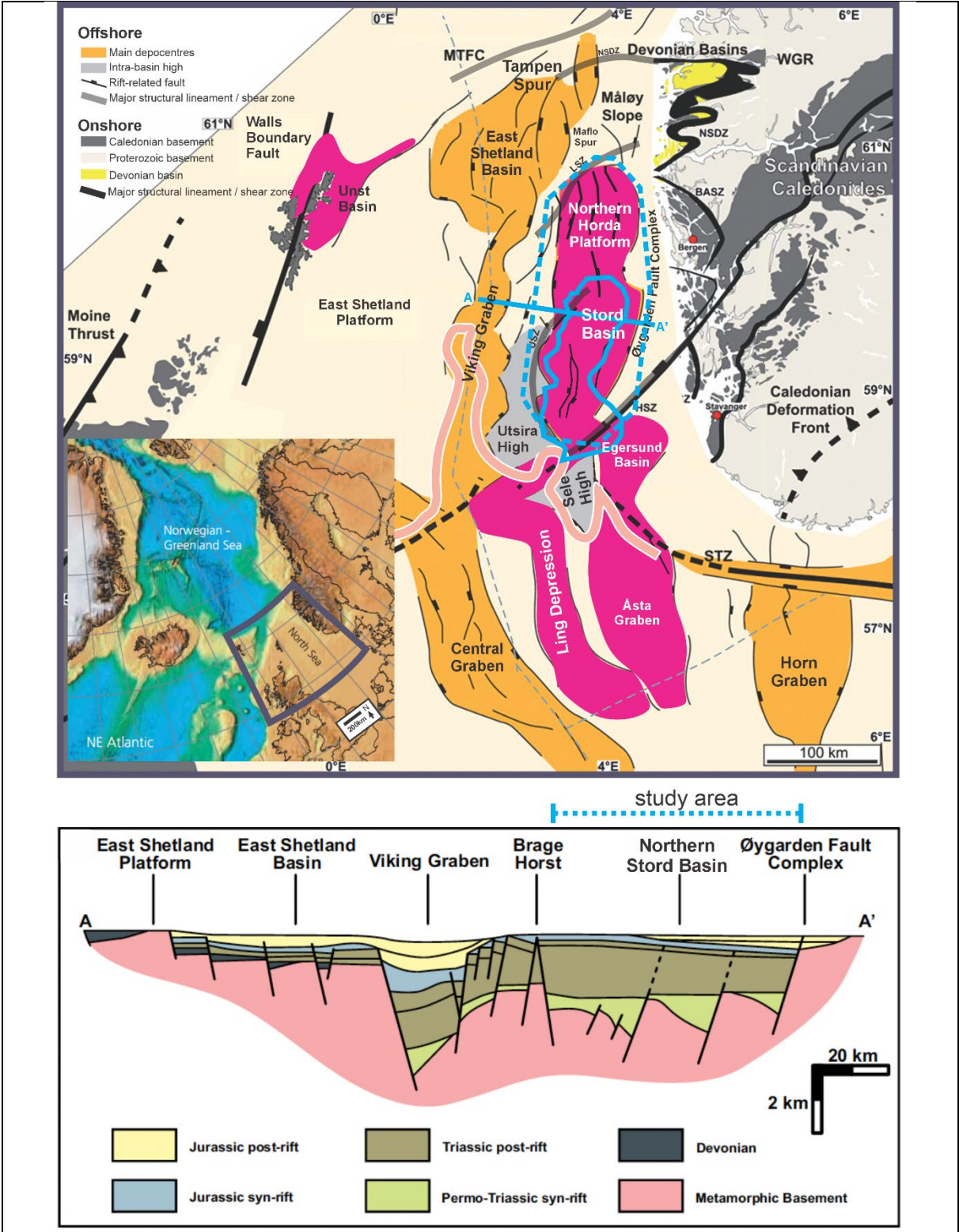


Figure 2.1.1: Map of northern North Sea with geological features, modified from Lundin, 2002; Fazlikhani 2017 and Fossen 2016; Osagiede et al., 2020.

2.2. Geological evolution

The North Sea has undergone numerous geological events dominated by phases of stretching, thinning, and subsiding over millions of years, resulting in the formation of rift basins and the accumulation of thick layers of sedimentary rocks (Phillips *et al.*, 2019). The basin is underlain by a basement of tectonostratigraphic terrain consolidated into crystallinum (Lervik, 2021; Riber *et al.*, 2015; Spørensen & Tangen, 1995). The region's geological history comprises several orogenic events, including the Paleoproterozoic Gothian event, the formation of the Sveconorwegian mountain belt, and the breakup of Rodinia. These tectonic activities culminated in the Late Ordovician-Devonian period with the creation of the Laurussia continent (Biddle & Rudolph, 1988; Phillips *et al.*, 2019). The initiation of the North Sea rift system's tectonic evolution and the basin's current configuration followed the Devonian orogenic collapse, which marked a peak in orogeny during the Middle Silurian to Early Devonian epochs (Corfu *et al.*, 2014). The transition from contractional stress to extension was driven by the reactivation of the Basal Caledonian Thrust decollement, leading to the formation of substantial detachment shear zones, such as the Nordfjord-Sogn Detachment Zone and the Bergen Arcs and Hardangerfjord shear zones (Fossen *et al.*, 2017). This development was instrumental in shaping key structures within the basin, such as the Øygarden Fault and Utsira High fault complex, which were reactivated in subsequent geological periods (Phillips *et al.*, 2019; Würtzen *et al.*, 2021; Patruno *et al.*, 2015; Osaigede *et al.*, 2020; Fazlikhani *et al.*, 2020; Tillmans *et al.*, 2020, Lervik *et al.*, 2021; Fossen *et al.*, 2016). According to Fazlikhani *et al.* (2020) and Phillips *et al.* (2019), the Stord Basin is structurally delimited by two primary shear zones: the Hardangerfjord Shear Zone (HSZ) on the east and the Utsira Shear Zone (USZ) on the west. These structures and processes collectively influenced the formation of the North Sea rift system (Fossen *et al.*, 2017; Fazlikhani *et al.*, 2017; Phillips *et al.*, 2019; Osaigede *et al.*, 2020).

The geological evolution of the Northern North Sea is marked by significant orogenic events and plate tectonic movements. The collision of terrains during the Paleozoic resulted in the creation of the Caledonides (fig. 2.2.1), a faulted belt that was subsequently displaced westward onto the Baltican coastal plain as a nappe, forming the exposed basement between Stavanger and Bergen in Norway (Faleide *et al.*, 2015; Biddle & Rudolph, 1988; Phillips *et al.*, 2019). Notably, the compression of the basement played a critical role in the formation of the Caledonides mountain belt (Færseth *et al.* 1995). The area's rifting history further contributed

to its current geological structure (Badely et al., 1998; Gabrielsen et al., 1990; Ziegler, 1990; Færseth et al. 1995).

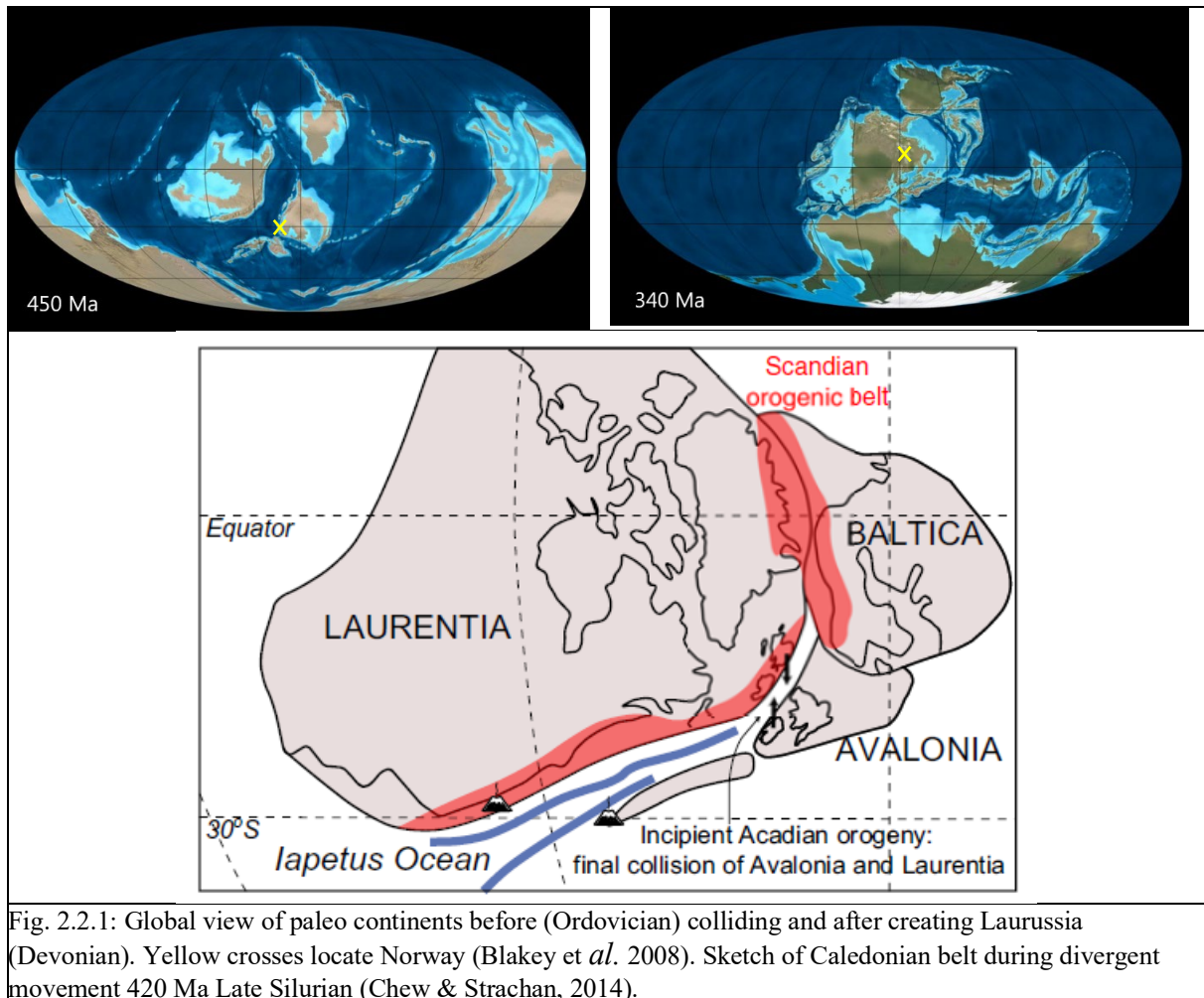


Fig. 2.2.1: Global view of paleo continents before (Ordovician) colliding and after creating Laurussia (Devonian). Yellow crosses locate Norway (Blakey et al. 2008). Sketch of Caledonian belt during divergent movement 420 Ma Late Silurian (Chew & Strachan, 2014).

Throughout this extensive process, the Northern North Sea area underwent a transition from orogeny to rifting. Extensional movement in a rift basin is predominantly attributed to the divergence of tectonic plates, with the separation of plates inducing tensional forces within the lithosphere, leading to the emergence of rift zones (Ziegler, 1990). Along these zones, the lithosphere undergoes weakening and fracturing, resulting in the formation of normal faults and subsequent subsidence of the basin (Ziegler, 1990; Phillips, 2019; Fazlikhani, 2020). The formation of a half-graben, a basin with a steeply dipping fault known as a normal fault, typically occurs during the initial stages of rifting when tensional forces induce stretching and thinning of the lithosphere (Burchfiel et al., 1972; Biddle & Rudolf, 1988; Spørensen & Tangen, 1995; Osagiede, 2020 Lervik, 2021).

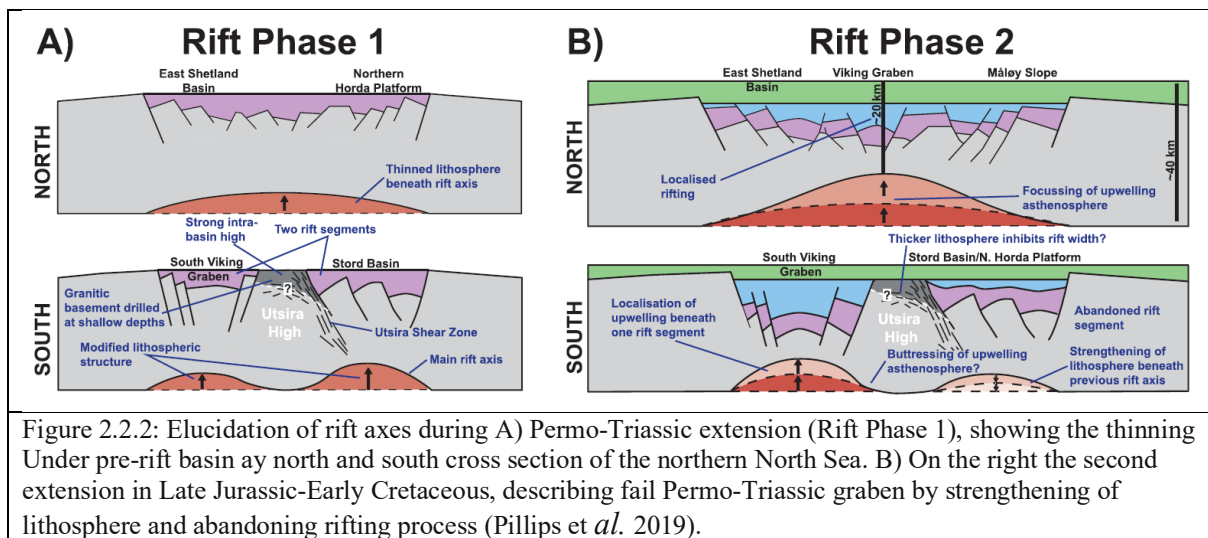
The Northern North Sea now comprises a diverse structural framework of platforms, rift basins, and horsts, formed largely through extensional tectonics (normal separation). Notably,

the most significant hydrocarbon reservoirs and source rocks were developed during the Permian-Triassic and Jurassic periods.

Later, during the Late Carboniferous to Early Permian period (approximately 330 to 290 million years ago), the Variscan orogeny took place as a result of the collision between the African and European plates (Ziegler, 1990). This process led to the formation of the Variscan Mountains, which served as a source for deposition into a rift basin that later emerged during the Permo-Triassic rifting event (Badely et al., 1998; Gabrielsen et al., 1990; Ziegler, 1990; Færseth et al. 1995).

Some older Devonian, Triassic normal faults were in tertiary reactivated into reverse faults (Biddle & Rudolph, 1988)

The Late Palaeozoic to Late Mesozoic rifting in the northern North Sea began with the Permo-Triassic rift phase or Rift Phase 1 (RP1), creating various basins and structural features (Færseth, 1996; Fazlikhani et al., 2017; Phillips et al., 2019). This phase also witnessed major volcanic activity and the formation of deltaic sequences such as the Brent Sandstone Group during the Late Triassic and Early Jurassic epochs (Ziegler, 1992; Helland-Hansen et al., 1992).



These are Jurassic-Cretaceous features, and the main crustal thinning took place in the late Middle to Late Jurassic, followed by thermal subsidence and sediment loading in the Cretaceous. However, the Viking Graben and its margins are underlined by an older major rift basin of assumed Permian-Early Triassic age. The axis of this rift system is thought to lie beneath the present Horda Platform. Fig. 2.2.2. shows axes of those 2 rifts. From Phillips *et al.* 2019.

Fazlikhani *et al.* (2020) and Phillips *et al.* (2019) provide valuable insights into the rift evolution and fault reactivation history of the North Sea and The Stord Basin. Fazlikhani *et al.* (2020) undertook an analysis of seismic and well data from the flank of South Viking Graben, Utsira

High, Ling Depression and Stord Basin to delineate three critical rift phases during the *Cretaceous-permian*, *Late Permian-Early Triassic (RP1)*, and *Late Jurassic-Early Cretaceous (RP2)* (fig.2.2.2). Fazlikhani’s work underscored the significance of pre-existing weaknesses in the geological structure, with reactivation of older faults representing a significant aspect of rift progression. The final phase of faulting was primarily localized to the South Viking Graben, with boundary faults playing a crucial role. In the Stord Basin faults were active throughout first RP1 till syn-RP2 except for the central faults, which were active only till Early post-RP1. Horda Platform faults active in RP1 and in Late syn-RP2 and Early post-RP2 had their reactivation. The basin geometry at the kilometer-scale is influenced by two main factors: (a) extension in an east-west direction, and (b) the presence of pre-existing Caledonian/Devonian structures, specifically the Utsira Shear Zone (USZ) in the west and the Hardangerfjord Shear Zone (HSZ) in the east.

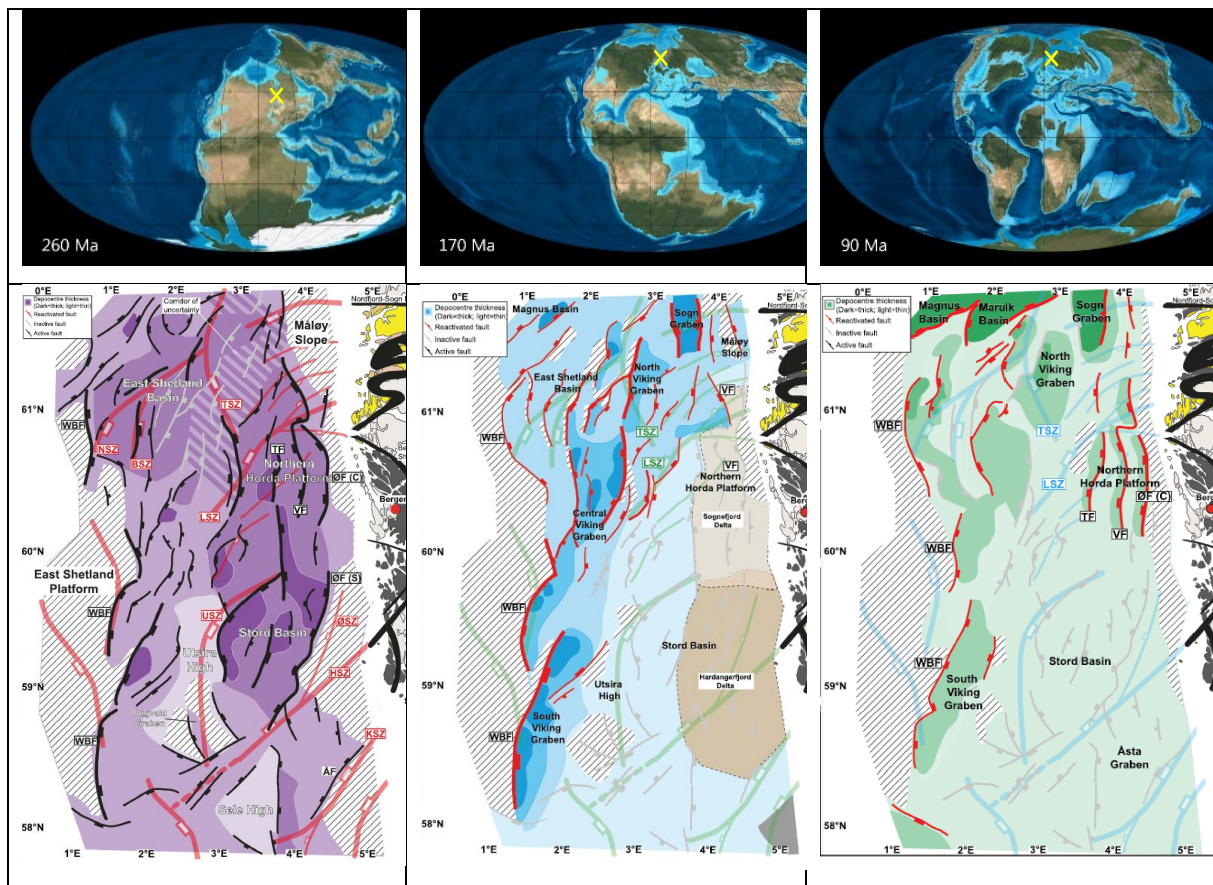


Figure 2.2.3: In Phase 1 (RP1), the Stord and East Shetland Basins, shaped by Devonian shear zones, became the main areas of rift activity. During Phase 2 (RP2), activity shifted to the Viking and Sogn Grabens and East Shetland Basin, leaving the Stord Basin and Northern Horda Platform quiet. After RP2, the activity moved northwards, focusing on the NE trending Marulk and Magnus Basins, with occasional fault reactivations in the Northern Horda Platform (Phillips et al., 2019). Above a paleo geographical position of Norway (marked as yellow cross) related to the stage of rifting (...).

Additionally, smaller-scale structures in the pre-rift basement may contribute to the reorientation of fault segment tips during RP1. The basin's sedimentation patterns are primarily

influenced by thermal subsidence during RP2, where significant depocenters are linked to or situated near the Hardangerfjord Delta of the Middle to Late Jurassic period (Fazlikhani et al., 2020).

Complementarily, Phillips et al. (2019) mapped similar rift phases in the North Sea. The Late Permian-Early Triassic, referred to as Rift Phase 1, saw rift activity stretch across the northern North Sea rift, marked by significant fault activity in the South Viking Graben and Stord Basin rift segments. The main depocenters in this phase were in the *Stord Basin, Northern Horda Platform, and East Shetland Basin* in the west, depositing up to 4 km of strata. Notably, Phillips et al. (2019) documented that RP1 strata were considerably thin over the Utsira High and absent on platform areas beyond the main rift (fig.2.2.3).

Then, the Alpine orogeny took place during the Late Jurassic to Early Cenozoic period, around 150 to 30 million years ago, due to the collision between the African and Eurasian plates (Baig et al., 2021). This led to the basin of the North Sea reaching its greatest depth of subsidence and some of the Devonian and Triassic normal faults being reactivated into reverse faults (Biddle & Rudolph, 1988). During the Late Jurassic to Early Cretaceous, the second rift phase, Rift Phase 2 (RP2), was marked by renewed extensional tectonics (Ziegler, 1992; Færseth, 1996; Duffy et al., 2015; Fazlikhani et al., 2017; Phillips et al., 2019). The subsequent Cretaceous phase saw widespread thermal subsidence with some local syn-rift activity (Phillips et al., 2019).

The post-rift development in the Northern North Sea is described by Gabrielsen et al. (2001) as a three-stage model: Initial post-rift stage, Medial stage, and Final stage. This development is complex due to the continued activity of the basin bounding master faults (Bell et al., 2014) and variations in subsidence rates throughout the area due to plate separation in the Norwegian-Greenland Sea, intraplate tectonics, and basin-flank tectonics (Nøttvedt et al., 1995).

2.3. Stratigraphy

The boreholes featured in this study offer valuable perspectives on the stratigraphic layers and geological progression of these regions (Table 2.3.1). This allows an examination of defined strata from the south (17/3-1), west (25/6-1), and north (31/11-1s) of the region. Each well provides insight into diverse geological formations, thereby enriching our understanding of the region's stratigraphy and geological evolution.

In the following section, I will provide a detailed overview of the primary stratigraphic units and present a stratigraphic chart. This is based on the analysis of the afore-mentioned wells, supplemented by extensive literature review.

The most accurate chronostratigraphic chart of the Stord Basin is provided by the NORLEX project, a collaborative work of Noreco, Lundin, and ConocoPhillips. This project based its findings on a selection of wells with predefined main groups and formations, and an evaluation of published research, including works by Gradstein et al., 2005; Phillips et al., (2019); Fazlikhani et al., (2020), and others. Phillips (2019) constructed a regional stratigraphic chart for the North Sea, which includes the Stord Basin. However, his research tends to align the Stord Basin closely with the adjacent Permian Åsta Graben, with presence of Tau Formation as an equivalent to Draupne Formation. Fazlikhani (2020), in contrast, presented a simplified version of the chart, focusing only on the stratigraphic groupings. He selected the Brent Group, as the following authors: Færseth (1996), Whipp et al. (2014), and Bell et al. (2014), who all studied the stratigraphy of the Horda platform. The NORLEX project, however, interprets the underlying strata as the Vestland Group, specifically the Heather/Hugin Formation. It seems that the Sognefjord delta of the Brent Group transgressed, allowing younger sediments from the Hugin Formation to invade the Stord Basin. This interpretation aligns with the depositional environment descriptions by other authors ... and corroborates with data available on the Norwegian Petroleum Directorate (NPD) fact page (refer to fig. 2.3.1.1, 2.3.3.4).

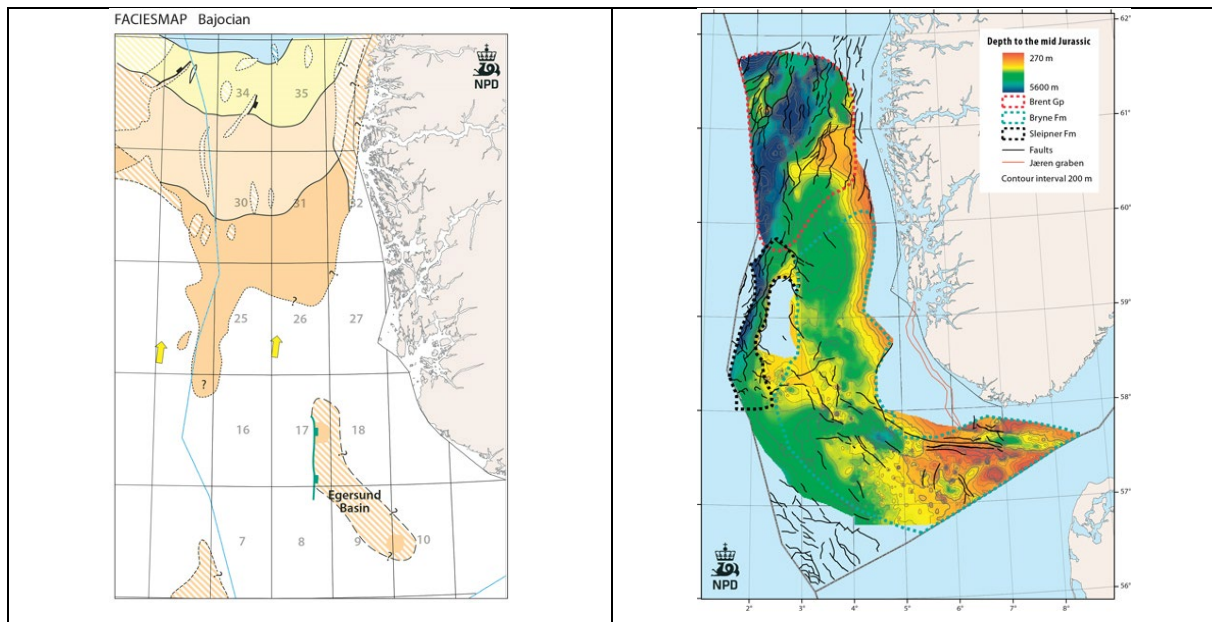


Figure 2.3.1.1: Distribution of Mid Jurassic regional sediment spread of Brent, Vestland Group (Sognefjord delta distribution on left, mid Jurassic depth contour with outlined Formations on the right-hand side (from NPD fact page)

Past classification of lithostratigraphical division were created without seeing the basin as the entire body (Lervik K.S., 2006). The lithostratigraphy of the northern North Sea has been composed or adapted in multiple major publications. Stratigraphy follows the determination from the northern part of Horda platform based on data obtained from drilled wells (Patruno et al. 2014; Deegan & Scull, 1977; Vollset & Doré 1984; Cameron et al.1993). Other studies also consider Utsira and Sele high stratigraphy (Jackson et al. 2010) for interpretation stratigraphy of Stord basin. Because the western part of the Stord Basin is bound by the South Viking Graben with slightly different tectonic framework described in a Geology evolution chapter, where the Jurassic rifting were active while Stord basin ceased. For adapting the stratigraphic chart, it is less important. But it still needs to be viewed when research will see the Stord basin as a whole succession structure. The most robust and detailed chart division of Norway's offshore lithostratigraphy can be provided by Lundin (Fig. 2.3.1.2) focusing on main geological feature (basins, grabens and heights) on English, Norwegian and Danish side.

Stratigraphy at some intact places of a Stord basin is challenging and requires different methods to predict strata development, methods of tracing reflection horizons from identified nearby boreholes.

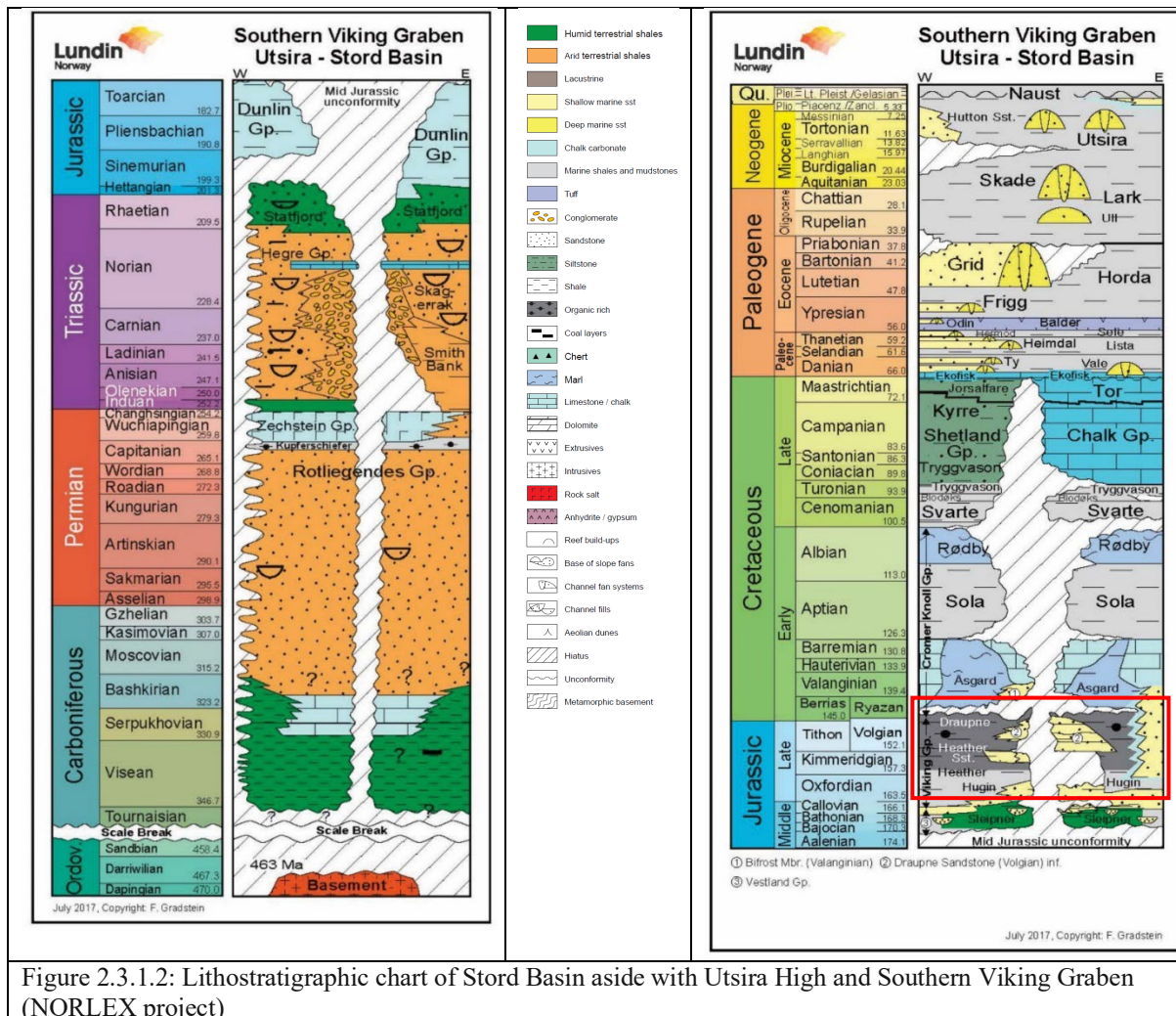


Figure 2.3.1.2: Lithostratigraphic chart of Stord Basin aside with Utsira High and Southern Viking Graben (NORLEX project)

Stratigraphic units and depositional development

The complex geological history of the Stord Basin, in the Northern North Sea, began with Permian-Carboniferous depositions (Fazlikhani et al., 2020; Phillips et al., 2019; Faleide et al., 2010; Lervik, 2021; Gabrielsen et al., 2001). These times were marked by the Zechstein Group formations, which can be seen today in the Danish Basin, the Southern and partly Central Viking Graben, and the Sele High.

During the early Carboniferous, Norway was primarily arid land with an overthrust of older, crystalline rock and marine sediments. Extensive faulting and volcanic activity occurred in the late Carboniferous and persisted into the early Permian, which saw dramatic environmental changes. The climate was predominantly hot and humid, leading to a diverse mix of deposits, from sandstone and mudstone to coal and evaporites, forming in varied environments from riverine to swampy terrains and narrow rifts to broad depressions (Ziegler, 1990).

A noticeable shift occurred as Gondwana drifted northward at the end of the Carboniferous period, leading to the formation of the Variscian (Hercynian) mountain belt by the late Permian (Ziegler, 1990). This northward shift transformed the geological landscape, with southern North Sea, Northern Germany, Denmark, and the British Isles becoming part of the Variscian foreland basin.

As we moved into the Permian era, the climate became cooler, and Norway began to shift northward, becoming part of a continental shelf sea that extended to the Boreal Ocean. The landscape was arid, periodically encroached upon by the sea, but some areas remained scarcely submerged. In several locales, Upper Permian strata lie directly on the Caledonian or Precambrian basement, indicating significant geological transformations over time.

However, the Late Permian witnessed a dramatic drop in sea levels, leading to extensive desiccation and the creation of widespread evaporite strata (Ziegler, 1990). The landscape was transformed, with remnants of earlier sediments eroded away.

The Triassic period introduced new geological phenomena, marked by signs of alluvial deltas, indicating the ongoing breakup of the last supercontinent which continued into the Early Triassic (Ziegler, 1990). The Boreal Ocean advanced southward, merging with the opening proto-Tethys Ocean. Intense weathering of the land led to oxidation of gravel, sand, and mud, resulting in the characteristic, red-colored deposits in both continental and marine basins. As the Triassic period concluded, sea levels rose, and the climate shifted towards a more humid state.

However, the boundary between the Permian and Triassic Statfjord formation is not characterized by sharp strata. Rather, it's defined by a transition from reddish to overlying greenish mudstone or a coarsening-upward sequence (Lervik, 2021). This observation facilitated the recognition of the transition between the Permian and Triassic strata across selected wells in both the UK and Norwegian sectors of the North Sea (Lervik, 2021).

To unify UK and Norwegian lithostratigraphic nomenclature, Volset & Doré (1984) reviewed and defined the lithostratigraphic group, the Hegre group, including Teist, Lomvi and Lunde formations (Lervik et al., 2006). Uncertainties still exist, specifically regarding the Sognefjord formation, which some wells classify as part of the Jurassic strata group [citation needed].

This complex geological history of the Stord Basin underscores the difficulty of stratigraphic correlation and indicates the potential for further exploration and understanding, as more exploration wells penetrate foot-wall basement (Spencer & Larsen, 1990), and as seismic resolution improves, core-material data is expanded, and basement-penetrating wells become more commonplace (Goldsmith et al., 2003., Nystuen et al., 2014, Würtzen et al., 2021)

Bedrock

The bedrock, or basement, of the Stord Basin consists of highly metamorphosed and consolidated volcanic and sedimentary rocks originating from the Precambrian and early Paleozoic eras (Basset M.G., 2003-NPD page). More precise details are provided in the Geological Evolution chapter. Wells 25/6-1, at Utsira High horst, and 17/3-1, at the border with the Åsta Graben crest, have been utilized to study the pre-Devonian basement. However, the specific formation or group remains undefined. Indications of metamorphic mineral content and weathered sediment textures suggest varying degrees of temperature and pressure conditions over time, such as the albitization of plagioclase in the hinterland of the Cambrian peneplain (Basset M.G., 2003(NPD), Baig et al., 2019).

The Stord Basin's stratigraphic history is intricately layered, extending to the Devonian period and potentially even deeper. Like the Horda Platform, Devonian sediments are presumed to reside in the lower sections of the Triassic half-graben beneath the Stord Basin. This assumption is supported by the presence of terrestrial plant fossils, indicating continental depositional conditions (Jones and Smith, 2008). Unfortunately, exploration of these sediments has been minimal due to the limited well penetration in these areas (Smith et al., 2010).

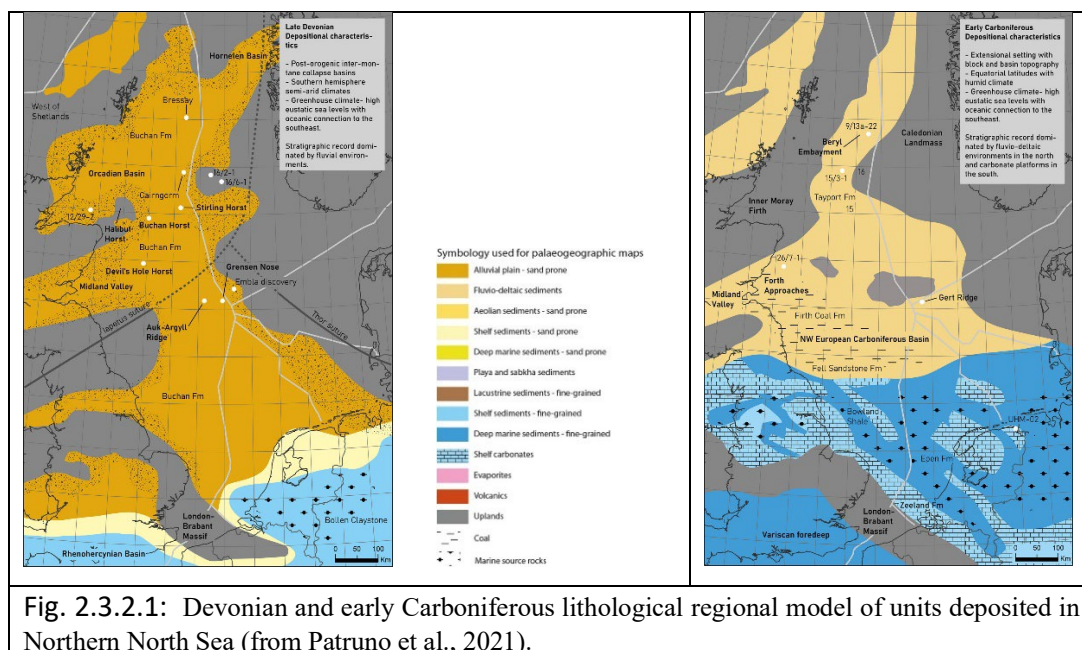


Fig. 2.3.2.1: Devonian and early Carboniferous lithological regional model of units deposited in Northern North Sea (from Patruno et al., 2021).

Rotliegende and Zechstein group

The geological formation of the northern North Sea region, including the Central Viking Graben, Ling Depression, and Utsira High, showcases a rich diversity of strata and structures. Significant among these are the Late Carboniferous to Early Permian Rotliegende Group and the Late Permian Zechstein Group (fig. 2.3.2.2).

The Rotliegende Group is renowned for its reddish sandstone and siltstone layers, born out of arid conditions, and serves as a crucial source of hydrocarbon reservoirs in the North Sea (Glennie, 1998; Ziegler, 1990). Meanwhile, the Zechstein Group consists of cyclic deposits of carbonates, evaporites, and clastics that accumulated in a restricted sea environment, offering immense economic value in the form of potash and salts, as well as substantial hydrocarbon reserves (Stewart, 2007; Johnson et al., 2012). The formations differ in their geographical prevalence. Massive evaporite fields in the southern North Sea have given rise to impressive salt domes, significantly shaping the structural and depositional evolution of nearby basins (Ziegler, 1990). In stark contrast, the Carboniferous-Permian units within the Horda Platform and Stord Basin, characterized by extensive erosion in arid, hot conditions, either remain largely unexplored due to a scarcity of well data or have been subjected to weathering and erosion (Johnson et al., 2012).

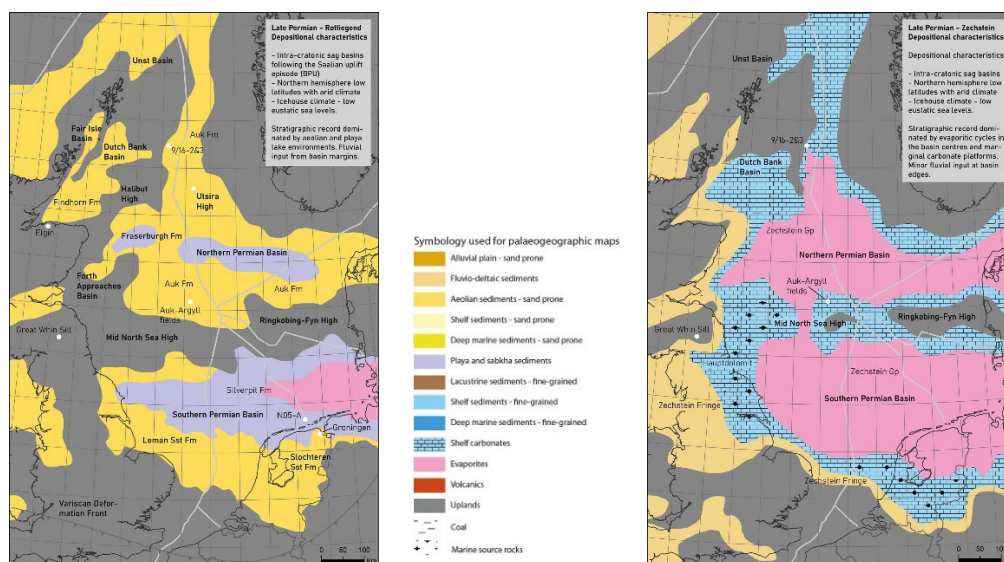


Fig. 2.3.2.2: Late Permian lithological Rotliegende and Zechstein group evaporites in regional model of units deposited in Northern North Sea (from Patruno et al., 2021).

Hegre Group

During the Permian and Triassic eras, the Stord Basin experienced significant geological shifts, with the deposition of sandstones and mudstones from the Hegre Group forming the foundation of the inter-rift strata (Johnson et al., 2012). Sediments during this period primarily came from the surrounding uplifted regions, indicating a continental depositional environment. The Hegre Group is composed of five distinctive lithological strata (Fig. 2.3.2.3), reflecting diverse depositional conditions. While Triassic deposition has been frequently linked to terrestrial environments (Patruno et al., 2021), an analysis of cuttings and logs suggests a range of environments spanning alluvial, deltaic, to subaqueous sedimentation, as evidenced in the

Smith Bank and Alke formations (Lervik, 2019). These formations, situated at the lowermost part of the syn-rift basins, are predominantly made up of mudstones, indicative of deposition in distant underwater settings. The nearby Lunde and Skagerrak formations contrastingly host considerable deltaic sand deposits, manifesting as substantial clastic wedges. Lervik (2021) notes that the primary source of this sand influx originated from prominent valley systems stemming from the Sognefjord and Hardangerfjord regions.

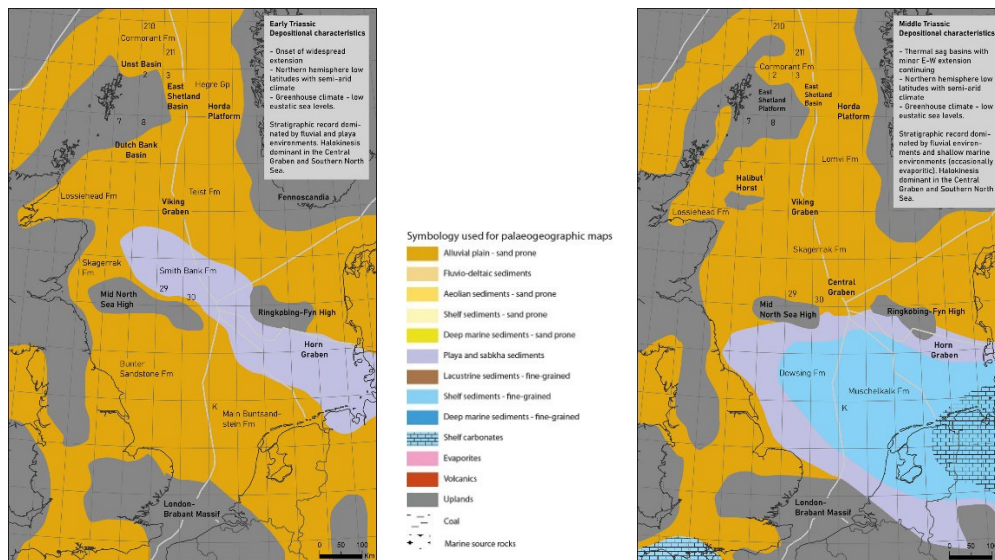


Fig. 2.3.2.3: Triassic Formation deposition spread of clastic and deltaic sediments in regional model of units deposited in Northern North Sea (from Patruno et al., 2021).

Statfjord, Dunlin and Brent/Vestland Group

During the Early to Middle Jurassic, the Stord Basin underwent a significant phase of geological transformation, marked by the deposition of fluvial, deltaic, and shallow marine sediments. This led to the formation of the Brent, Statfjord, and Dunlin Groups (Anderson et al., 1994; Steel, 1995). This period also saw the commencement of the Second Rift Event, indicated by the deposition of the Ness and Tarbert Formations (fig. 2.3.2.4) within the Brent Group (Anderson et al., 1994; Deng et al., 2018). The Vestland Group is an equivalent to Brent Group deposited at the western and southern part of northern North Sea (NPD fact page).

Moreover, this epoch was characterized by the notable uplift and eastward tilting of the Stord Basin, particularly during the deposition of the Brent Group. This significant geological activity provides evidence for the inception of fault lines along the eastern boundary of the Stord Basin during the Late Bajocian to Middle Callovian periods (Whipp et al., 2015). These structural

alterations fundamentally transformed the basin's geological configuration and had profound impacts on the deposition patterns of the groups.

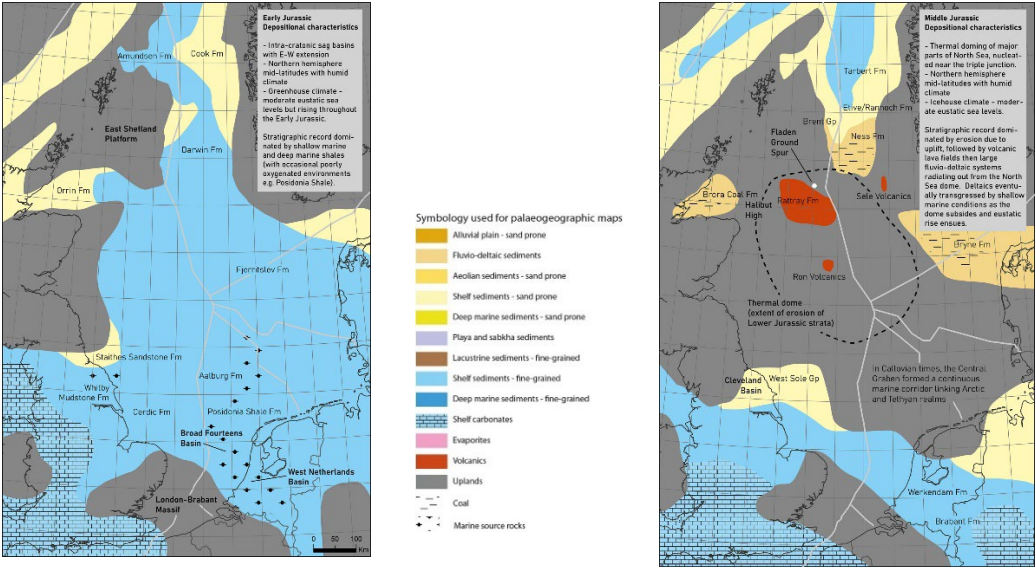


Fig. 2.3.2.4: Early and Middle Jurassic deposition and hiatus in regional model of units deposited in Northern North Sea (from Patruno et al., 2021).

Viking Group

During the Late Jurassic to Early Cretaceous periods, the Viking Group's sandstone and shale strata were deposited within the North Sea's geological features such as the Stord Basin, Horda Platform, and Viking Graben. This group, first identified in the Viking Graben area, comprises marine formations like the Krossfjord, Fensfjord, Sognefjord, and Draupne Formations (Fig. 2.3.2.5). These represent stacked, regressive, shallow marine clastic sequences, deposited amidst increasing rates of fault-driven subsidence during the Second Rift Event (Dreyer et al., 2006; Bell et al., 2015).

The Viking Group's deposition culminated with the Cretaceous Unconformity, ending the Second Rift Event. This was caused by reduced strain rates rather than a halt in fault activity. The resulting uplift of surrounding clastic sources and tectonic subsidence heavily influenced the sedimentary architecture of the Cenozoic Stord Basin. Overlying the Viking Group's deep-water clastics and Cromer Knoll and Shetland groups' carbonates were mud-dominated Cenozoic sediments.

Among the formations, the Heather Formation of the Viking Group comprises silty claystones deposited in an open marine environment. This deposition resulted from a marine transgression following the youngest formation of the Brent Group (Norlex, bulletin 3).

The Sognefjord Formation is a crucial feature within the Stord Basin and is also found east of the North Sea's Troll field. This Upper Jurassic formation is notable for its reservoir sandstone,

characterized by high porosity, permeability, and low clay content, especially in the lower unit, Zone-3. Moreover, the formation contains two carbonate stringers in Zone-3, possibly acting as flow barriers due to their high resistivity, density, and low porosity/permeability (Mondol et al., 2018).

The Draupne Formation, an equivalent to the Kimmeridge Clay Formation in the Northern North Sea, consists of dark grey-brown to black, non-calcareous, carbonaceous, occasionally fissile claystone. It is marked by high radioactivity due to its organic carbon content, and low velocity, high resistivity, and low density. This formation was deposited in a marine environment with restricted bottom circulation, often under anaerobic conditions. Sandstones within the Draupne Formation, believed to be of turbiditic origin, range from Oxfordian to Ryazanian, corresponding to the Late Jurassic to Early Cretaceous periods (Offshore Record of Geology and Stratigraphy, Norlex, bulletin 3).

These intricate formations offer insight into the geological history of the area, serving as potential hydrocarbon reservoirs, influencing the sedimentary architecture of the region, and guiding our understanding of the area's tectonic history.

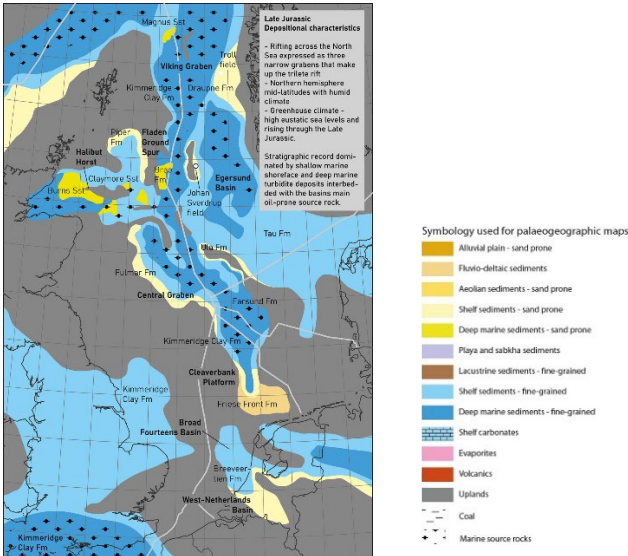


Fig. 2.3.2.5: Draupne Formation within Late Jurassic in regional model of units deposited in Northern North Sea (from Patruno et al., 2021).

Cromer Knoll Group and Shetland Group

The Cromer Knoll Group and Shetland Group are significant lithostratigraphic groups of the North Sea basin. The Cromer Knoll Group is predominantly characterized by carbonates such as chalk or limestone (fig. 2.3.2.6), indicative of a marine depositional environment during the Late Cretaceous (Cameron, 1992). The Shetland Group, predominantly composed of Tertiary-

aged clastic sedimentary rocks, shows a transition to more siliciclastic deposition in the Cenozoic era (Cameron et al., 1992).

In the context of the Stord Basin, both groups contribute to the basin's complex stratigraphy. They overlie the Viking Group formations, illustrating the sedimentological and tectonic evolution of the region (Ziegler, 1982). Importantly, certain formations within these groups, particularly those consisting of shales and dense limestones, may serve as effective seals for hydrocarbon reservoirs in specific locations (Evans et al., 2003). Detailed analysis of the stratigraphic and structural context is required to confirm the full extent of their roles as seals.

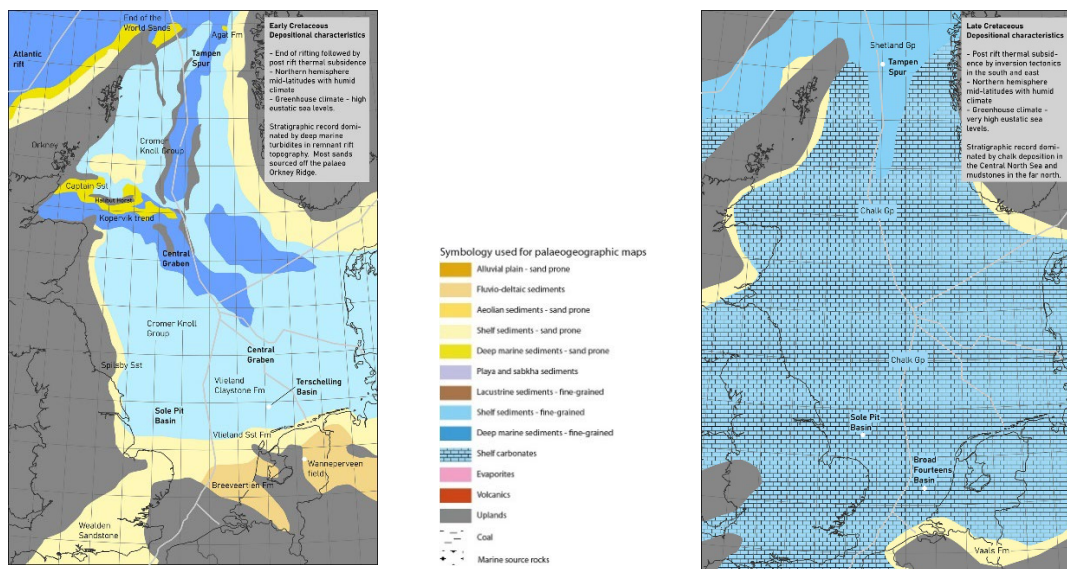


Fig. 2.3.2.6: Cretaceous units' disposition of Cromer Knoll Group and Shetland Group in regional model of units deposited in Northern North Sea (from Patruno et al., 2021).

Rogaland Group, Hordland Group and Nordland Group (Fig. 2.3.2.6)

Rogaland Group: Late Cretaceous to Paleocene formations that contribute to the North Sea's sediment fill. It includes Våle, Lista, Sele, and Balder formations, offering a combination of claystone, siltstone, chalk, limestone, and sandstone. These formations could serve as reservoir and source rocks for hydrocarbons, influencing the area's petroleum prospectivity (NPD fact page).

Hordaland Group: Early Eocene to Early Miocene formations primarily made up of claystone and siltstone. They have been deposited under varying marine conditions and can function as a seal in hydrocarbon systems, depending on their thickness and continuity (NPD fact page).

Nordland Group: From the Miocene to Pliocene epochs, this group consists of sandstones and siltstones in the Utsira, Skade, and Kvitnos Formations. They range from shallow to deep marine settings and can serve as potential reservoir rocks or seals, depending on their distribution and continuity (Underhill & Partington, 1993).

In the Stord Basin, these groups contribute to the basin's sediment fill, geological history, and petroleum potential. The Rogaland and Nordland Groups, with their reservoir-quality sandstones, can store hydrocarbons, while the Hordaland Group's claystones can prevent hydrocarbon migration, acting as a seal in the petroleum system (NPD fact page).

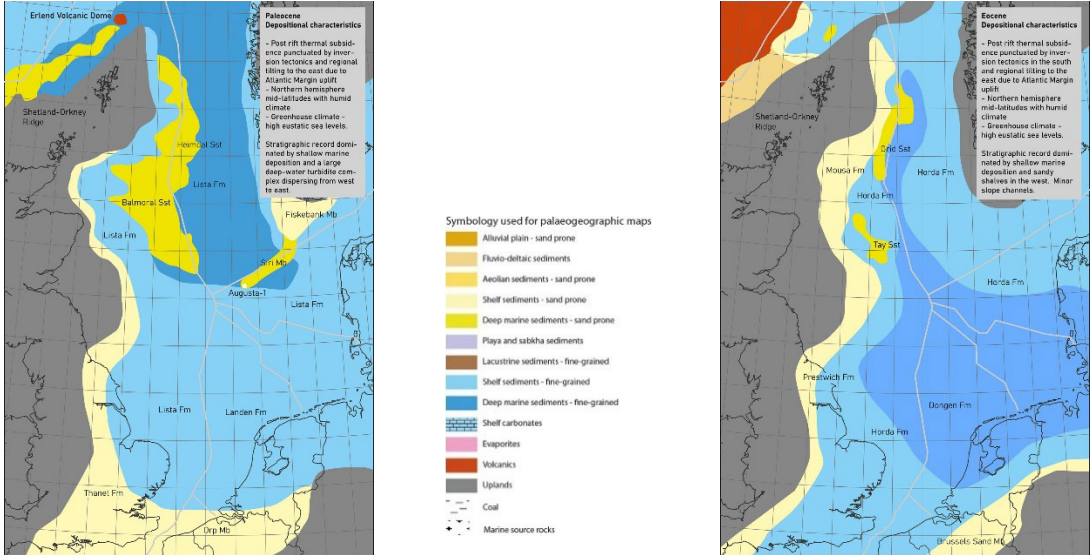


Fig. 2.3.2.6: Cenozoic disposition of Rogaland, Hordaland and Nordland Group in regional model of units deposited in Northern North Sea (from Patruno et al., 2021).

3. Theory, data, and methodology

3.1. Theory

In this section of my thesis, I embark on a comprehensive journey through several significant theories in the fields of seismology and sedimentology. This exploration serves as a vital foundation, paving the way towards their application in the critical real-world practice of Carbon Capture and Storage (CCS). My exploration commences with reflection seismology, a key technique used to interpret the earth's subsurface characteristics. This is closely followed by study of seismic resolution, alongside reflection configurations, are deciphered.

Building upon these seismic understandings, I then delve into the realm of sedimentary principles. Here, I concentrate on seismic sequence stratigraphy and seismic facies, aiming to unravel the complex processes of sediment deposition and the manner in which these deposits are detected seismically and what parameter of clinoform are important to understand.

In the final part of this theoretical journey, these concepts find their practical application as I venture into the field of Carbon Capture and Storage. In highlighting its importance as an integral strategy in mitigating climate change, I introduce a case study of a saline aquifer in the Stord basin. This will offer practical insights and underscore the real-world implementation and impacts of CCS, thereby intertwining theory with practice in the sphere of geological studies.

3.1.1. Reflection seismology

Seismic reflection theory is one of the tools helping to obtain stratigraphic information, knowledge about depth, structure, thickness, and properties of rock like density or rock type which has been layered, folded, or metamorphosed under the surface. Reflection seismology uses 2D or prospected in seismic profiles. From this it is possible to interpret geological structures, horizons and seismic facies in the Stord Basin and outline clinoforms of upper Jurassic prograding coastal shelf. 2D data of certain seismic surveys which are listed in Methods (Chapter 3), are projected in a seismic profile, and read in Petrel 2022 Schlumberger AS. Seismic facies are seismic reflection patterns packaged into discrete units that have recognizable, mappable shapes or geometries. These patterns are interpreted to represent a specific depositional environment and associated set of geologic circumstances. The term 'facies' is borrowed from sedimentology and stratigraphy, where it refers to distinctive characteristics of a rock unit, formed in a particular depositional environment, that distinguish

it from other rock units (Sangree & Widmier, 1977; Mitchum et al., 1977, Quiquerez & Dromart, 2006). In the context of seismic data, seismic facies analysis involves the classification of seismic data into different facies, based on the characteristics of the seismic reflections. These characteristics can include reflection amplitude, frequency, geometry, continuity, and others. Each seismic facies unit is thought to represent a unique set of depositional and/or erosional processes (Sangree & Widmier, 1977; Mitchum et al., 1977, Quiquerez & Dromart, 2006).

Reflection horizons in a seismic reflectivity profile or a 2D line section are created due to changes in physical parameters such as density and seismic velocity. This creates an acoustic impedance, which can be defined by a reflection coefficient. When interpreting geological features, the seismic amplitude, phase and polarity (trough or peak, seen as positive or negative, respectively, in relation of European or American) give information about the physical properties of the reflector (in fig.3.1.1.1).

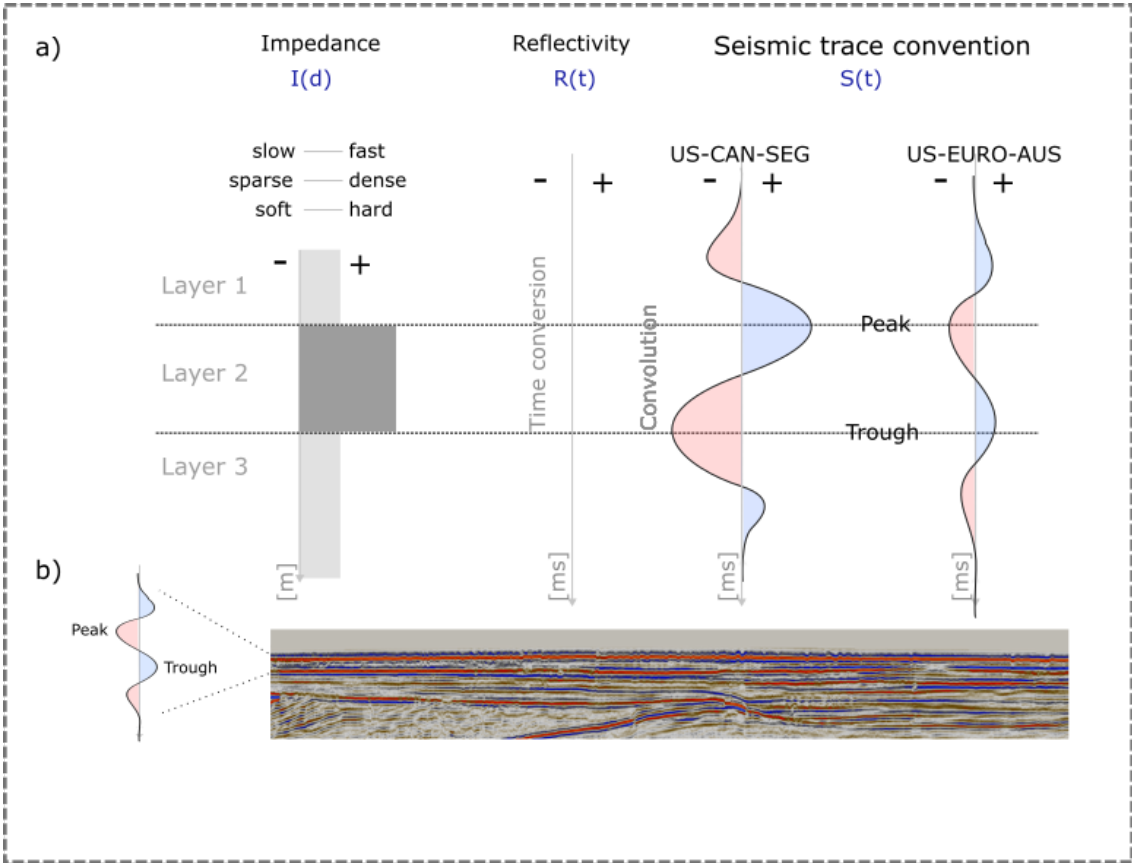


Figure 3.1.1.1: a) example of Impedance, reflectivity, and seismic profile showing relation of Impedance, Reflectivity and seismic velocity wave while entering different density on an interface of the rock layers b) In a 2D seismic section shows example of a hard event, here seabed. Modified from SubSurfWiki..

Acoustic Impedance is denoted as Z and is equal to density ρ - rho multiplied by seismic velocity v , equation (eq.2.1.1.1) is shown below. The impedance value is related to the type of rock. The change in acoustic impedance defines the *reflection coefficient* R (eq.2.1.1.2).

eq.2.1.1.1

$$Z = \rho v$$

The wave in non-normal incidence on interface (between two rocks) can be reflected, refracted, or transmitted. The coefficient represents how much of the seismic wave energy is reflected. In normal incidence the coefficient is defined by a ratio of the subtraction of both rock's impedance (Z_1, Z_2) divided by the sum of those impedance values. The value range from -1 to 1 (Ikelle, L. T. & Amundsen, L., 2006, Yilmaz, Öz.2001):

eq.2.1.1.2

$$R = Z_1 - Z_2 / Z_1 + Z_2$$

Seismic velocity refers to the speed at which seismic waves travel through different materials in the Earth's sub-surface, in other word it is a distance divided by a travel-time, two-way-time (father referred as TWT), duration of signal from source through the layer and back to receiver. Seismic velocity determines elasticity of a layer in which the seismic wave penetrates with different speeds. Seismic velocity can be measured using vertical seismic analysis or velocity various analysis of seismic data. These measurements are essential for accurately imagining and understanding the subsurface during exploration or geotechnical studies.

By other words seismic waves are generated at the surface and travel into the subsurface. As the waves encounter different rock layers with varying densities and elastic properties, their velocity changes. The seismic waves can travel faster or slower depending on the characteristics of the subsurface materials. For example, seismic velocities are generally higher in denser, more consolidated rocks and lower in less consolidated or fluid-filled layers. By analyzing the travel times and velocities of the seismic waves, it is possible to construct velocity models of the subsurface.

3.1.2. Seismic resolution

Seismic resolution refers to the ability of a seismic survey to accurately distinguish and resolve subsurface features or boundaries. It is a measure of the level of detail that can be captured and resolved by seismic data. Resolution depends on frequency, velocity and wavelength (inversely proportional to frequency). Seismic waves show a diminishing frequency value as the depth increases while the other two increase (fig. 3.1.2.1). This results in worsening of resolution quality (Nanda, 2006, Kearey et al., 2002). Several factors affect seismic resolution besides wave frequency (Kearey et al., 2002, Sheriff, R.E., 2006) like Source receive spacing, acquisition geometry, signal-to-noise ratio (SNR) and at last rock properties (Kearey et al., 2002, Yilmaz, Öz, 2001).

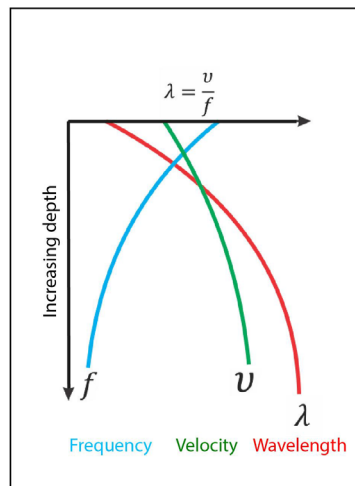


Fig. 3.1.2.1: Plot of frequency, velocity and wavelength. While the seismic wave travels deep in a subsurface the three parameters show inverse relation between frequency with other two parameters. Decreasing of frequency influence quality of resolution. Figure modified from Brown (1999).

Achieving higher resolution often comes at the expense of increased cost, time, and data complexity. It is a balance between the desired level of detail and practical considerations. Ultimately, seismic resolution plays a crucial role in accurately imaging and interpreting subsurface structures, geological features, and potential hydrocarbon reservoirs (Kearey *et al.*, 2002, Yilmaz Öz, , 2001).

The detectability of these acoustic impedance contrasts is determined by both vertical and horizontal resolution, as explained by Brown (1999). Seismic resolution refers to the minimum spatial or temporal distance between two reflection events needed to distinguish and resolve

them separately. Two types of resolution are considered: vertical and lateral. Both are influenced by the signal bandwidth.

3.1.2.1. Horizontal and vertical resolution

Seismic resolution, which determines the minimum spatial or temporal separation between two reflection events distinguishable as separate, comprises two aspects: vertical and horizontal. Vertical resolution, roughly a quarter of a wavelength, helps to differentiate closely spaced reflectors in seismic data. It's influenced by the pulse length on the recorded seismic section and decreases with depth due to energy absorption within sediments and increased sediment compaction (Kearey *et al.*, 2002). On the other hand, horizontal resolution is linked to the distance between source and receiver, and it specifies the minimum lateral distance at which two points on a reflector can be resolved as separate entities. The level of horizontal resolution affects our ability to accurately define geological features and boundaries. Both these dimensions of resolution are governed by the signal bandwidth and can significantly influence seismic data interpretation (Brown, 1999).

3.1.2.2. Reflection configuration

Seismic data's reflection configuration provides information about gross stratification patterns that correspond with sedimentary processes and deposition environments. There are several principal reflection configurations which are subdivided into categories such as parallel, divergent, chaotic, and reflection-free configurations (Mitchum *et al.*, 1977; Veeken, 2007). Each suggesting a unique depositional environment and lithofacies distribution (Veeken, 2007).

Parallel and subparallel configurations result from uniform, stable sedimentation conditions and are typically found in sheet, sheet drape and fill units. These configurations' variations are largely determined by changes in seismic parameters like amplitude and continuity. *Divergent configurations*, on the other hand, are characterized by lateral sediment thickening, indicating asymmetrical sedimentation. They're typically wedge-shaped, signifying lateral variations in sedimentation rates, subsidence, and/or burial effects (Veeken, 2007).

Chaotic reflection configurations represent discontinuous and discordant reflections, implying a disorganized arrangement of reflection surfaces. They might indicate strata deposited in high-energy, variable environments or strata initially deposited as continuous layers that were later subjected to deformation processes. Reflection-free configurations coincide with areas with

weak or no acoustic impedance contrast, which can be related to certain lithologies like igneous masses, salt features, or homogenous shales or sandstones (Mitchum *et al.*, 1977).

Several other factors, such as *reflection amplitude, continuity, and frequency*, provide additional insight into geological aspects (Kearey *et al.*, 2002; Veeken, 2007). High amplitude reflections typically indicate vertical alternation of contrasting lithologies, whereas low amplitude ones suggest similar properties on either side of the interface (Mitchum *et al.* (1977). High continuity suggests uniform deposits with great lateral extent, while discontinuous reflections point to environments with rapid energy changes. Frequency, while related to the nature of a seismic pulse, can also inform about geological factors like reflector spacing or lateral interval velocity changes, particularly in the context of gas occurrences (Mitchum *et al.*, 1977; Veeken, 2007).

3.1.3. Sedimentary principles

Sedimentary facies are specific stratigraphic segments characterized by distinct features that mirror the prevailing conditions during their formation. These features, which include sedimentary structures, dimensions, grain size and shape, color, and biological content, provide valuable insights into the nature of the sedimentary rock. When descriptions focus solely on the physical and chemical aspects of sediment transportation and deposition, the term "lithofacies" is used. The facies concept extends beyond mere stratigraphic unit descriptions to form the foundation for facies analysis. This analysis, a methodical approach to interpreting sedimentary strata, aids in reconstructing ancient environments (Nichols, 2009).

3.1.3.1. Seismic sequence stratigraphy

Originally developed for marine succession in passive margins, the stratigraphic concept is primarily influenced by sea-level changes cycles (Van Wagoner *et al.*, 1988; Shanley and McCabe, 1994; Catuneanu, 2006; Jarsve *et al.*, 2014). Sequence stratigraphy, a recent significant advancement in sedimentary geology, revolves around the interpretation of stratigraphy and depositional facies from seismic data (Catuneanu *et al.*, 2008; Mitchum *et al.*, 1977).

This methodology clusters seismic reflections into genetically related, chrono-stratigraphically defined depositional periods known as depositional sequences, further split into system tracts

(Vail, 1987). These tracts, characterized by predictable stratal patterns and lithofacies, offer a way to create a chronostratigraphic correlation framework (Vail, 1987). Stratal stacking patterns reflect combinations of depositional events such as progradation, retrogradation, aggradation, and downcutting, defining specific deposit types like transgressive, regressive, or forced regressive (Catuneanu *et al.*, 2009).

Four key variables determine variations in stratal patterns and lithofacies according to Vail (1987). These include tectonic subsidence, which creates space for sediment deposition; eustatic changes in sea level, influencing stratal patterns and lithofacies distribution; sediment volume, impacting paleowater depth; and climate, determining the dominant sediment type in a specific area. For instance, temperature and humidity significantly affect the spread of carbonates and evaporites. Accommodation space, crucial for sediment deposition, refers to the available space for marine or non-marine sediments (Coe *et al.*, 2003).

Van Wagoner *et al.* (1988) gave general knowledge of sequence stratigraphy. The potential association of flooding surfaces with submarine erosion. This association implies that the deepening phase—corresponding to a rise in relative sea level and the inception of a new sequence—could involve minor erosional events. Such events might contribute to the complexity of stratigraphic records and introduce nuances to the interpretation of depositional environments and paleogeography (Helland-hansen, 1995)

Stratigraphic sequences should be based on both allocyclic (e.g., changes in sea level, tectonics) and autocyclic (e.g., sediment supply, river avulsions) controls, rather than strictly eustatic sea level changes, understanding the multiple controls on stratigraphic formation and their complex interrelationships (Catuneanu, 2006). However, it is also crucial to note the influences of both allocyclic and autocyclic factors on stratigraphic development. While sea-level changes are vital allocyclic controls, sediment supply and other local factors can significantly affect the stratigraphic patterns as autocyclic controls. Therefore, a comprehensive understanding of these systems tracts should incorporate the interplay between these factors to create a more holistic interpretation of basin history (Catuneanu, 2006).

Seismic boundaries

The commencement of seismic stratigraphy interpretation entails the delineation of genetic reflection packages via the surfaces that encapsulate seismic sequences and systems tracts. These enveloping discontinuities are discerned based on reflection termination patterns and their continuity (Vail *et al.*, 1987, 1991; Emery & Myers, 1996; Helland-Hansen & Hampson, 2009; Catuneanu *et al.*, 2009).

Seismic boundaries are identified within a seismic line through recognition of seismic reflector terminations at discontinuity surfaces. The terminations typically occur beneath a discontinuity, defining the upper sequence boundary, manifested in the form of a *toplap* or *truncation* (fig. 3.1.3.1.1). Toplap represents strata termination against an overlying surface, denoting non-deposition and/or minor erosion, while truncation entails strata deposition and subsequent tilting and removal along an unconformity surface, a reliable top-discordant criterion of a sequence boundary. Truncation may also occur because of termination against an erosional surface, such as a channel (Vail et al, 1987, 1991, Mitchum et al, 1977, in Payton; Catuneau, 2006, 2009)

On the other hand, terminations occurring above a discontinuity define the lower sequence boundary, evident in *onlap or downlap* (fig. 3.1.3.1.1). Onlap involves the progressive termination of initially horizontal strata against an initially inclined surface or vice versa, while downlap signifies the termination of inclined strata downdip against an inclined or horizontal surface. Instances of downlap surfaces include the top of a basin floor fan surface, a top slope fan surface, and a maximum flooding surface (Vail et al, 1987, 1991; Mitchum et al, 1977, in Payton; Catuneau, 2006, 2009).

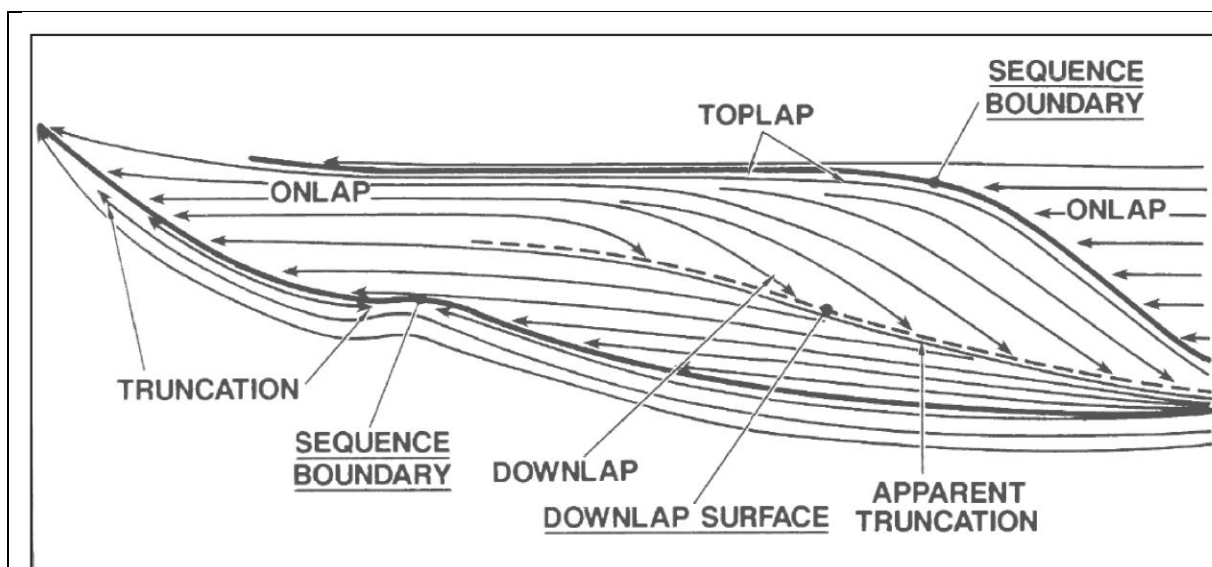


Figure 3.1.3.1.1: This section presents a depiction of a seismic sequence, showcasing the main reflection terminations employed in the categorization of sequence stratigraphy. Modified from Vail (1987).

System Tracts

Interpretations of systems tracts are based on stratal stacking patterns, their positioning within the sequence, and the nature of bounding surfaces (Van Wagoner et al. 1987, 1988, 1990; Posamentier et al. 1988; Van Wagoner 1995; Posamentier and Allen 1999). Systems tracts can

be classified as shoreline-related, linked to specific types of shoreline trajectories, or shoreline-independent, where a genetic connection to contemporary shorelines is undetermined.

Depositional sequences, as outlined by Van Wagoner et al. (1988), Brown and Fisher (1977), and Posamentier et al. (1988), can be subdivided into systems tracts. These are smaller stratigraphic units defined by their distinct stacking patterns and their correlation to cycles of sea-level change. Key among these is the *Highstand Systems Tract (HST)*, *Falling Stage Systems Tract (FSST)*, *Low stand Systems Tract (LST)*, *Transgressive Systems Tract (TST)*, and *Regressive Systems Tract (RST)*, which embody crucial stages of sea-level change and sediment supply dynamics (Van Wagoner et al., 1988; Hunt and Tucker, 1992; Embry and Johannessen, 1992).

The HST, FSST, LST, TST, and RST (Figure 3.1.3.1.2) form during specific phases of the relative sea-level cycle. FSST includes regressive deposits that accumulate after a relative sea-level fall initiates and before the start of the next relative sea-level rise. The LST comprises deposits that form after the onset of a relative sea-level rise, during a phase of normal regression. The TST is made up of deposits that gather from the start of a transgressive phase until the point of maximum coastal transgression. HST includes the progradational deposits that form when the rate of sediment accumulation exceeds the rate of accommodation increase during the later stages of relative sea-level rise. Lastly, RST is found above a TST and is overlain by the initial transgressive surface of the subsequent TST.

These systems tracts are valuable for interpreting depositional environments, predicting sedimentary facies, and reconstructing paleogeography (Allen & Allen, 2013). Emphasizing the role of sea-level change and tectonic subsidence rates, it's now understood that they are notably affected by variations in sediment supply. This distinction is particularly evident in the LST, which forms during rapid sea-level falls and is characterized by base-of-slope fans, slope fans, and lowstand wedges. In contrast, the Transgressive and Highstand Systems Tracts are associated with rapid and slow sea-level rise following maximum flooding, respectively (Catuneau et al., 2008).

These systems tracts, which are essential in both siliciclastic and carbonate-dominated systems despite their significant differences (Catuneau et al., 2008), are invaluable as they refer to different stratal stacking patterns, are characterized by different sediment dispersal patterns within the basin, and consequently are associated with different petroleum plays. This has significant implications for petroleum exploration and production development. Beyond these

shoreline-related systems tracts, there are also shoreline-independent systems tracts, stratigraphic units forming subdivisions of sequences in areas where sedimentation processes are independent of shoreline shifts (Catuneanu, 2006).

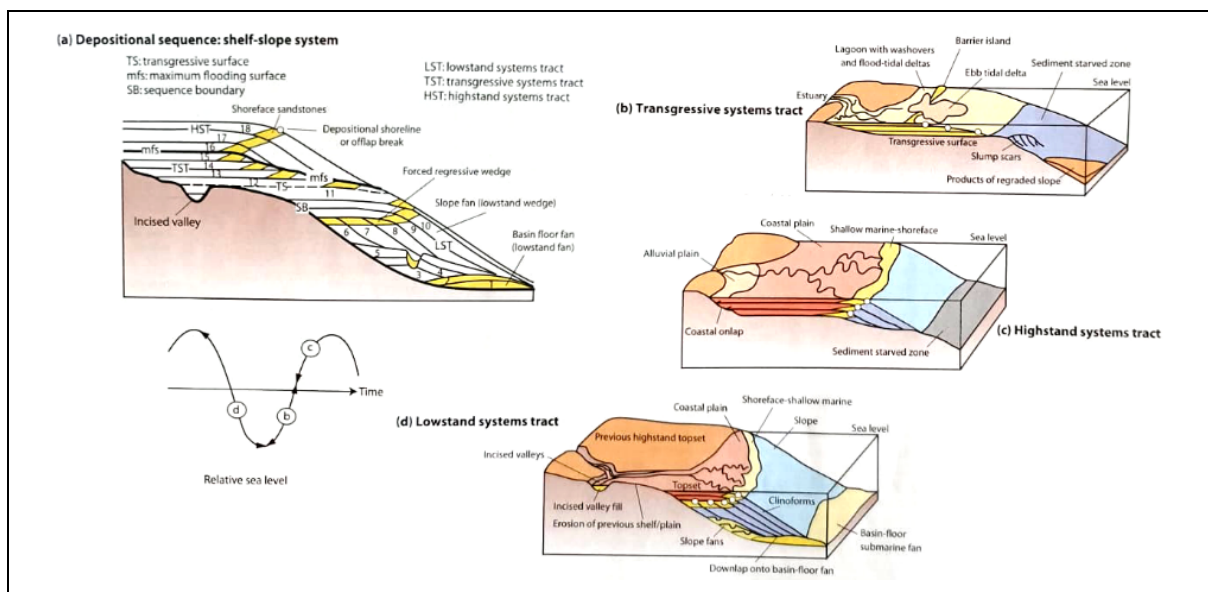


Figure 3.1.3.1.2: This section provides a theoretical illustration, showcasing the interplay between distinct systems tracts and their correlation to the relative sea-level curve, based on the Exxon group's work (Posamentier et al., 1988), further refined by Emery and Myers (1996). (a) Portrays how systems tracts are organized within a depositional sequence in an environment encompassing a coastal plain, continental shelf, and slope. The sequence's relative ages are represented numerically. (b), (c), and (d) Offer representations of transgressive, highstand, and lowstand systems tracts, respectively. The open circles in the illustration signify the depositional shoreline or shelf break.

Clinoforms

Clinoforms refer to large-scale sedimentary structures that exhibit a progradational wedge shape under water bodies, such as oceans and lakes where deltaic, lacustrine, or marine clastic sediments (like sand, silt, or clay) are transported and deposited (Reading, 1996, Reading & Levell, 1996; Catuneanu et al, 2011). These structures are characterized by a gentle, nearly horizontal topset, a steeply inclined foreset, and a more horizontal bottomset. The transitions between these three zones are often sharp, giving clinoforms their distinctive shape (Helland-Hansen & W., & Hampson, G. J. (2009); Patruno & Helland-Hansen, 2018; Pellegrini et al., 2020).

There are three primary types of clinoforms shown in a fig. 3.1.3.2.1 (Mitchum et al., 1977; Helland-Hansen & Hampson, 2009; Patruno & Helland-Hansen, 2018; Pellegrini et al., 2020):

1. **Deltaic clinoforms:** These are typically associated with river deltas, where sediment is transported by rivers and deposited at the river mouth. Deltaic clinoforms are relatively small-scale structures with a foreset slope typically less than 5° .

2. **Shelf-edge clinoforms:** These are larger-scale structures, typically found at the edge of continental shelves, where sediment is transported by ocean currents and wave action. Shelf-margin clinoforms may have foreset slopes ranging from 2° to 8°.
3. **Continental margin clinoforms:** These are the largest scale clinoforms, associated with deep-sea fan systems where sediment is transported by turbidity currents. Submarine fan clinoforms can have foreset slopes of up to 20°.

The dimensions of clinoforms can vary considerably, from tens of meters to several kilometers in thickness, and laterally from hundreds of meters to hundreds of kilometers (Steel & Olsen, 2002; Helland-Hansen & Hampson, 2009). The scale is dictated by numerous factors including the type of clinoform, sediment supply, sea level, and tectonic activity. The dimension, morphology, and geometry of clinoforms yield valuable information regarding sediment supply, sediment type, pre-existing basin floor topography, water depth, and the hydrodynamic regime under which they were deposited (Mitchum et al., 1977; Emery & Myers, 1996; Helland-Hansen et al., 2012; Anell & Midtkandal, 2015; Patruno et al., 2015a; b). Hansen, W., & Hampson, G. J., 2009). The dimensions of clinoforms vary. Commonly, shelf-margin slopes exhibit variations between 2 to 7 degrees (Steel & Olsen, 2002; Johannessen & Steel, 2005). Slopes with high quantities of coarse material are often steeper compared to slopes composed predominantly of muddy sediments (Johannessen & Steel, 2005). When the sediment flux from the shelf break is high, sand-prone slopes often result from channelized slopes or when sandy, shelf-edge-attached aprons are supported (Johannessen & Steel, 2005).

A key attribute of these structures is the slope gradient, which is influenced by factors such as the grain size of the sediment, sediment supply, and the energy of the depositional environment. As an illustration (3.1.3.1.3) deltaic clinoforms located in low-energy wave environments may exhibit steeper gradients in comparison to their counterparts in high-energy wave environments (Reading, H. G., & Levell, B. K., 1996).

Furthermore, it should be noted that clinoform slope gradients are not static over time but change in response to alterations in relative sea level and sediment supply. This implies that a single clinoform might exhibit varying slope gradients at different points in its history (Helland-Hansen & Hampson, 2009).

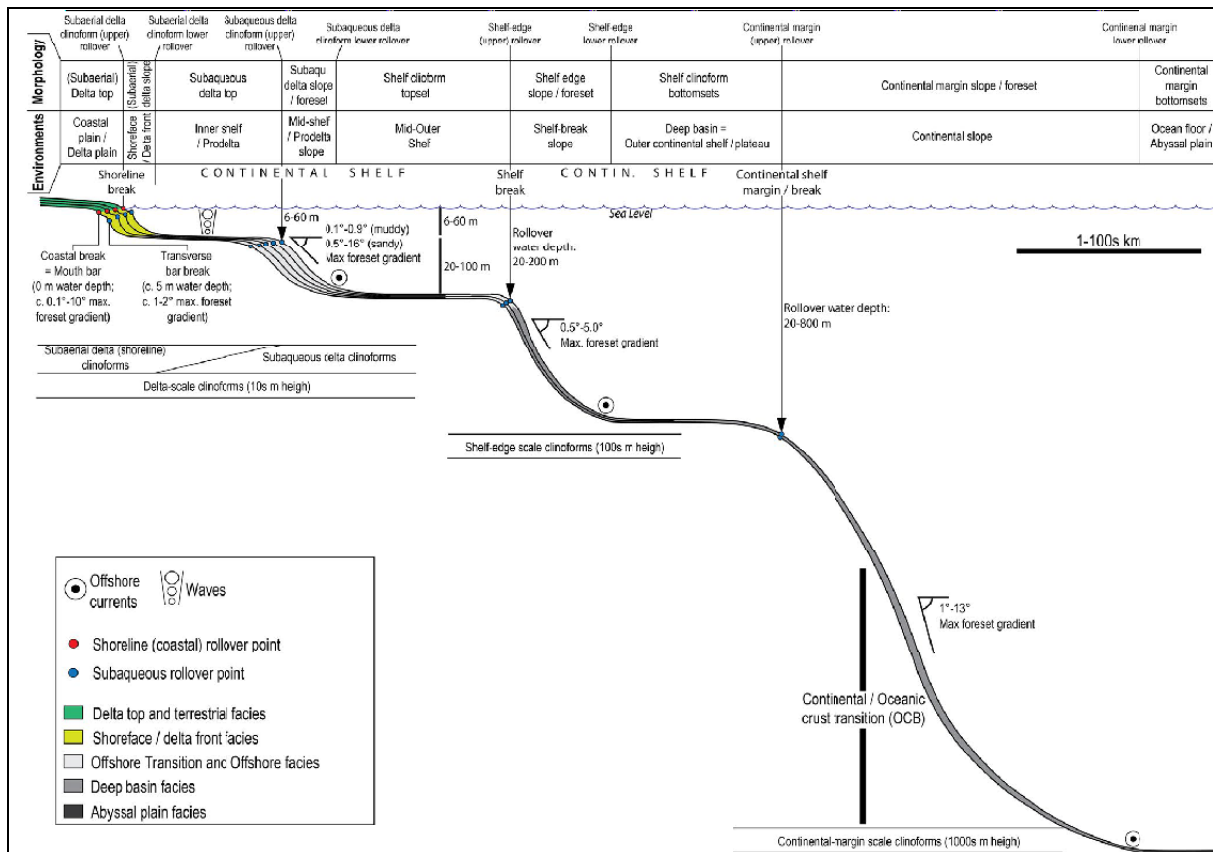


Figure 3.1.3.1.3: distinguish between continental-margin and shelf-edge clinoforms based on differences in depositional facies in their topset/bottomset, geometry, depositional rates, and geodynamic position. Continental margin clinoforms straddle the transition between continental and oceanic crust, while shelf-edge clinoforms are typically situated in continental crust. The differentiation of these four predominant types of clinoforms hinges upon factors such as vertical relief, the presence of specific sedimentary facies and facies associations within each segment of these varied clinothem types, degree of proximity along an idealized transect from shoreline to abyssal plain, oceanographic circumstances, and geodynamic context. Particularly, *continental-margin and shelf-edge clinoforms* are differentiated by their depositional facies in topset/bottomset, geometry, deposition rates, and geodynamic positioning. Continental margin clinoforms mark the transition from continental to oceanic crust, while shelf-edge clinoforms typically reside within the continental crust (Pellegrini et al., 2020).

Geometry of slope

The internal structure, slope geometry, and toe progression of clinothems are vital indicators of sediment redistribution processes. Details like erosion patterns or stratification in clinothems can hint at strong currents or sediment supply fluctuations. The slope's gradient and form can reflect sedimentation rate and nature, with steep and gentle slopes signifying high and slow sedimentation rates, respectively. Similarly, the rate of a toe's forward movement - the maximum extent of clinoform's reach - is indicative of sediment supply and redistribution efficacy. Rapid toe progression implies plentiful sediment supply or efficient redistribution, while the opposite might indicate limited sediment supply or less effective redistribution (Wolinsky & Pratson, 2007; Anell & Midtkandal, 2015). Shelf-edge progression, trajectory angle, slope angle, and foreset angle offer additional insights into the sedimentary environment (fig. 3.1.3.1.4).

Toe advance - refers to the seaward movement or progradation of the edge, or "toe," of a delta, alluvial fan, or similar sedimentary deposit. It is the distance between upper rollover point to

lover one. This movement is usually the result of sediment accumulation outpacing erosion and subsidence, pushing the deposit's outer boundary further into the body of water (fig. 3.1.3.1.4).

Shelf-edge advance - reveals the equilibrium between sediment supply and accommodation space creation, with fast and slow advances suggesting high sediment supply rate or decrease in accommodation space, and low sediment supply rate or increase in accommodation space, respectively (Helland-Hansen & Hampson, 2009).

Slope relief - indicates the vertical variation from the base to the summit of a slope, measuring the terrain's rise or fall. It is considered synonymous with "foreset height," a term from sedimentary geology, referring to the vertical difference from the top to the base of inclined sediment layers (from the rollover lower one to upper one, vis fig. 3.1.3.1.4), often found on a delta's front slope. These layers result from sediment deposition.

The trajectory angle - the steepness of the path traced by the shelf as clinothems accrue over time - indicates the balance between accommodation creation and sediment supply. Steep and gentle angles typically signify that accommodation creation is surpassing or falling behind sediment supply, respectively (Patruno et al., 2015).

Slope angle - the tilt of the basin margin or seafloor slope from the horizontal, informs about the seafloor's sediment stability and occurring processes. Steeper angles encourage gravity-driven processes like turbidity currents, while gentler slopes host tractional processes (Patruno et al., 2015, Anell & Midtkandal, 2015)).

Foreset angle - which is the angle of the sloping strata within a clinoform, provides insights into the sedimentary processes, sediment characteristics, and flow conditions during deposition. Greater angles suggest coarser sediments and high-energy environments, whereas gentler angles hint at finer sediments or low-energy conditions (fig. 3.1.3.1.4).

In essence, these parameters, their interplay, and influences offer a comprehensive understanding of the sedimentary system's architecture, enabling geologists to decode the depositional history and environmental changes of a sedimentary basin. The understanding of these parameters allows geologists to reconstruct the depositional history and environmental changes of a sedimentary basin. By integrating the data on trajectory angle and shelf-edge advance with other characteristics of clinothems, they can gain a more comprehensive understanding of the paleoenvironment and the processes that shaped it (Patruno et al., 2015).

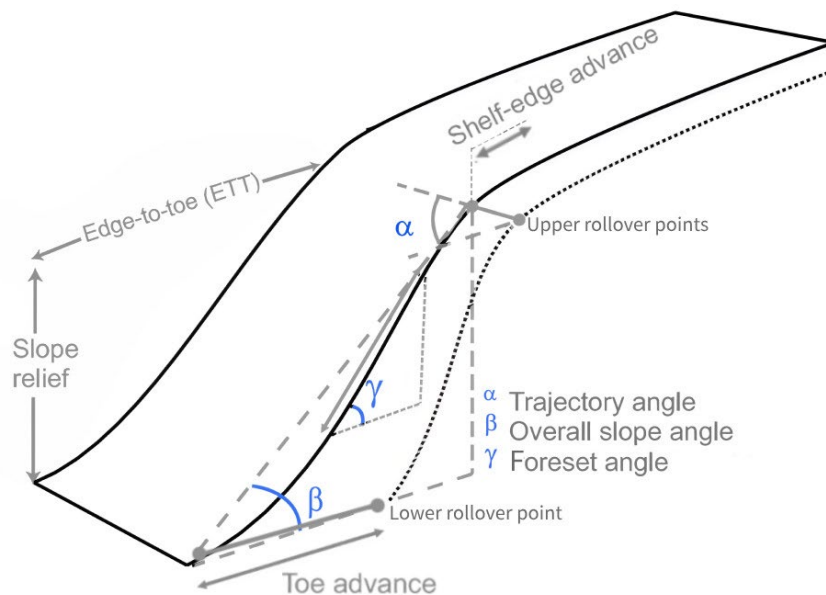
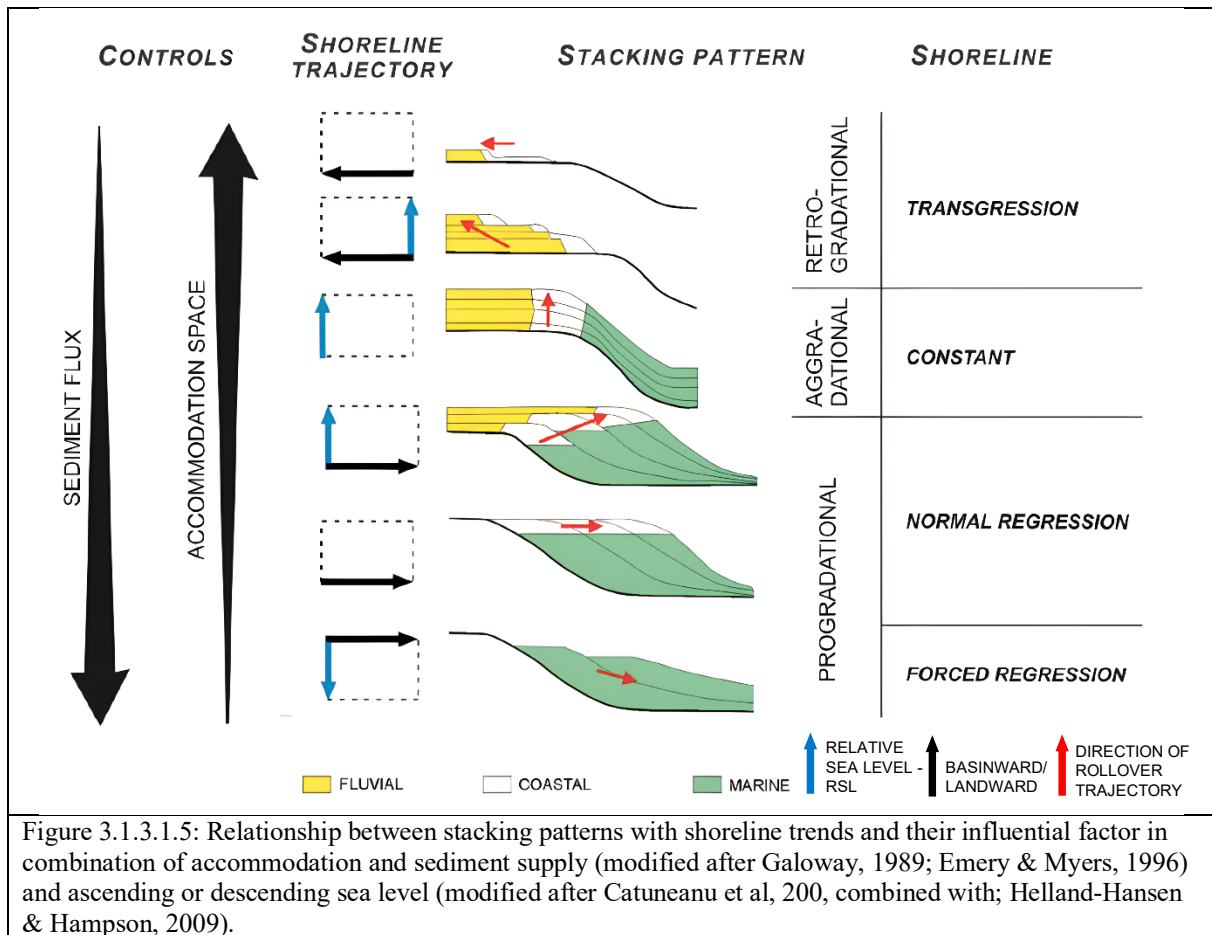


Figure 3.1.3.1.4: Simplified image of clinoform with important parameters. Angles and distances, used later for calculation (modified from Anell & Mitkandal, 2015; Patruno et al, 2015a).

Stacking pattern and Trajectories

In alignment with the organization of chronostratigraphic units, sets of clinothems can be classified into three fundamental accumulation patterns: *aggradational*, *progradational*, and *retrogradational* (Van Wagoner et al., 1988). The aggradational pattern represents the vertical assembly of repeated cycles with persistent facies and no discernable sideways shift in facies belts over time. In contrast, progradation characterizes the upward growth of the cycles, distinguished by more proximal facies at the top, while the retrogradational pattern presents younger, distant deposits situated above proximal units. The translation of depositional systems, either landward or basinward, is controlled by the interplay between sediment accumulation rates and accommodation space changes (Van Wagoner et al., 1988; Posamentier & Allen, 1999; Catuneanu, 2002; Catuneanu et al., 2009; Helland-Hansen & Hampson, 2009, fig. 3.1.3.1.5). For instance, during transgressive periods, an increase in relative sea level exceeding sediment supply generates accommodation space, causing facies belts to migrate landward and form retrogradational stacks. Conversely, a decrease in relative sea level reduces accommodation space, forcing the system to prograde, regardless of sediment discharge (forced regression). This behavior is different from sediment-driven progradation (normal regression), which happens when sea level remains constant or the rate of accommodation creation cannot match sediment supply (Catuneanu et al., 2008). These patterns provide insights into the past environments in which the sediments were deposited (Catuneanu et al., 2009; Helland-Hansen & Hampson, 2009).

The path drawn by the shelf during the accumulation of clinoforms, known as the shelf-edge trajectory, plays a crucial role in stratigraphic studies (Johannessen & Steel, 2005). This trajectory facilitates the examination of the spatial-temporal movements of the shelf-edge. The existence of a break-in-slope often provides a critical physical marker for tracking both lateral and vertical shifts within depositional systems (Helland-Hansen & Hampson, 2009). The shelf break serves as a significant boundary, signaling substantial shifts in depositional mechanisms and their resulting products. This break separates the shelf and slope regions, dictating processes like sedimentation, bypass, and channeling. The dominant processes on the shelf include regular migration of deltas and shorelines and the influence of tidal and wave activities (Helland-Hansen & Hampson, 2009). The trajectory of the shelf break results from a combination of factors such as bathymetry, sediment supply, eustatic sea-level fluctuations, and subsidence (Helland-Hansen & Hampson, 2009). With the addition of clinoforms, the shelf-edge trajectory may undergo changes in its inclination or gradient, leading to its classification as ascending, flat, or descending (Johannessen & Steel, 2005; Helland-Hansen & Hampson, 2009). An ascending shelf-edge trajectory indicates a long-term increase in relative sea level, caused by sediment accumulation on the shelf break outpacing sea-level rise. Consequently, less sediment reaches deep waters, with a greater proportion settling on the existing shelf and coastal plain (Johannessen & Steel, 2005; Helland-Hansen & Hampson, 2009; Helland-Hansen et al., 2012). In contrast, flat and descending shelf-edge trajectories suggest long-term stability or a relative sea-level decrease. During lowstand phases, sediment transfer across the shelf is promoted, potentially forming channelized deposits on the slope and basin floor (Steel & Olsen, 2002).



Clinoforms are sedimentary structures that reflect the lateral migration of a depositional environment. They are most found in deltaic, lacustrine, or marine settings where clastic sediments (like sand, silt, or clay) are transported and deposited. Clinoforms can form large-scale bodies that are many kilometers in thickness and extend across entire basins, or they can be smaller features just a few meters in size.

Clinoforms consist of three main parts: the topset, foreset, and bottomset (Reading, 1996, Reading & Levell, 1996; Catuneanu et al, 2011).

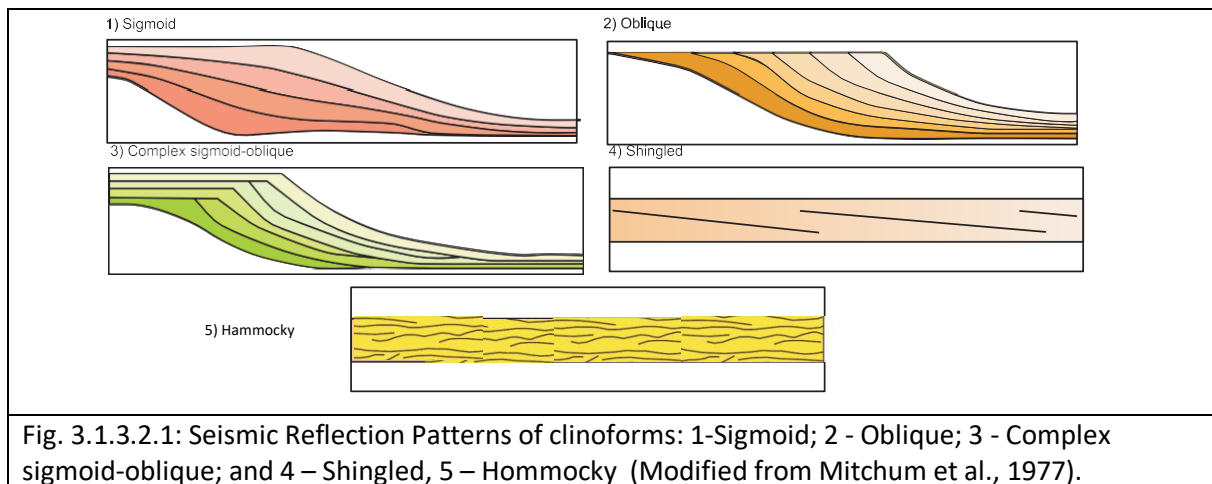
1. **Topset:** The topset consists of relatively horizontal layers of sediment that are deposited when the sediment transport system reaches a body of water. The layers are typically flat or gently sloping (Reading, 1996, Reading & Levell, 1996; Catuneanu et al, 2011).
2. **Foreset:** The foreset forms when sediment begins to pile up at the edge of the water body, causing it to slough off and create a sloping face. This is usually the most visually distinct part of the clinoform. The foreset slope can range from a few degrees up to nearly vertical, depending on the type of sediment and the water depth (Reading, 1996, Reading & Levell, 1996; Catuneanu et al, 2011).

3. **Bottomset:** The bottomset consists of horizontal layers of sediment that spread out at the foot of the foreset, typically under the influence of gravity and underflows (Reading, 1996, Reading & Levell, 1996; Catuneanu et al, 2011).

The evaluation of clinoforms can reveal important information about past environmental conditions, including changes in sea level, sediment supply, and tectonic activity. For example, a change in the angle of the foreset slope can indicate a change in sea level, with lower angles typically associated with rising sea levels and steeper angles (Reading, 1996, Reading & Levell, 1996; Catuneanu et al, 2011).

3.1.3.2. Seismic Reflection Patterns of clinoforms

Sangree & Widmier (1977) initially proposed a classification of clinoform end members as two distinct types, sigmoid and oblique shape). This categorization was further elaborated by Mitchum et al. (1977), who suggested an additional division encompassing five seismic reflection patterns for different clinoform types. Sigmoid, which displays curves at the top and base, indicative of balanced sedimentation. Oblique (both tangential and parallel), shows a straight, downward pattern, suggesting sediment supply exceeds accommodation. complex sigmoid-oblique combines elements of both, indicating mixed depositional environments, the shingled pattern, similar roof shingles, occurs in high-energy, high sediment supply environment, and lastly hummocky (Fig.3.1.3.1). These classifications served to underscore the rich diversity and inherent complexity of clinoform formations.



Anell & Midtkandal (2015) proposed a tripartite division which serves as a foundation for their clinotherm classification (fig. 3.1.3.2.1). This detailed categorization framework takes in consideration the importance of several factors, including rollover trajectories, stacking patterns, and the symmetric relationships among genetically related clinoforms. Furthermore, it considers the internal composition of clinotherms. Their comprehensive scheme suggests nine

distinct types of clinothems: Oblique, Tangential oblique, Tangential oblique chaotic, Sigmoidal symmetrical, Sigmoidal divergent, Sigmoidal chaotic, Asymmetrical top-heavy, Asymmetrical bottom-heavy, and Complex (Anell & Midtkandal, 2015). The slope curvature can be linear (oblique), exponential (tangential), or Gaussian (sigmoidal). The study also differentiates between chaotic and non-chaotic clinothems, as well as between symmetrical and divergent sigmoidal clinothems. Furthermore, it distinguishes between top-heavy and bottom-heavy asymmetrical clinothems (Anell & Midtkandal, 2015).

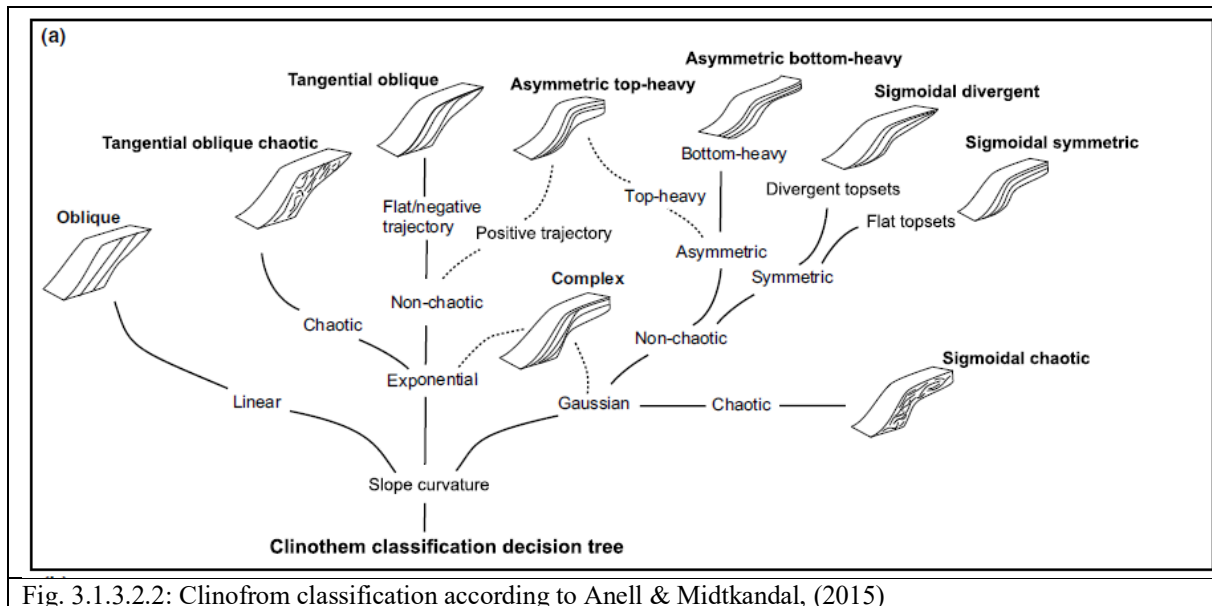


Fig. 3.1.3.2.2: Clinofrom classification according to Anell & Midtkandal, (2015)

Oblique Clinothems: These clinothems have a linear slope with tabular foresets and no clear topsets or bottomsets. They are truncated and may not represent classic oblique examples.

Tangential Oblique Clinothems: These clinothems have tangential slopes with flat or descending trajectories and no topsets. Sediment bypasses the shelf area, supplying sediment increasingly to the foreset and bottomset.

Tangential Oblique Chaotic Clinothems: Similar to the tangential oblique clinothems, these clinothems have tangential slopes. However, they exhibit chaotic characteristics, likely due to sediment redistribution and slope backfilling.

Sigmoidal Symmetrical Clinothems: These clinothems have classic S-shaped Gaussian-type curvature. They have a convex slope defining the shelf edge and a concave lower slope. Sediment accumulation is relatively symmetrical.

Sigmoidal Divergent Clinothems: These clinothems exhibit S-shaped curvature with lower trajectory angles. They have low shelf-edge advance and similar characteristics to the other sigmoidal types.

Sigmoidal Chaotic Clinothems: Similar to sigmoidal symmetrical clinothems, these clinothems have S-shaped curvature. However, they exhibit chaotic characteristics, likely due to sediment redistribution and slope erosion.

Asymmetrical Top-Heavy Clinothems: These clinothems have a rounded shelf edge and typically exponential slopes. They have a positive trajectory and preserved topsets. Sediment accumulates more in the upper part of the clinothems.

Asymmetrical Bottom-Heavy Clinothems: These clinothems have sigmoidal slopes with sediment accumulating beyond the shelf edge, resulting in a gentle slope and asymmetrical profile. Sediment is sequestered downslope, leading to limited shelf-edge advance.

Complex Clinothems: These clinothems have intermediate external and internal shapes between sigmoidal and tangential. They exhibit a combination of characteristics from both types.

3.1.4. Carbon Capture and Storage (CCS)

Carbon Capture and Storage (CCS) involves isolating carbon dioxide (CO₂) produced from industrial activities before it's released into the atmosphere and storing it deep within geological structures underground. This process helps industries reduce their greenhouse gas emissions, effectively contributing to the reduction of man-made CO₂ in the atmosphere. The storage, however, needs to be safe, environmentally sound, and affordable.

These storage sites can be onshore or offshore, each with unique benefits and challenges. The idea is to securely store CO₂ within subsurface formations. The U.S. Department of Energy (DOE) is currently exploring five such geological formations (fig.: 3.1.9.1: saline formations, oil and natural gas reservoirs, unminable coal seams, organic-rich shales, and basalt formations (+enhanced coal bed methane recovery). The DOE's Carbon Storage Program is also conducting extensive research on CCS, and developing best practice manuals.

One way to store CO₂ is in a supercritical state, where the CO₂ is maintained at temperatures above 31.1°C (88°F) and pressures beyond 72.9 atm (around 1,057 psi). Supercritical CO₂ behaves somewhat like a gas and a liquid, being dense like a liquid but having the viscosity of a gas. This state significantly reduces the required storage volume compared to standard pressure conditions.

At depths below approximately 800 meters (about 2,600 feet), the Earth's natural temperature and fluid pressures surpass CO₂'s critical point, meaning that injected CO₂ would naturally remain supercritical at these depths due to the ambient conditions (Rodosta *et al.*, 2017).

Carbon dioxide (CO₂) remains underground due to various trapping mechanisms. there are four main mechanisms that help trap CO₂ in the subsurface and prevent it from migrating to the surface.

Structural trapping physically contains CO₂ in rocks, which act as barriers to keep the gas from escaping. The CO₂ travels upwards until it's hindered by a non-permeable rock layer.

Residual trapping, on the other hand, is when CO₂ gets caught in the pore space of rocks as it moves through, leaving behind droplets that are effectively immobile.

Solubility trapping, some CO₂ dissolves into the brine water within the rock's pores. Some of this dissolved CO₂ combines with hydrogen atoms to form bicarbonate ions.

Mineral trapping happens when dissolved CO₂ in the rock's water reacts with minerals to form solid carbonate compounds, leading to permanent CO₂ storage.

CO₂ storage is ongoing globally, including large projects like the Sleipner CO₂ Storage Site in Norway and the Weyburn-Midale CO₂ Project in Canada, which each store more than 1 million metric tons of CO₂ annually. There are also sizable efforts in China, Australia, and Europe. Additionally, many other Carbon Capture and Storage (CCS) initiatives are ongoing around the world, validating the feasibility of geological storage for long-term CO₂ containment. Over 200 CO₂ capture and storage operations have been conducted globally, either completed or under development (Rodosta et al., 2017).

Around the world, CO₂ storage is being implemented. Commercial-scale projects such as Norway's Sleipner CO₂ Storage Site and Canada's Weyburn-Midale CO₂ Project, which each store over a million metric tons of CO₂ annually, have been active for years. Significant efforts are also ongoing in China, Australia, and Europe, affirming that it's feasible to securely store large quantities of CO₂ permanently.

Furthermore, diverse Carbon Capture and Storage (CCS) projects are progressing globally, showcasing the potential of geological storage technologies for future long-term CO₂ containment. So far, more than 200 CO₂ capture and storage operations, either completed or in progress, have been executed worldwide (Rodosta et al., 2017)..

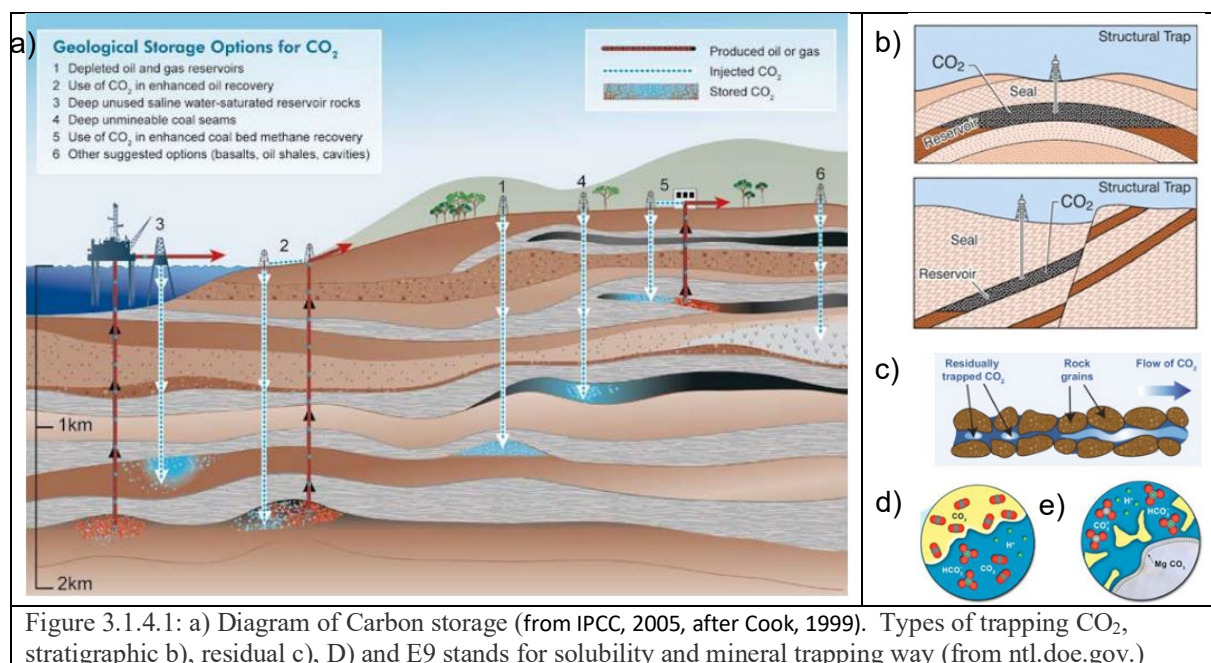


Figure 3.1.4.1: a) Diagram of Carbon storage (from IPCC, 2005, after Cook, 1999). Types of trapping CO₂, stratigraphic b), residual c), D) and E) stands for solubility and mineral trapping way (from ntl.doe.gov.) (National Energy Technology Laboratory. (n.d.))

Regional analyses suggest that the Norwegian Continental Shelf could potentially accommodate a substantial quantity of CO₂ storage. To fulfill ambitious climate goals (...), a thorough geological characterization is now needed to prioritize and mitigate risks associated

with potential new storage sites. Situated in the northern part of the North Sea and to the south of the Horda Platform—where current Carbon Capture and Storage (CCS) infrastructure is being developed—the Stord Basin may present feasible opportunities for CO₂ storage within stratigraphic and residual trapping, (Evans&Braathen, 2022) particularly of prograding delta-shelf of Draupne formation in Viking group. Faleide et al. (2021) delve into the issues and potential errors associated with the interpretation of normal faults. By juxtaposing objective and subjective uncertainties, the study elaborates on how these uncertainties can be recognized, addressed, and reduced. Jackson et al. (2022) render insight to depositional development of Johansen Formation targeted as primary CO₂ storage unit.

In the Jackson's et al. (2022) analysis of sedimentological data obtained from core images of the recent 31/5-7 (Eos) validation well aligns with the earlier interpreted depositional model: a wave-influenced delta front that experienced three stages of growth, build-up, and desertion, referred to as the "lower Johansen, upper Johansen and Cook deltas." The findings suggest that variations influencing the spread and connectivity of high-permeability sandstones in the middle and closer delta-front (for example, delta shape, clinoform slope, and the extent of facies associations interweaving along the clinoforms) markedly affect both horizontal and vertical permeability, the Lorenz coefficient, and pore volumes injected at the time of breakthrough.

Additionally, the lateral persistence of carbonate-cemented layers along transgressive surfaces has a profound effect on effective vertical permeability. The intensity of bioturbation—physical disturbance of sediment by living organisms—also significantly impacts both effective horizontal and vertical permeability, as well as the Lorenz coefficient. Combined effects of these heterogeneities also play a critical role.

As such, the significant influence of sedimentological variations on the movement and storage of CO₂ can't be overlooked. It serves as an initial blueprint for trapping via capillary action, dissolution, and mineral processes (Jackson et al., 2022).

In a similar deposition setting, of westward delta prograding shelf, such an overlook is not possible due to none well penetration in a clinoforms set. Focus remains on knowing the shape and layout of a delta (**clinoform geometry**), sediment supply source or nature of receiving the sediments, and possibly the energy of the current. Also, focus lay within **clinoform dip** which helps to determine depositional environment and **facies-Association Interfingering** - various sedimentary environments (represented by different facies) intermingle and overlap along the sloping surfaces of the clinoforms. This can provide insights into changes in the depositional environment over time and space, including shifts in sea level, sediment supply, and sediment transport mechanisms.

Understanding depositional heterogeneity can help to better predict and model the behavior of injected CO₂ and manage potential risks associated with its storage. High-quality 3D, 2D seismic data, well logs, and other geological and geophysical data are key for accuracy (Jackson *et al.*, 2022).

Depositional heterogeneity (fig. 3.1.9.2) refers to the variability in a geological system due to different conditions of deposition. It plays a critical role in various subsurface processes, such as oil and gas extraction, water supply, contaminant transport, and carbon dioxide (CO₂) storage.

In the context of CO₂ storage, depositional heterogeneity can significantly affect the storage capacity, injectivity, and containment security of a reservoir. Here are some specific implications:

Storage Capacity: The total volume of pore space available for CO₂ storage is influenced by depositional heterogeneity. Different sedimentary layers have varying porosity and permeability, leading to different storage capacities. For instance, more permeable layers will allow CO₂ to flow more freely, thus offering potentially larger storage spaces.

Injectivity: Injectivity refers to the ease with which CO₂ can be injected into a storage reservoir. Higher permeability layers allow for better injectivity. However, too much heterogeneity could create preferential pathways for the CO₂, potentially bypassing some of the available storage space.

Containment Security: Once injected, the CO₂ must be securely stored to avoid leakage back into the atmosphere. Some depositional environments may create potential leakage pathways, such as fractures or faults. Others may result in trapping mechanisms, such as cap rocks or stratigraphic traps, that enhance containment security.

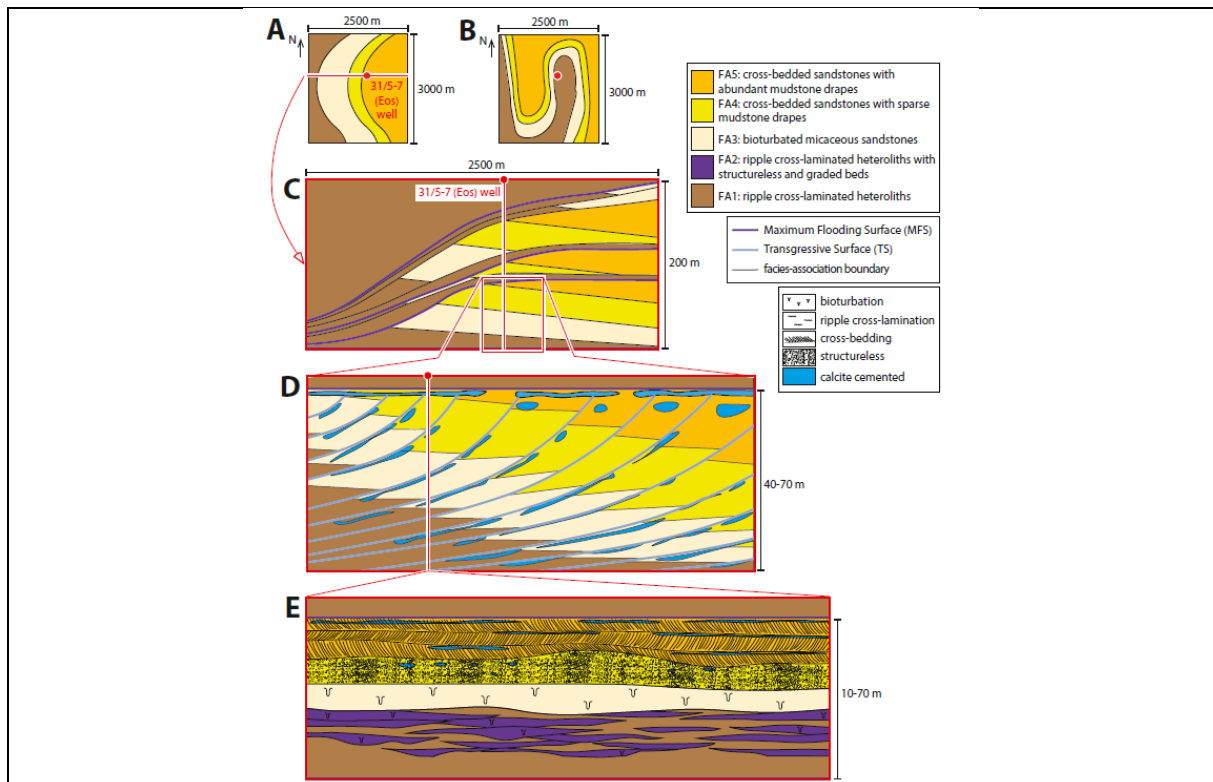


Fig. 3.1.4.2: An example of hierarchy of heterogeneity of lower Johansen upper Johansen and Cook delta in Horda Platform (Jackson *et al.*, 2022). (**A**, **B**) plan-view maps for two morphological configurations of the delta systems (**C**) vertically stacked regressive-transgressive tongues (clinoform sets) within the lower Johansen, upper Johansen and Cook formations (**D**) an individual regressive-transgressive tongue (clinoform set), showing selected clinoforms (**A**) marked by interfingering of facies associations across minor transgressive surfaces (**B–D**) and calcite-cemented concretions along and between the transgressive surfaces (**E**) idealized facies succession showing selected heterogeneities within facies association.

3.2. Data

In this chapter, we will delve into the data that underpins this study. Furthermore, we will provide a detailed account of the methods and workflow employed in this study to accomplish the primary objectives.

3.2.1. Software

This study incorporates the tool Petrel E&P software 2022 (Schlumberger Limited.) for interpreting selected 2D seismic surveys (tab. 3.2.2.1), to project well, clinoform parameter computation, and map creation. Unless explicitly specified, the depiction of all interpreted features and cross-sections is in two-way time (TWT). In this study, a detailed velocity model was not implemented, thus we assume an average overburden velocity of 2000 m/s at 2000 m depth to simplify calculations. Modifications of illustrative figure interpretation were done with vector graphics software Corel Draw X7 and Inkscape 1.2.

3.2.2. Data set

In the context of this study, two important sources of data were utilized: wellbores and seismic reflection data. The overview tab of wells and seismic surveys are presented below.

3.2.2.1. Wellbores

All wells used in this study help to understand stratigraphic charts defined in other studies. The stratigraphic defined groups and units obtained from NPD fact page were assessed. Only 3 wells lay within the basin. The well 17/3-1 was targeted to tectonic high between the Åsta graben and the Stord Basin. Two other wells, 31/11-1s and 25/5-1, were drilled as a part of Stovegolvet and Storbarden prospect, respectively. The other wells are in surrounding closes at the western or northern part of Stord basin (detail location in tab. 3.2.2.2.1, location of wells is fig. 3.2.2.1.1). Furthermore, the strata revised from NPD fact page are collected in a tab. 3.2.2.2.

WELBORE NAME	LOCATION IN STRUCTURE	OLDEST PENETRATED FORMATION AND AGE	OPERATOR	TOTAL DEPTH (MD) [m]	RELEASE YEAR
17/3-1	Horst between Åsta graben and Stord Basin	Basement Pre-Devonian	Elf Petroleum Norge AS	2852	1997
17/4-1	Ling Depression between Utsira and High	Rotliegend Group Early Permian	Elf Petroleum Norge AS	3997	1970
25/6-1	Utsira High Fault Zone footwall	Basement Pre-Devonian	Saga Petroleum ASA	2881	1988
25/12-1	SE part of Utsira High block footwall	Undefined Devonian	A/S Norske Shell	2865	1975
26/4-1	Utsira High Fault Zone footwall	Undefined Triassic	BP Norway Limited U.A.	3690	1989
26/5-1	Stord basin	Tryggvason Late Cretaceous	Rocksource Exploration Norway AS	1910	2015
30/9-15	Between Brage Horst and Northern Horda Platform Footwall	Statfjord Group Early Jurassic	Norsk Hydro Produksjon AS	2764	1996
30/12-1	Between Brage Horst and Northern Horda Platform Footwall	Statfjord Group Early Jurassic	Norsk Hydro Produksjon AS	3641	1996
31/8-1	Boundary Northern Horda Platform and Stord basin Tusse Fault edge	Krossfjord Formation Middle Jurassic	E.ON Ruhrgas Norge AS	2629	2012
31/11-1 s	Stord basin	Late Triassic	Equinor Energy AS	3284	2022
31/5-7	Northern Horda platform (CO ₂) Footwall of Tusse Fault	Statfjord Group Early Jurassic	Equinor Energy AS	2915	2020

Tab. 3.2.2.1.1: The Overview of wells used in this study, with depth, with drilling operator, and date of release. Colors are used to visually divide the age of the oldest strata drilled.

Well indication - lithostratigraphic unit at drilled depth [m]															
25/12-1	25/6-1	26/4-1	26/5-1	17/3-1	17/4-1	31/11-1s	30/12-1	30/9-15	31/8-1						
169 NORDLAND GP	47 NORDLAND GP	144 NORDLAND GP	292 NORDLAND GP	398 NORDLAND GP	132 NORDLAND GP	319 NORDLAND GP	135 NORDLAND GP	128 NORDLAND GP	336 NORDLAND GP						
902 HORDALAND GP	725 UTSIRA FM	768 UTSIRA FM	292 UNDIFFERENTIATED	396 HORDALAND GP	544 HORDALAND GP	319 NAUST FM	648 UTSIRA FM	657 UTSIRA FM	315 HORDALAND GP						
1457 ROGALAND GP	886 HORDALAND GP	792 UNDIFFERENTIATED	874 HORDALAND GP	873 ROGALAND GP	1041 ROGALAND GP	692 HORDALAND GP	772 UNDIFFERENTIATED	718 UNDIFFERENTIATED	1253 ROGALAND GP						
1457 BALDER FM	990 SKADE FM	1094 HORDALAND GP	874 UNDIFFERENTIATED	873 BALDER FM	1041 BALDER FM	692 UNDIFFERENTIATED	899 HORDALAND GP	842 HORDALAND GP	1253 BALDER FM						
1500 SELE FM	1013 NO FORMAL NAME	1682 GRID FM	1495 ROGALAND GP	942 SELE FM	1080 SELE FM	1434 ROGALAND GP	2136 FRIGG FM	1014 SKADE FM	1366 SELE FM						
1567 LISTA FM	1373 GRID FM	1733 NO FORMAL NAME	1495 BALDER FM	966 LISTA FM	1108 LISTA FM	1434 BALDER FM	2156 ROGALAND GP	1028 UNDIFFERENTIATED	1386 LISTA FM						
1597 SHETLAND GP	1395 NO FORMAL NAME	2050 ROGALAND GP	1566 SELE FM	1001 VÅLE FM	1150 VÅLE FM	1456 SELE FM	2156 BALDER FM	1177 NO FORMAL NAME	1466 VÅLE FM						
1597 TOR FM	1910 ROGALAND GP	2050 BALDER FM	1572 LISTA FM	1030 SHETLAND GP	1163 SHETLAND GP	1476 LISTA FM	2205 SELE FM	1194 UNDIFFERENTIATED	1483 SHETLAND GP						
1707 HOD FM	1910 BALDER FM	2106 SELE FM	1853 VÅLE FM	1030 TOR FM	1163 TOR FM	1565 SHETLAND GP	2270 LISTA FM	1901 ROGALAND GP	1483 EKOFISK FM						
1908 CROMER KNOLL GP	1962 SELE FM	2142 LISTA FM	1857 SHETLAND GP	1271 HOD FM	1370 HOD FM	1565 KYRRE FM	2416 VÅLE FM	1901 BALDER FM	1494 TRYGGVASON FM						
2187 VIKING GP	2032 LISTA FM	2246 TY FM	1857 TOR FM	1380 CROMER KNOLL GP	1408 BLODØKS FM	1595 TRYGGVASON FM	2429 SHETLAND GP	1964 SELE FM	1527 BLODØKS FM						
2187 DRAUPNE FM	2137 VÅLE FM	2322 VÅLE FM	1883 TRYGGVASON FM	1380 RØDBY FM	1438 HIDRA FM	1614 BLODØKS FM	2429 HARDRÅDE FM	2009 LISTA FM	1540 SVARTE FM						
2244 VESTLAND GP	2154 TY FM	2350 SHETLAND GP		1425 SOLA FM	1444 CROMER KNOLL GP	1628 SVARTE FM	2544 KYRRE FM	2151 VÅLE FM	1599 CROMER KNOLL GP						
2425 NO GROUP	2164 SHETLAND GP	2350 HARDRÅDE FM		1505 ÅSGARD FM	1673 RØDBY FM	1673 CROMER KNOLL GP	2610 SVARTE FM	2156 SHETLAND GP	1599 RØDBY FM						
	2164 HARDRÅDE FM	2584 CROMER KNOLL GP		1875 BOKNFJORD GP	1706 ÅSGARD FM	1673 RØDBY FM	2622 CROMER KNOLL	2156 HARDRÅDE FM	1673 SOLA FM						
	2192 CROMER KNOLL GP	2584 RØDBY FM		1875 FLEKKEFJORD FM	2080 MIMME FM	1895 SOLA FM	2622 RØDBY FM	2242 CROMER KNOLL GP	1811 ÅSGARD FM						
	2192 SOLA FM	2623 SOLA FM		1980 SAUDA FM	2122 VIKING GP	1942 ÅSGARD FM	2693 SOLA FM	2242 ÅSGARD FM	1999 VIKING GP						
	2222 MIMME FM	2637 VIKING GP		2311 TAU FM	2122 DRAUPNE FM	2191 VIKING GP	2712 ÅSGARD FM	2249 BRENT GP	1999 DRAUPNE FM						
	2234 VIKING GP	2637 DRAUPNE FM		2339 EGERSUND FM	2217 HEATHER FM	2191 DRAUPNE FM	2795 VIKING GP	2249 NESS FM	2109 HEATHER FM						
	2234 DRAUPNE FM	2725 HEATHER FM		2388 VESTLAND GP	2265 VESTLAND GP	2313 HEATHER FM	2795 DRAUPNE FM	2265 UNDIFFERENTIATED	2123 SOGNEFJORD FM						
	2256 HEATHER FM	2753 VESTLAND GP		2388 SANDNES FM	2352 NO GROUP DEFINED	2317 SOGNEFJORD FM	2852 HEATHER FM	2276 DUNLIN GP	2367 FENSFJORD FM						
	2277 VESTLAND GP	2753 HUGIN FM		2410 BRYNE FM	2532 SKAGERRAK FM	2412 HEATHER FM	2903 BRENT GP	2276 DRAKE FM	2498 KROSSFJORD FM						
	2277 HUGIN FM	2820 SLEIPNER FM		2440 NO GROUP DEFINED	2532 SMITH BANK FM	2615 FENSFJORD FM	2903 TARBERT FM	2466 COOK FM							
	2290 SLEIPNER FM	2872 DUNLIN GP		2440 SMITH BANK FM	2665 ZECHSTEIN GP	2678 KROSSFJORD FM	2989 NESS FM	2489 AMUNDSEN FM							
	2297 DUNLIN GP	2872 DRAKE FM		2811 BASEMENT	2665 UNDIFFERENTIATED	2721 HEATHER FM	3133 DUNLIN GP	2616 STATFJORD GP							
	2297 DRAKE FM	3095 NO FORMAL NAME			3829 KUPFFERSCHIEFER FM	2758 BRENT GP	3133 DRAKE FM								
	2344 AMUNDSEN FM	3308 STATFJORD GP			3834 ROTLEGEND GP	2758 RANNOCH FM	3409 COOK FM								
	2437 STATFJORD GP	3665 NO GROUP DEFINED				2827 DUNLIN GP	3417 BURTON FM								
	2503 NO GROUP DEFINED					2827 DRAKE FM	3549 AMUNDSEN FM								
	2503 SKAGERRAK FM					2898 COOK FM	3596 STATFJORD GP								
	2651 SMITH BANK FM					2906 BURTON FM									
	2851 BASEMENT					2929 JOHANSEN FM									
						2998 AMUNDSEN FM									
						3008 STATFJORD GP									
						3008 NANSEN FM									
						3043 EIRIKSSON FM									
						3120 HEGRE FM									
						3120 LUNDE FM									

Tab. 3.2.2.1.2: Overview of main stratigraphic groups found in the wells, selected here and used for correlation of Jurassic strata, namely Top Viking group, Top of Sognefjord Formation. Data are copied and modified into tab from NPD fact depositary page (NPD fact-page). Coloring is there for better overview, outlining main groups. Nordland, Hordaland and Rogaland are in one frame.

3.2.2.2. Seismic reflection data

For this study the 2D seismic data survey was used, presented in a regional map of study area. The shows the survey used in this study for interpretation faults, correcting the horizons and interpretation of clinoform. Only some surveys were chosen for the evaluation of clinoforms. Consideration factor was to quality throughout the whole delta profile cover. The direction related to quality, as well. Some lines appear to be great in quality at crossing direction than the needed one. Whole list with resolution quality and example is in a tab. Tab. 3.2.2.1 and map of

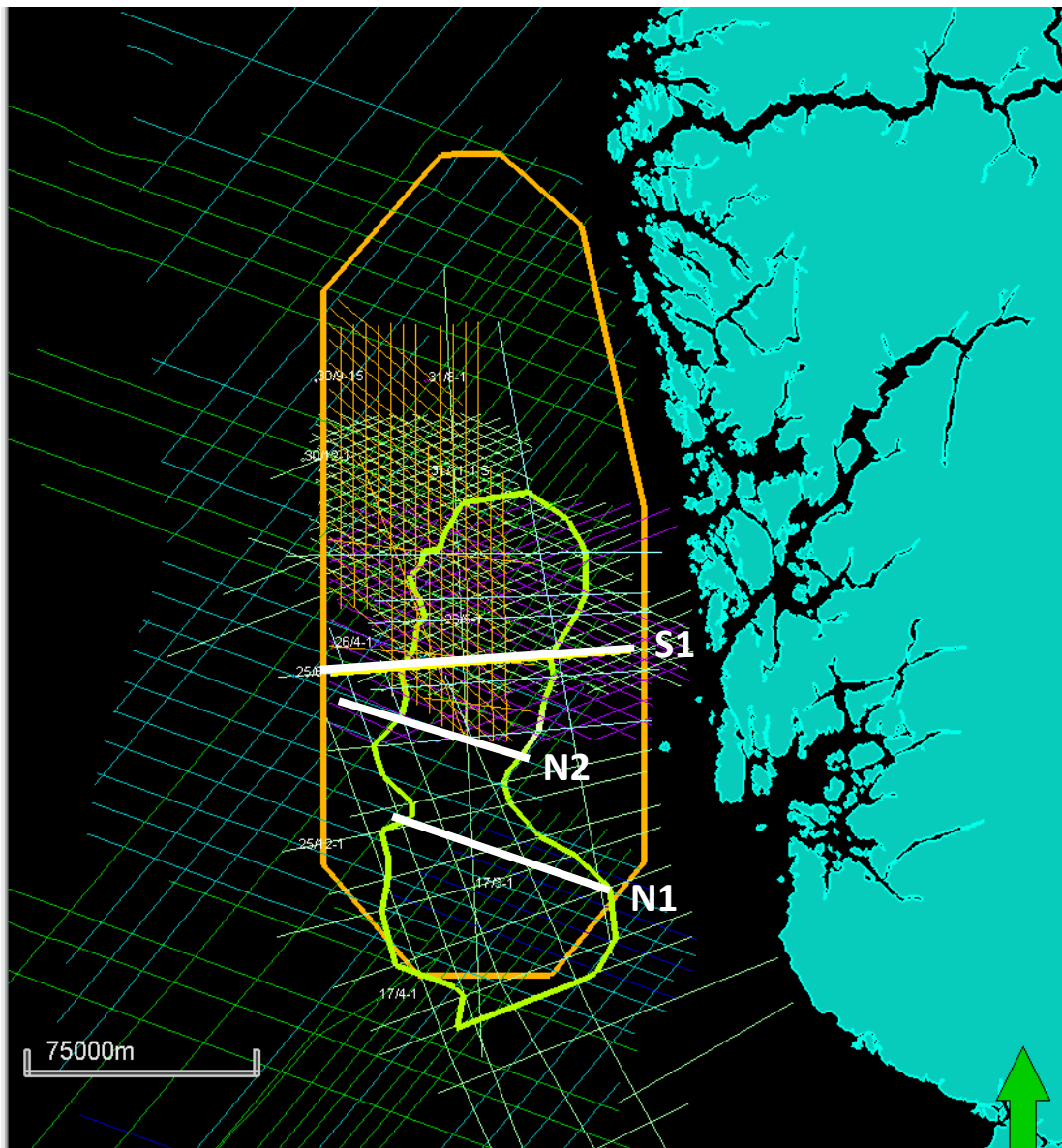
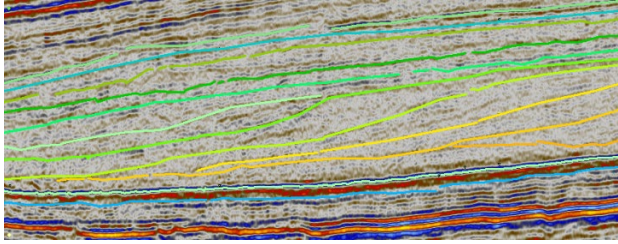
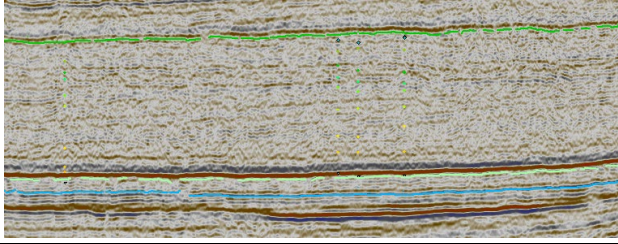
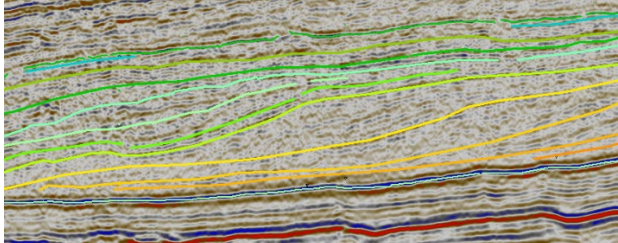
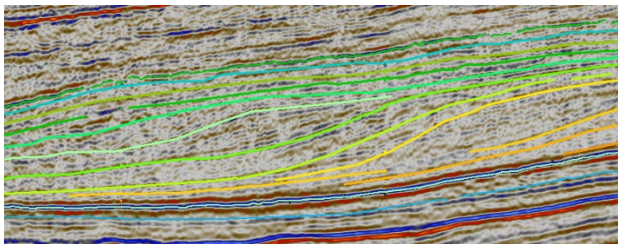
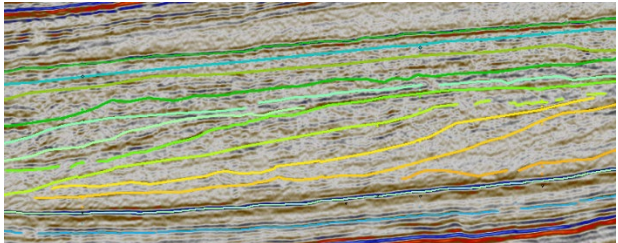
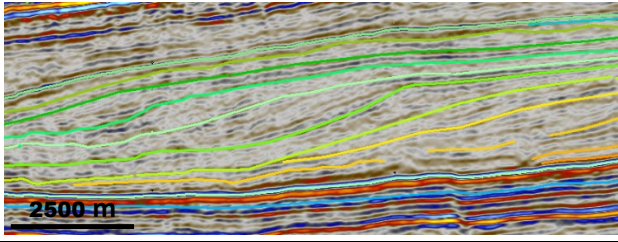


Fig.: 3.2.2.2.1: Map of study area, with norwegian land. Seismic surveys with a location of wells. The orange polygon outline the study area, and the Green one outline the traced interpreted clinoform. The line border on left hand sit with a toes of delta (downlaps) and on the rigth hend side is partly bordered with the maste fault zone (Øygarden Fault Complex). The with lines representing the 3 out of 21 seismic lines, S1, N2 and N1.

SURVEY	QUALITY OF REFLECTION		COMPANY	SURVEY YEAR
ST8201	Low		STATOIL	1982
GSB-85R97	Low		GECO	1985
SBGS-87	Low		NOPEC AS	1987
SBGS-RE-94	Medium		NOPEC AS	1987
HRTRE00	Low		GEOTEAM	2000
NSR-06 A	Good		TGS NOPEC GEOPHYSICAL COMPANY ASA	2006

Tab. 3.2.2.2.2: Listed seismic surveys used for construction of faults, correlation of horizons and interpretation of clinoforms. Stratigraphic boundary (Neon), Upper Jurassic tops - Viking Group (dark green) and Sognefjord Formation (blue). Tab includes Company producer and a year of drilling.

21 seismic lines used for interpretation of clinoform. There are 2 in-lines used to support further interpretation. Especially, at the northern part due to sufficient change in seismic facie of clinoform, the interpretation stopped there. Uncertainty which clinoform to follow, before termination the interpretation there the most probable clinoform to be followed was the younger ones.



Fig. 3.2.2.2.2: Overview of used seismic profiles for interpretation clinoforms (21 in total).

3.3. Methods

In this chapter, I outline a thorough methodology leading to measurement and calculation of key clinoform parameters (The elements under measurement include the dip of the topset, the angle of trajectory, and parameters of the rollover and toe advance).

Seismic data has been analyzed through different horizon interpretations. Some reflections are mapped as positive amplitudes (Trough) while others involve tracing negative amplitudes (Peaks). In the visualization in fig. 3.3.1.1, troughs are represented by rage yellow-red, peaks by light to dark blue, and thin grayish bands indicate the zero crossings.

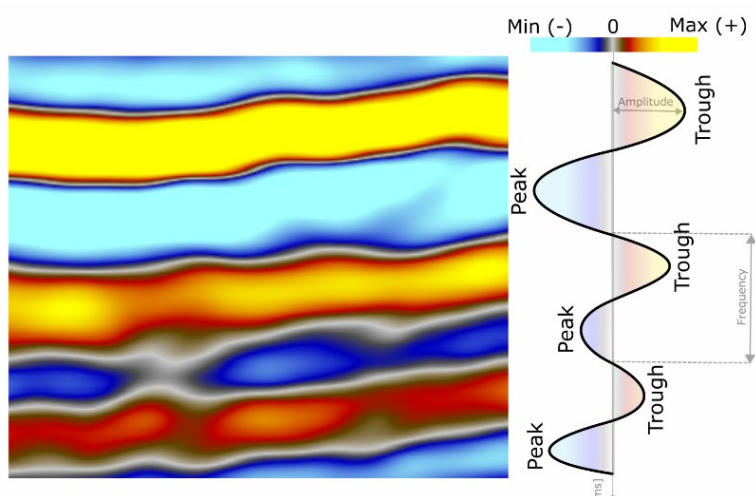


Figure 3.3.1.1: The illustration shows different amplitude with polarity and frequency, implication on seismic horizon (European type of polarity vs trough and peak is presented here).

- Identification and mapping of unconformities and correlated conformities, choosing proper amplitude polarity.
- Determination of termination style (e.g., onlap, toplap, downlap, offlap, etc.).
- Recognition of internal reflection pattern (e.g., parallel, wavy, divergent, etc.).
- Determination and designation of clinoforms, structural highs and lows.
- Categorization isochor map, thicknesses and surfaces maps

3.3.1. Viking Group and Sognefjord correlation

The main faults are interpreted with regional knowledge of fault present in Study area (Fazlikhani et al., 2020; Phillips et al., 2019) and seismic surveys evaluation, all sets used in this study are present in regional map and tab with detail description (Fig.: 3.2.2.2.1, tab. Tab. 3.2.2.2.2). The main stratigraphic group, including Viking Group, horizons were interpreted by Osmond et al. (2018, 2022). Some of the wells were used to clarify the horizon interpretation (Tab. 3.2.2.1.1, Tab. 3.2.2.1.2), especially for Top Viking Group and Sognefjord Formation. The strong reflection, interpreted as sequence boundary.

Correct position of horizons evaluations of delta in study area (Stord Basin) was checked using selected wells, 10 in total, information based on previous study (Fazlikhani et al., 2020; Phillips et al., 2019) and already defined strata (NPD fact-page). The tops of Viking Group and Sognefjord Formation were partly re-assisted and re-interpreted to be more accurate, in places where the interpretation was done by software calculation. The horizons example in a seismic line can be seen at fig.

Sognefjord Group of Åsta graben at the southern part of northern North Sea is an equivalent to Viking group in other documented wells. Sognefjord is defined on the strata Sauda Formation in a project. The same for Brent Gr. (Horda platform, North Graben), with Vestland Gr, which is present at Stord basin, Egersund, Åsta graben and Utsira, Sele High (NPD fact-page). The interpretation was obtained from 2D seismic lines of seismic surveys listed in tab. 3.2.2.2.2. From a seismic profile either the horizon is pinching out or continues, followed the peak (positive) or trough (negative), in a tab. 3.3.1.2 are listed the horizons with the seismic amplitude. The sequence boundary was recognized within the Viking Group as the horizon the clinoform downlap onto (fig. 3.3.1.2).

Knowledge of main stratigraphic units was studied through previous research and information provided on official web of NPD depository info, to understand the basin in a regional scale due to limited well-defined information within the studied area. The seismic boundary for Sognefjord and Viking Group of Stord Basin were correlated with few nearby selected wells (17/3-1, 17/4-1, 25/6-1 and 31/11-1 s) nearby.

INTERPRETED HORIZON	SEISMIC AMPLITUDE
TOP OF SHETLAND GROUP	TROUGH - POSITIVE
TOP OF CROMER KNOLL GROUP	TROUGH - POSITIVE
TOP OF VIKING GROUP	PEAK - NEGATIVE
SEQUENCE BOUNDARY	PEAK - NEGATIVE
TOP OF SOGNEFJORD FORMATION	TROUGH - POSITIVE
TOP OF STATFJORD	TROUGH - POSITIVE

Tab.: 3.3.1.2: Listed horizons with their followed seismic amplitude (European convention).

From seismic profile the bottom of Draupne Formation is marked by sharp contact with high impedance showing in negative amplitude on crosslines and positive amplitude in in-lines. This contact gradual thinned and disappeared westward as it is onlapping pre-Upper Jurassic rocks, Sognefjord Formation which was traced by positive through based on well, 26/4-1(2), 25/12-1, 26-/6-1. And 17/3-1 as Sauda Formation due to not present of Sognefjord formation.

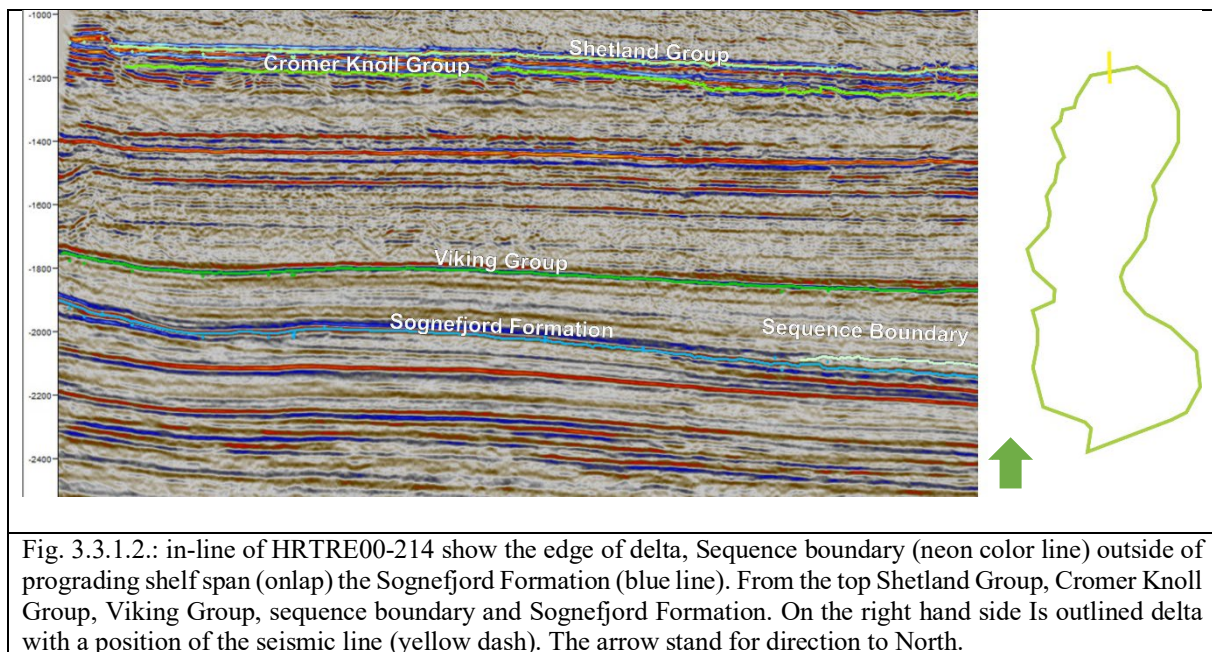


Fig. 3.3.1.2.: in-line of HRTRE00-214 show the edge of delta, Sequence boundary (neon color line) outside of prograding shelf span (onlap) the Sognefjord Formation (blue line). From the top Shetland Group, Cromer Knoll Group, Viking Group, sequence boundary and Sognefjord Formation. On the right hand side Is outlined delta with a position of the seismic line (yellow dash). The arrow stand for direction to North.

3.3.2. Clinoform analysing and measurement

The naming or numbering of key features and measurement parameters are in fig 3.3.2.1 in red color. To obtain results require certain steps, were undergone. Workflow of process can be break down into points.

Tracing clinoforms: This process involves identifying and tracking the consistent seismic reflections that symbolize the surfaces of clinoforms. The method includes tracing patterns of downlap, onlap, and truncation (for the theory behind this, specifically I refer to chapter 3.1.3

Sedimentary principles). The clinoforms are generally found along strong surfaces, which are typically characterized by positive (red) reflectors.

Naming or numbering the clinoforms: For seismic analysis, each clinoform was uniquely identified. The 21 cross-sections were interpreted and 2 in-line (fig. Fig. 3.2.2.2) as a supporting cross profile for evaluation the clinoform at the northern and partly middle section of Whole delta form. 14 Clinoforms in total were identified: K1, K2, K3, K4, K5, K6, K6/K7, K7, K8, K8/K9, K9, K10, K11, K12. K6/K7 and K8/K9 has in between label. Those clinoform were traced all the way to Øygarden Fault Complex hanging wall displacement (fig. 4.2.5) and partly were onlapping on younger clinoform topset. The further navigation is based on label and chosen color for every each identified clinoform.

Locating the Upper and Lower rollover and inflection points: The rollover is where the topset transitions into the foreset, while the inflection point is where this curvature is the greatest (fig. 3.3.2.1, fig. 3.1.3.1.4).

Outlining the rollover and inflection points between clinoforms: By tracing rollover points across the seismic lines (in a Petrel E&P software was use the fault interpreting tool for making the visual trajectory between rollover points, for both Upper and Lower one) following the rollover advance and creating a 2D map view (Figure 4.3.1) of the clinoform geometry.

Measuring the dip of the topset: This gives the initial slope of the topset before deposition. will use this value to convert other values back to their original position. The topset would initially dip between 0-0.4 degrees. 0.2 can be good value to use. For ex. when the angle dips at 1 degree needs to be subtracted by 0.8 from 1. Another measurement is from the dip of the slope (foreset), it to the trajectory angle (which will have decreased during subsidence.)

Measuring and recording the Real od foreset: first was measured ETT and Slope Relief to calculate tangent then Shelf-edge advance needed to be measured to calculate tangent of the angle and get Dip of topset. Then the values can be subtracted from Ideal dip of foreset by Dip of foreset corrected with subtraction 0.2. Now we got the Real dip of foreset.

Measuring and recording the Trajectory angle: first Rollover advance was measured on each chloroform at celeste lines (S1, N2, N1) with careful considering of coordination system, the values in height and length can be in negative value. In petrel the values shoe positive but the lateral length is actually in negative quadrant (that is important form deviate which values are backstepping in trajectory between Upper rollover points). The further calculating process is the same as at the point above for Real dip foreset. The results are Trajectory angle. Needs to be corrected by subtraction of 0.2 and adding the Dip of topset. Results is the Trajectory angle in a paleo setting where deposited.

Measuring other geometric parameters: These include height, length, maximum vertical thickness, total advance of the rollover, thickness of the topset, the advance of the toe, and the dip of the slope.

All recorded measurements are in a tabs. Tab. 4.4.1 – 3 in a Results sub-chapter 4.4.

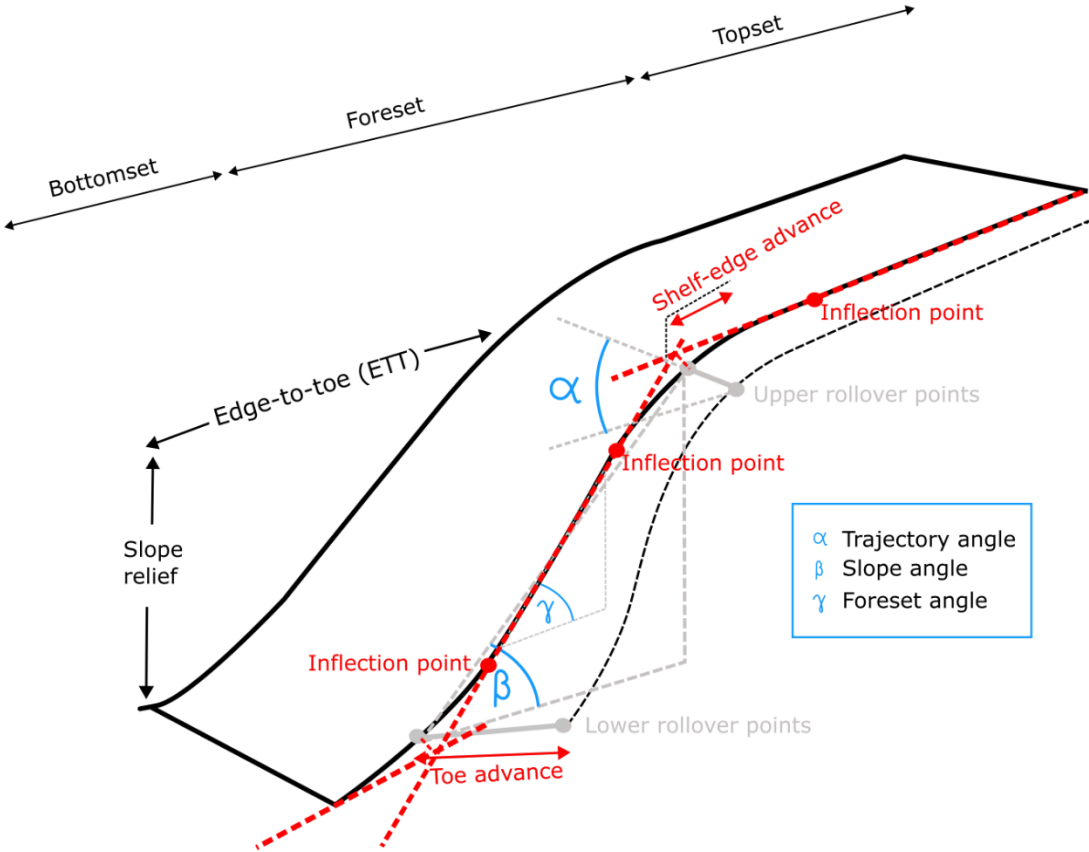


Fig. 3.3.2.1: Simplified image of clinoform with important parameters. Angles and distances, used later for calculation (modified from Anell & Midtkandal, 2015; Patruno et al, 2015a).

4. Results

This section describes and examines the geological architecture and crucial parameters of a prograding deltaic sequence. The focus is on the Draupne Formation's clinoform package in the Stord Basin, and their depositional environment and history. Detailed interpretations of clinoforms are provided through three carefully selected seismic profiles, chosen for their resolution quality and minimal tectonic influence. The complexity of interpretation is heightened in the delta's northern part due to the chaotic seismic facies of the thin clinoform bodies, resulting in some uncertainty in interpretation. This part also shows fewer clinoforms than the southern end. In-depth analysis of major fault systems and clinoform geometry is included, noting the cyclical development and deposition history. Shelf-edge clinoform trajectories are identified to decipher sea-level and sedimentary environment fluctuations. Calculated shelf-edge parameters offer valuable insights into sediment supply dynamics, basin subsidence rates, the potential redistribution of sediments, acknowledging the influence of compaction, which varies across different segments of the delta profile.

4.1. Architecture of a prograding deltaic sequence

The upper boundary of the Viking Group, which contains the Draupne Formation, is correlated with the Base Cretaceous Unconformity (BCU). This regional unconformity pervades the entire stratigraphic sequence and is attributed to erosion that altered the last interpreted clinoform K12 the foreset and toe of the delta. While these erosional effects were not factored into the trajectory calculations, they were accounted for in the stratigraphic interpretation that established the upper limit of clinoform K11.

The lower boundary of the Viking Group correlates with the Upper Jurassic Sognefjord Formation. However, the clinoform package itself is underlain by a younger Jurassic unit, which is interpreted as a sequence boundary (4.2.3-5). This boundary is characterized by a sharp contact that can be traced until it eventually onlaps or pinches out. This pinch-out occurs at the distal extent of the deltaic system.

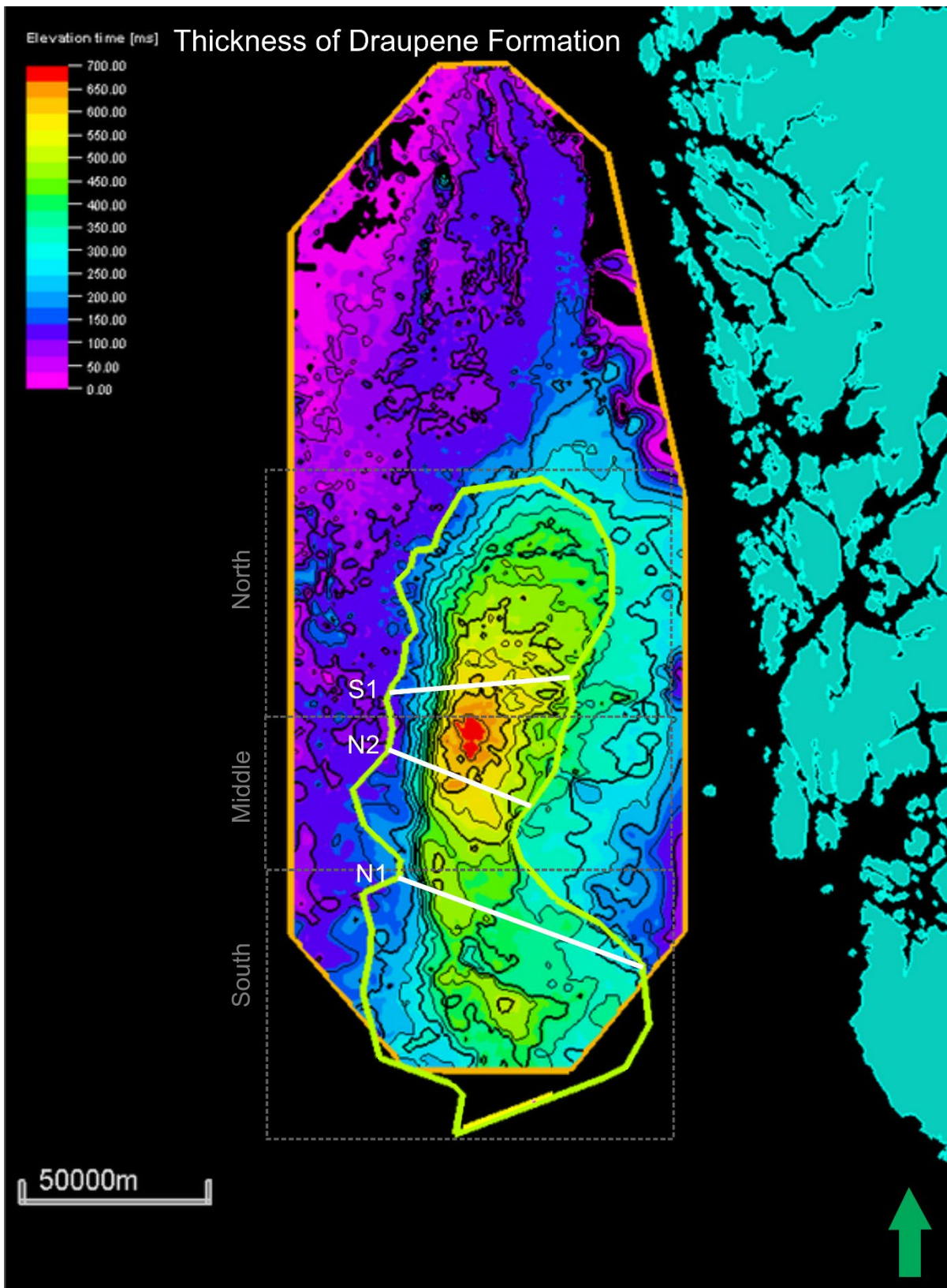


Figure 4.1.1: Thickness map of Draupne Formation (Top Viking Group-top of Sognefjord). The light green outlining the interpretation area of delta. The orange outline study is of Stord Basin together with northern Horda Platform. The map of delta is divided into sectors (South, Middle and North). White lines represent the seismic profile (S1, N2, N1), picked for further description of main geological features.

The thickness map of the Draupne Formation, presented in Fig. 4.1.1, shows an elongated shelf-edge delta lobe. This feature extends roughly 150 km in the north-south direction and averages

approximately 50 km in width. Within this deltaic system, the Draupne Formation reaches its maximum thickness of about 700 ms, which occurs predominantly in the distal central part (middle sector) of the delta.

In Fig. 4.1.1, the green line delineates the seismic trace of the delta's edge. As the observer approaches the toe of the clinoform set, the sedimentary succession visibly thins out, culminating in an almost flat profile over a horizontal distance of around 10,000 meters. The Orange frame outlines the study together with the northern Horda platform.

Structure map

The Top Draupne (Top Viking Group) is presented here to describe key structural features (fig. 4.1.2) and surface geometry. The map shows the major fault systems that demarcate the Stord basin (Øygarden and Utsira East) with incline orientation. Other major intra-basinal faults are also shown (F1-F8) with incline orientation. These faults terminate at depth, beneath the Viking Group (formed during the Permo-Triassic rift stage). The map visualizes also the northern Horda Platform, with major N-S trending faults bordering the Troll oil and gas field. The overall geometry of the surface is dipping smoothly westward into the basin from approx. 250ms to 2500ms.

Seismic section profile S1, N2 and N1

Figures 4.1.3-5 show interpreted and uninterpreted seismic cross sections for lines S1, N2 and N1, respectively. The basin-bounding faults, Øygarden and Utsira East, frame the basin. From the Triassic era, significant faults (F1-5) have been identified along with numerous other normal faults within the upper Triassic Statfjord Group. The interpretation divides the key stratigraphic units, highlighting the Draupne Formation, and the Sognefjord Formation. The clinoform set downlaps onto a strong reflection, possibly Heather Formation, which is interpreted as a sequence boundary (maximum flooding surface).

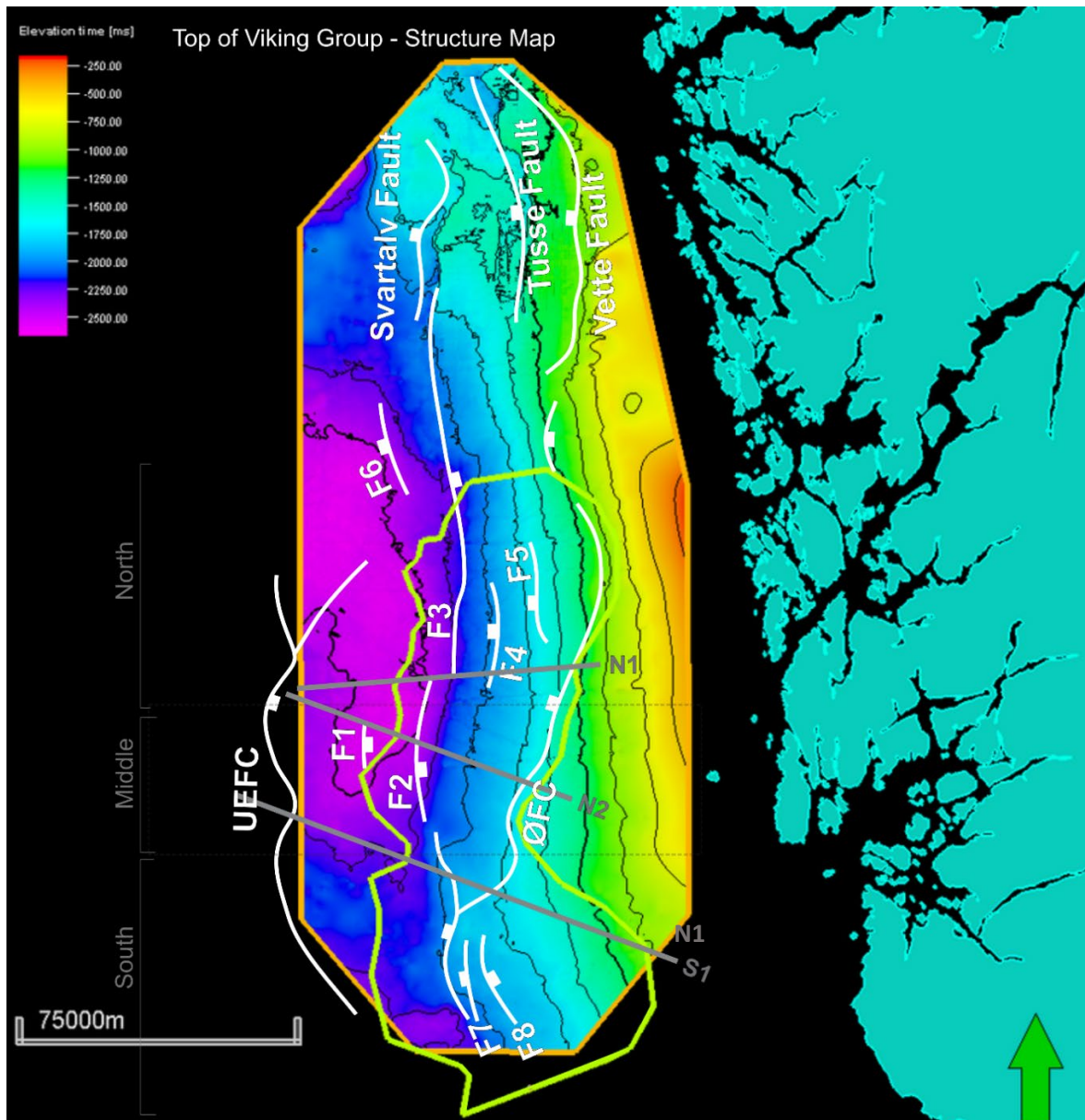
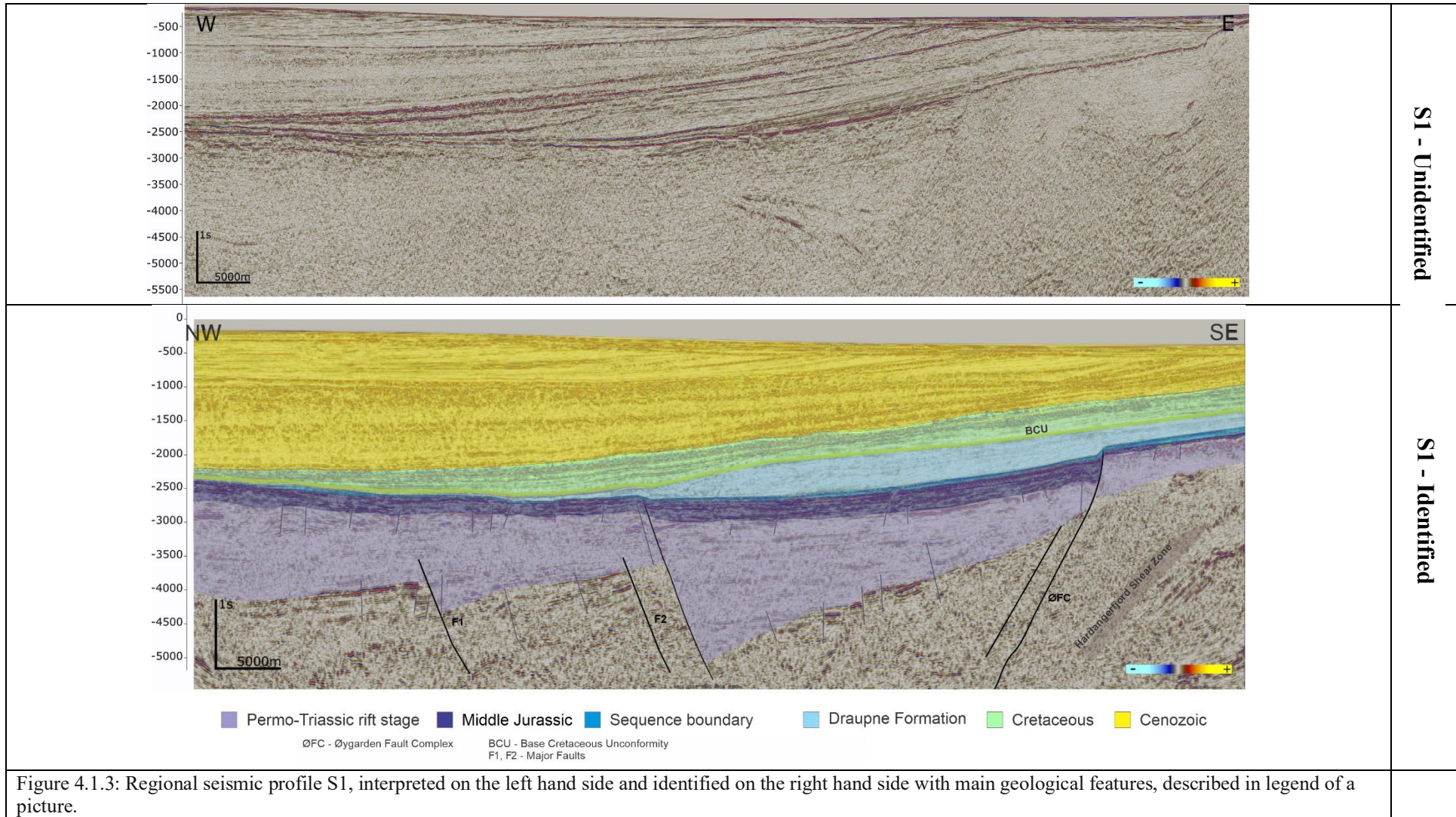
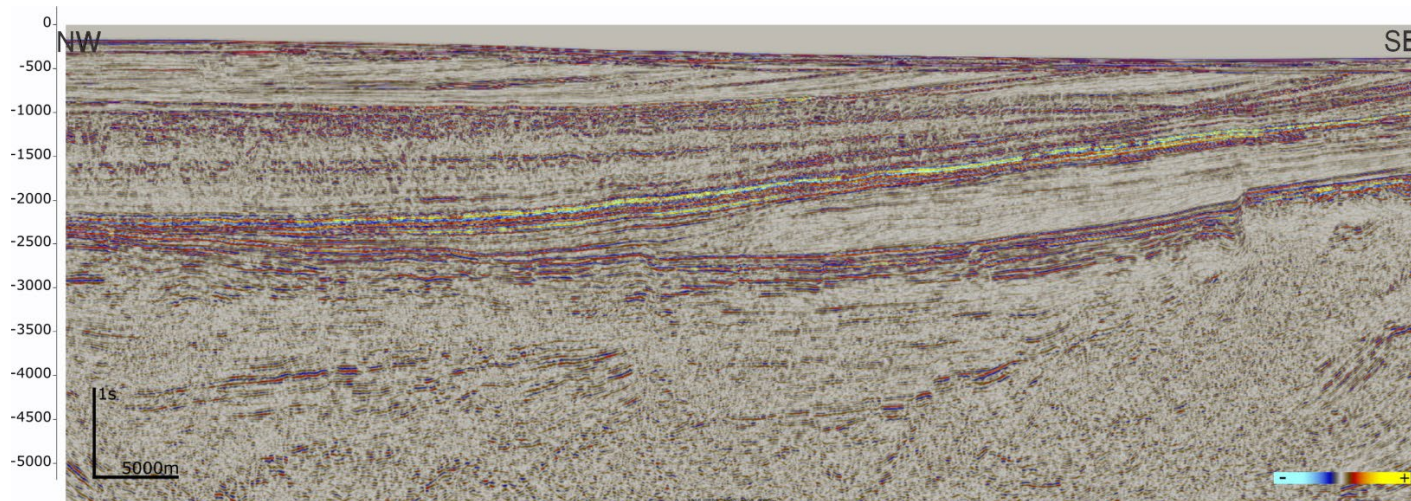
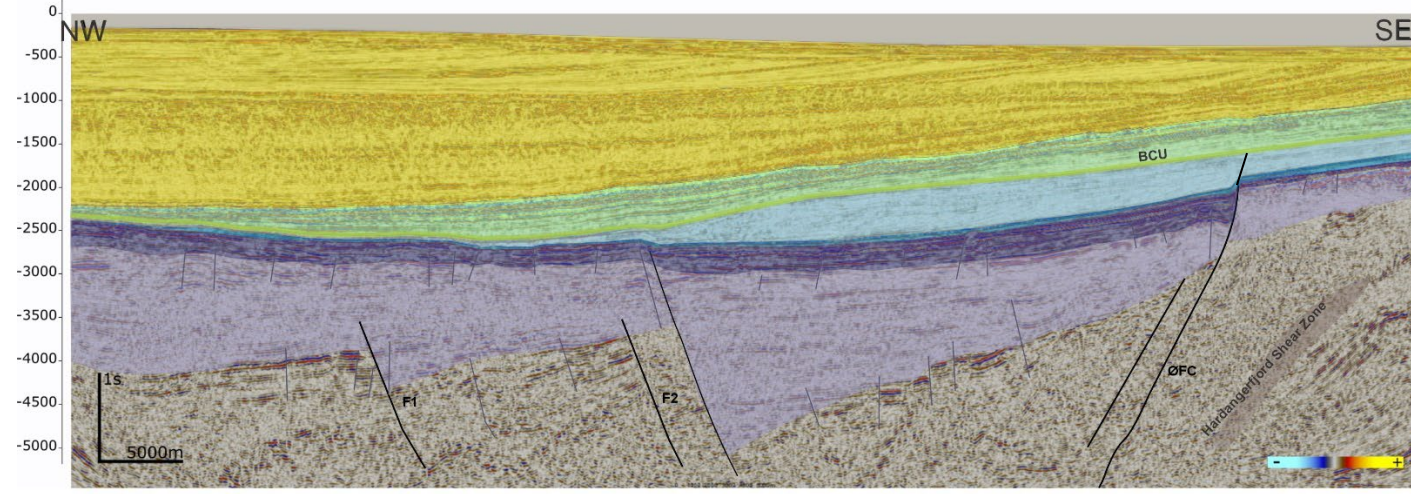


Figure 4.1.2: Surface-structure map top of Draupne. Main fault system, Øgarden Fault Complex (right hand side) – ØGC, Utsira East (left hand side) -UEFC, main fault zones at northern Horda platform, Svartalv, Tusse, Vette; and minor faults (F1-F8) within the Stord Basin. The gray lines represent the seismic section used for further description in this study S1, N2, N1.





N2 - Unidentified



N2 - Identified

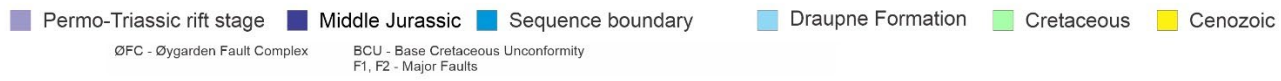
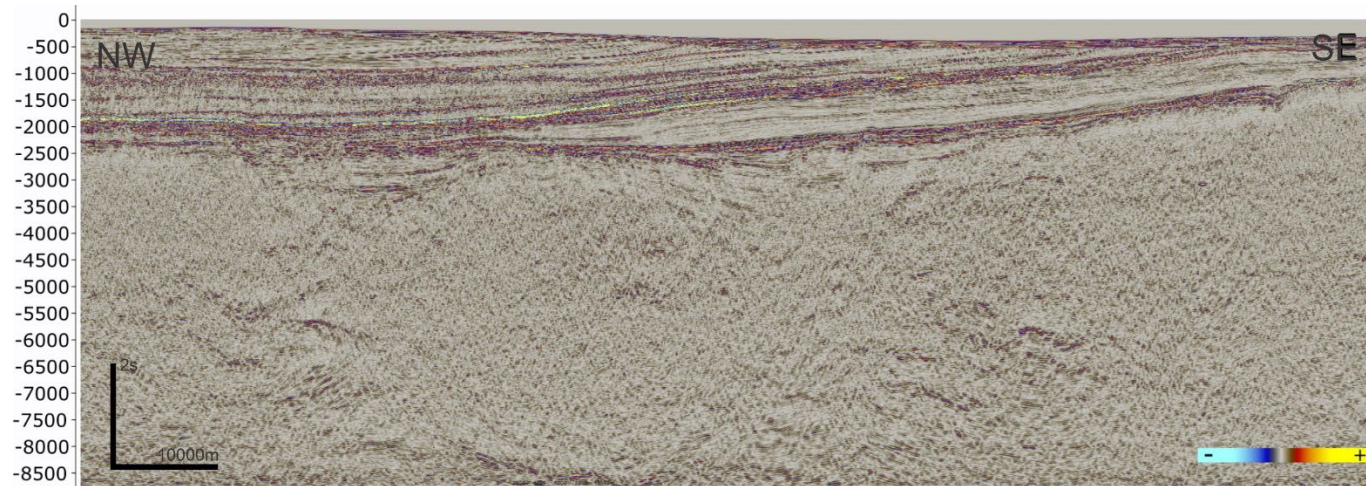
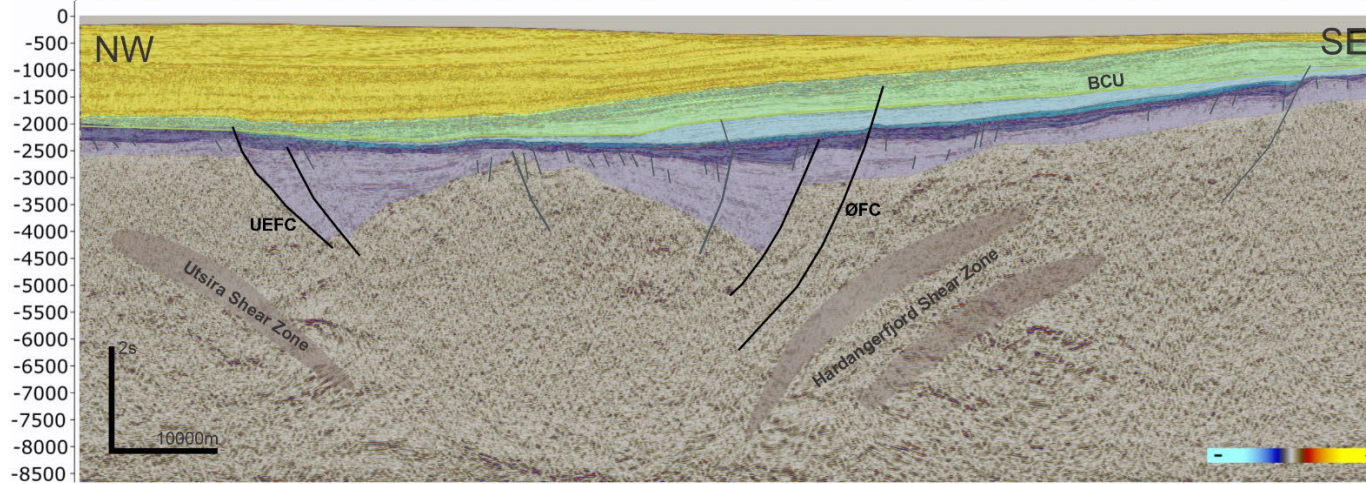


Figure 4.1.4: Regional seismic profile S1, interpreted on the left hand side and identified on the right hand side with main geological features, described in legend of a picture.



N - Unidentified



N1 - Identified

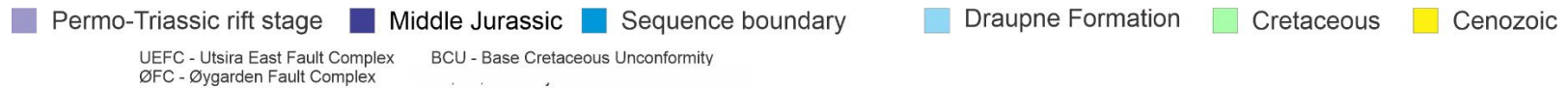


Figure 4.1.5: Regional seismic profile N1, interpreted on the left hand side and identified on the right hand side with main geological features, described in legend of a picture.

4.2. Clinoform geometry

From all three cross-sections S1, N2 and N1, detailed pictures of the prograding sequence have been provided here in fig. 4.2.5, 4.2.6, and 4.2.7, respectively, with 14 clinoforms in total interpreted and listed in methods (tab. 3.3.2.x). The interpreted version with seismic profile in a background is presented with the separated clinoform interpretation below. The Øygarden Fault Complex (ØFC, solid line on figures) serves here as a boundary of eastern termination of topsets of all named clinoforms, where the whole set is cut through. The exception to this is the southern part of delta, where the first 4 clinoforms (K1-K4) start to propagate before the fault zone on its Foot Wall (Figure 4.2.7). The rest of the presented interpreted clinoforms are downlapping on the Hanging Wall on a horizon with strong seismic impedance reflection, here referred as a sequence boundary into a long and flat bottomset. The rollover trajectory of the present clinoform package is shown in bold. The transparent line shows the corrected trajectory, accounting for post-depositional tilting of the sedimentary sequence. The correction is based on an average of all calculated values of every particular seismic line (S1, N2 and N1) of Dip topset angle, the values are seen in a tabs. 4.4.1 – 3.

Detail profile S1 (fig. 4.2.5)

The figure gives an overview of 14 interpreted clinoforms, with colored labeling. The deeper fault interpretation can be seen on a structure map of Top Viking Group (fig. 4.1.2). The rollover trend shows a progradation with low topset height, except K10 and K11. K12 is showing a prograding basin-ward, but that is due to missing part of clinoform foreset due to BCU. The first third of the succession appears to have longer and flat foreset and bottomset (from K1 to K4). The second succession grows in foreset thickness and the last third aggregates at the topset part. Then ascending trend with shorter, longer and again shorter trajectory length belongs to clinoform K1 -K5. From K8 the clinoform starts to descend again until K9. The whole set was divided into groups according to their geometry and continuous or chaotic reflectance (seismic facie) using Anell & Midtkandal (2015) classification. No linear class was detected here. Most Gaussian shapes are observed both sigmoidal both symmetrical and asymmetrical. One type of exponential was detected, tangential oblique. Asymmetric top heavy come under both types gaussian and exponential.

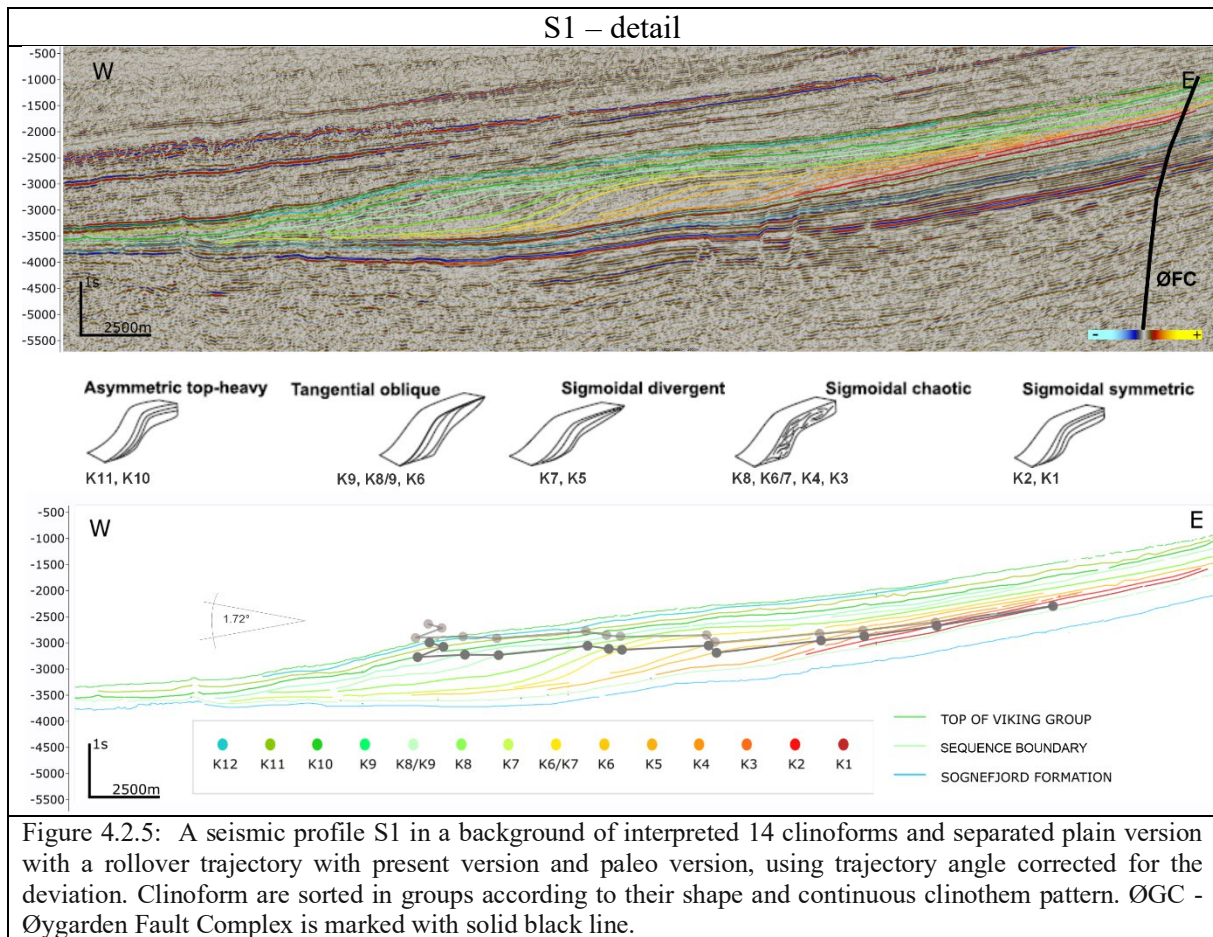


Figure 4.2.5: A seismic profile S1 in a background of interpreted 14 clinoforms and separated plain version with a rollover trajectory with present version and paleo version, using trajectory angle corrected for the deviation. Clinoform are sorted in groups according to their shape and continuous clinotem pattern. ØGC - Øygarden Fault Complex is marked with solid black line.

Detail profile N2 (fig. 4.2.6)

The same arrangement applies on the second figure of seismic profile, with the interpreted clinoforms, present trajectory, and corrected trajectory. A similar cyclicity can be observed here; a longer trajectory from K1 to K2, followed by a shorter trajectory from K2 to K3. Shorter (K4), shorter (K5), longer (K6), shorter (K7) and shorter (K8). Ascending trend seems to be present from clinoform K8. The ending members (K10, K11) show a backstepping trajectory. The clinoform set was sorted according to Anell & Midkandal (2015) classification with same picked clinoform shape type compared to section S1. There are fewer sigmoidal symmetrical clinoforms in this section compared to the northern and southern region of delta, only 2 of the clinoforms (K6/7 and K5) fall into this category. The majority of clinoforms show a sigmoidal divergent type compared to other two seismic profiles (K9, K7, K4, K2, K1).

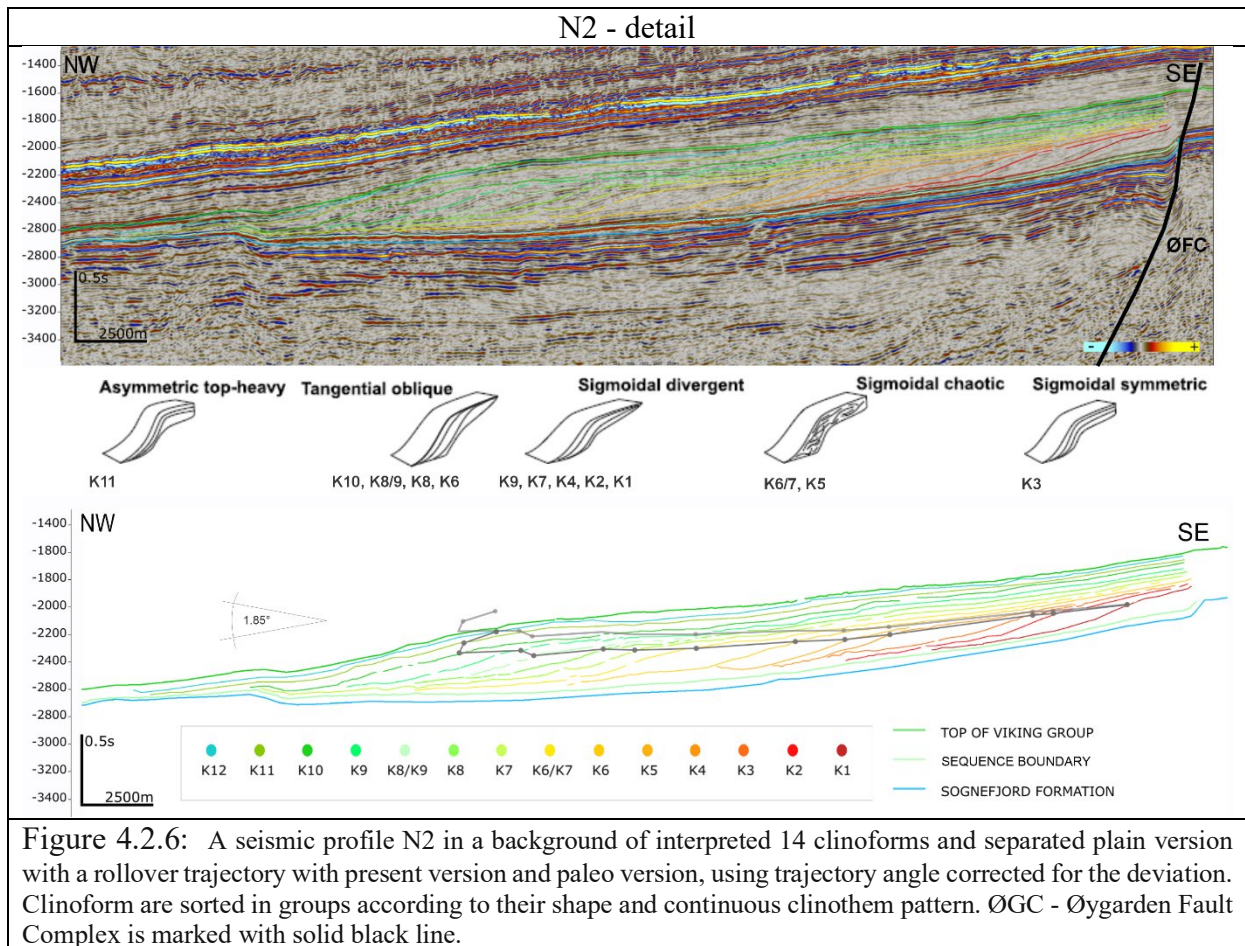


Figure 4.2.6: A seismic profile N2 in a background of interpreted 14 clinofolds and separated plain version with a rollover trajectory with present version and paleo version, using trajectory angle corrected for the deviation. Clinofolds are sorted in groups according to their shape and continuous clinofold pattern. ØGC - Øygarden Fault Complex is marked with solid black line.

Detail profile N1 (fig. 4.2.7)

On the southern seismic section, there is a minor fault at the distal part of the prograding sequence. The displacement caused by fault activity is also shown on the plain interpretation (without the seismic background). The trajectory shows similar development to sections S1 and N1; flat and slightly descending basinward over the first seven rollover points. At the K7 clinofold the sediment mass builds up and to the front. From K7 it is descending then ascending again in next clinofold, and the pattern repeats until the back stepping of K11. K12 shows prograding, however it is the last clinofold in contact with BCU. Therefore, the calculation on that clinofold performed at the tabs 4.4.1-3 are not included in graph projection in discussion part chapter 5.

The two most common types of clinofold shapes in this profile go within tangential oblique (K10, K8/9, K8 and K6) and sigmoidal symmetrical (K7, K6/7, K5, K3). Thicker Sigmoidal divergent clinofolds are observed in K9 and K4. Here at this profile only one complex type was classified (K1).

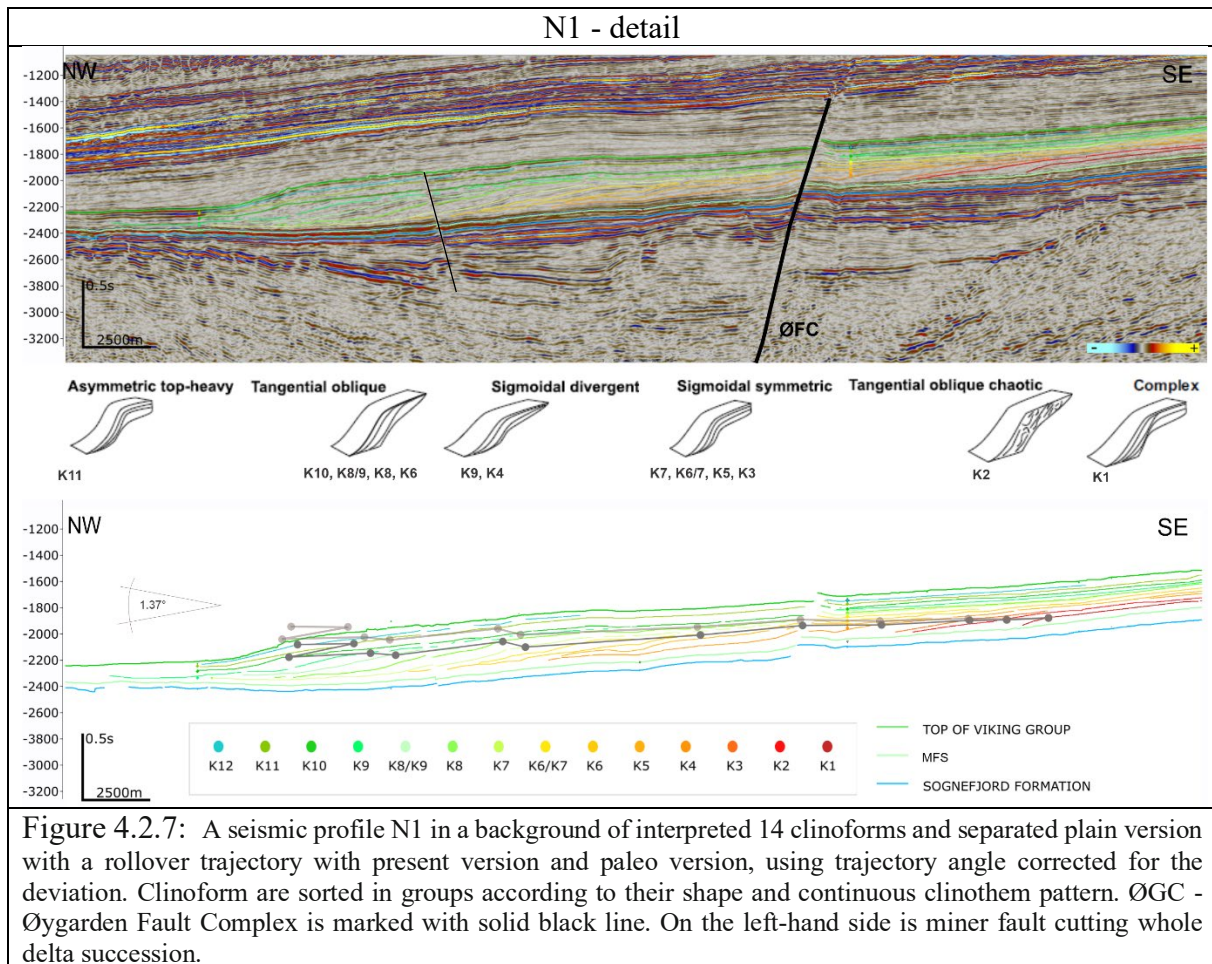


Figure 4.2.7: A seismic profile N1 in a background of interpreted 14 clinoforms and separated plain version with a rollover trajectory with present version and paleo version, using trajectory angle corrected for the deviation. Clinoform are sorted in groups according to their shape and continuous clinothem pattern. ØGC - Øygarden Fault Complex is marked with solid black line. On the left-hand side is minor fault cutting whole delta succession.

Overall asymmetrical tom heavy – K11, and tangential oblique - K8/9, K6 and sigmoidal symmetrical - K6/7 seem to have same pattern in deposition character across whole delta built. While tangential oblique - K10, K8, sigmoidal divergent - K9 and K4, and sigmoidal symmetrical – K5 are following same pattern (N1, N2) for south and middle part of widespread delta. Sigmoidal symmetrical - K3 and sigmoidal chaotic - K2 at north and south appear to be similar. The only complex – K1 shape falls on southern part of delta.

4.3. Trajectory of Shelf-edge scale clinoform

The clinoform trajectories of delta profile

The recognition of shelf-edge trajectories is crucial for comprehending the intricate geometry and depositional history of clinoforms, as it sheds light on sea level fluctuations and depositional environmental systems. Accordingly, I have depicted a regional scale map of the sedimentary delta in Fig. 4.3.1. The initial 11 clinoforms (K1-K10) within the clinoform succession display a prograding trend, while the final three exhibit a backstepping trend, as corroborated by the rollover trajectory angle calculations presented in Table 4.3.1-3. However,

clinoform K12 should be approached with caution as it resides near a sequence boundary affected by the Base Cretaceous Unconformity (BCU). In the southern region, determining the rollover points proved challenging due to tectonic influences. Meanwhile, in the northern region, tracing was not included in the image as the layer readings were visually unmanageable. The existence of the majority of clinoforms remains uncertain. Moreover, seismic facies changes have influenced the pattern of the delta's middle and southern sections.

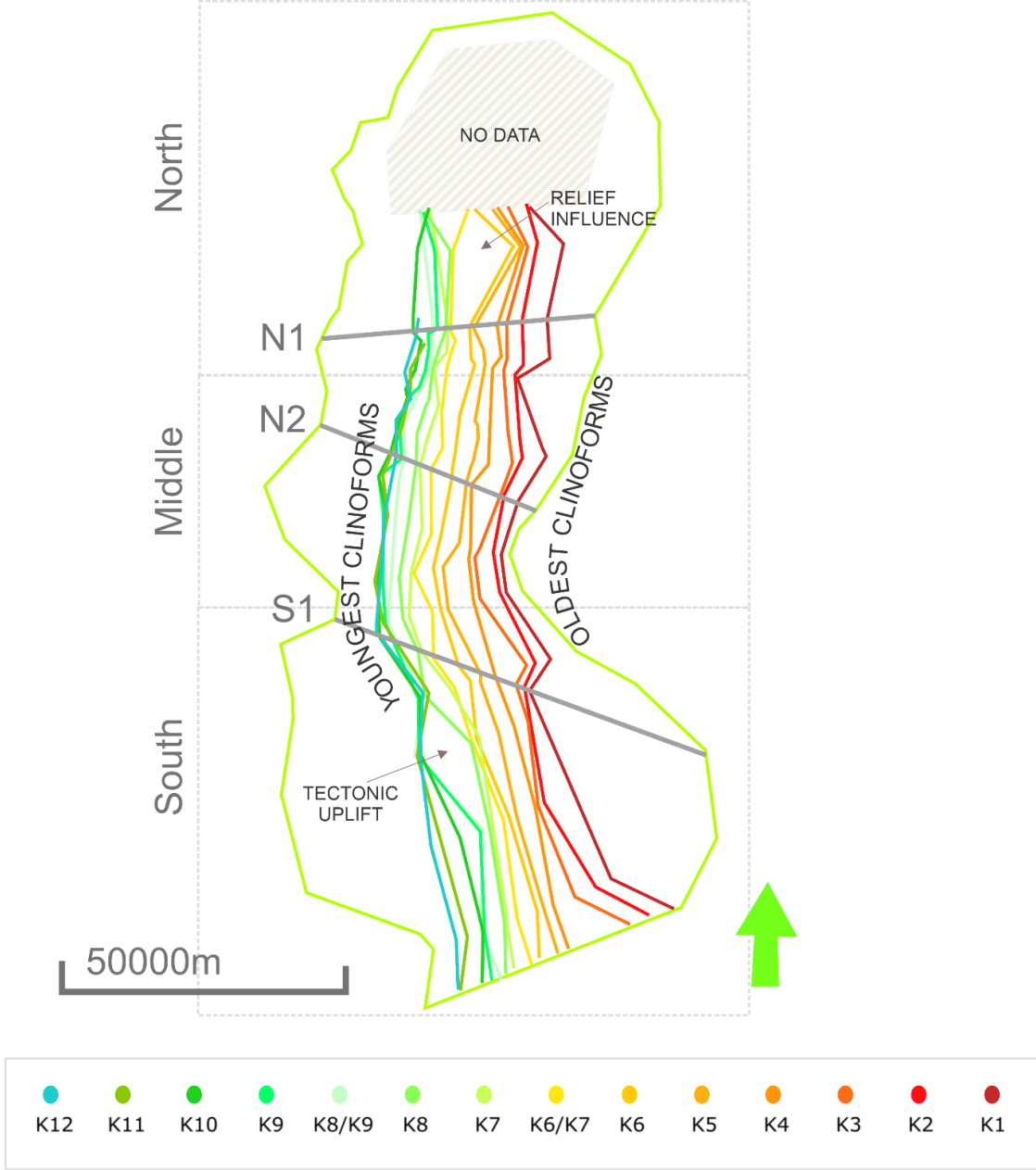


Figure 4.3.1: Regional map of shelf-edge trajectories with the interpreted seismic lines and legend for every each interpreted clinoform (K1-K12) in legend. The northern part of shelf-edge scale clinoform are not presented due to chaotic and packed topsets for tracking in seismic survey. The map breaks up the profile into South, Middle and North sectors. The tectonic and relief influence on prograding of delta can be seen on seismic facie example in appendix.

Trajectory variations across profiles and role of tectonic influence striking feature that can be inferred from the clinoform trajectory analysis is the cyclical nature of their development, particularly visible in profile N1 (Figure 4.2.6). This cyclical behavior is visible in a Middle sector of delta profile. From the oldest, shorter distances between clinoform are followed by longer distances till K7. The progradation rate gets balanced before back-stepping of clinoform K10 and K11. At the southern part of delta profile, the rate of prograding is less significant, but is influenced by tectonic uplift (refer to appendix). At the northern sector some specific difficulties for a normal prograding occur. Relief is a factor here, wherever the tectonic alteration of the relief can be taken into consideration (refer to appendix).

Influence of Base Cretaceous Unconformity (BCU)...The impact of the BCU is especially visible in the interpretation of clinoform K12. The missing part of its foreset due to BCU complicates its analysis. The BCU is a geological marker representing a significant erosional event or hiatus. In the map it was drawn to frame the delta set and to visualize its influence on the depositional environment of the sedimentary delta the erosion on a structure (fig. 4.2. 5-7).

Cliniform Body Thickness

The thickness maps of individual clinoform bodies present a significant aspect of the study, providing a visual interpretation of the lateral and vertical distribution of sediments within the deltaic system. These maps, along with individual seismic profiles, can further illuminate the sedimentation patterns and processes responsible for the evolution of the clinoform structures. On the figure 4.3.2 are presented selected clinoform bodies: K9-K8, K6-K5, K5-K4 and K4-K3. On the southern and northern sector is visible the compaction influence (refer to appendix), the mass at those locations rich less in thickness compared to the central part. The Amount in height of thickness decreases from youngest to oldest. From 200ms for K9-K8, 110 for K6-K5, 100ms for K5-K4 and lastly 90ms for K4-K3. At the very southern part the sediment supply is redistributed almost equally, compared to the rest of delta profile. According to previous analysis the clinoform K9 and K4 appear to have sigmoidal divergent shape, meaning biggest sediment mass at the foreset, while sigmoidal symmetric, K5, the redistribution is thinner over across a delta. Bothe for south and central part of profile. At the north the K9 and K5 seem to be tangential oblique and sigmoidal symmetrical, respectively. K6 is tangential oblique throughout whole profile, from south to north. K4 is at the northern part sigmoidal symmetrical and at the rest of profile sigmoidal divergent (higher in thickness appearance in a map).

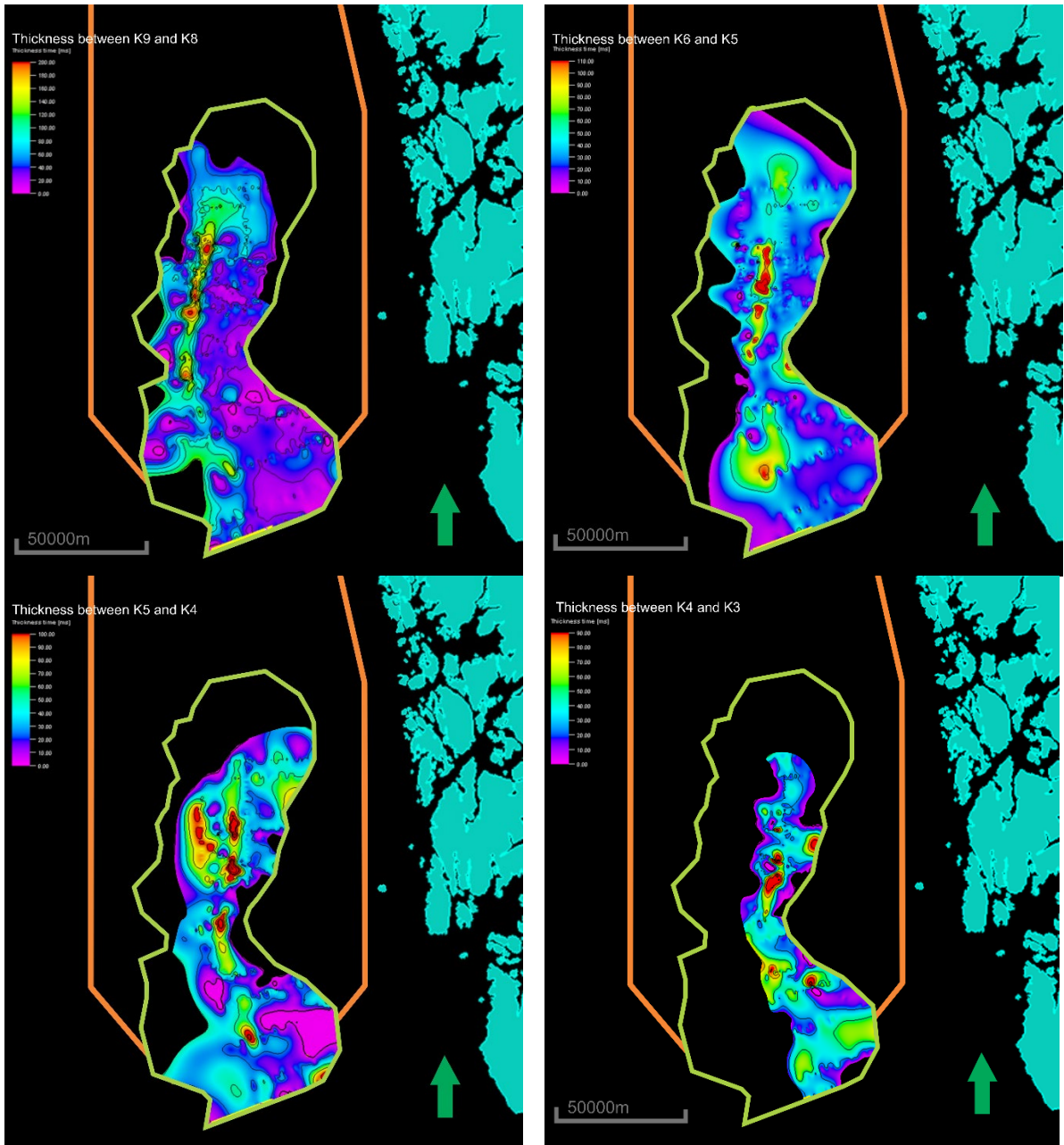


Fig. 4.3.2: The thickness seismic attribute map shows the redistribution and thickness of selected clinoform bodies from the top: K9-K8, K6-K5, K5-K4, K4-K3

4.4. Calculation of Shelf-edge parameters

For understanding the detailed geometry of clinoforms and their depositional history the recognition of shelf-edge trajectories, real angle of foreset and rollover trajectory angle as critical parameters in the interpretation of ancient depositional systems. Shelf-edge parameters provide insights into past sea-level changes, sediment supply dynamics, basin subsidence rates, and climatic variations. This section focuses on the calculation of shelf-edge parameters in order to interpret the depositional environments and history of the clinoforms within the Draupne Formation.

Below are three tabs. (Tab. 4.4.1-3), were constructed for S1, N2 and N1 seismic line. Comparing north, middle and south, respectively, Trajectory angle for forward stepping descending and ascending trend in average number is 2.22. significantly higher than for other 2 with numbers for angle 1.47 (N2) and 1.37 (N1). Those numbers are seen as correction for shelf edge paleo-trajectory. Another look in comparison between regions is with foetal Foreset dip angle. In direction N to S, the gradient of slope decreases (2.83 S1, 1.85 for N2 and 0.64 for N1). The relation of Rollover points is shown in figures 4.3.5-7. Furthermore, the Dip of foreset in present time shows an average number same for north and south, on the north the Ideal foreset dip is almost double steeper than south, in average numbers. Corrected angles (Foreset and Trajectory) were using number 0.2 to get on paleo (real) gradient.

S1	Edge-to-toe (ETT)	Slope relief	Rollover advance		Shelf-edge advance		Toe advance	Ideal dip of foreset	Dip of topeset	Real dip of foreset corrected	Trajectory angle	Trajectory angle corrected
	[m]	[ms]	[m]	[ms]	[m]	[ms]	[m]	arctang [°]	arctang [°]	arctang [°]	arctang [°]	arctang [°]
K1	6882	283	4459	-158	2004	76	2511	2.36	2.17	0.38	-2.02	-0.05
K2	4887	222	2821	-85	1822	73	1256	2.60	2.28	0.52	-1.72	0.36
K3	3375	186	1622	-41	1894	56	1065	3.16	1.71	1.65	-1.46	0.05
K4	2836	175	4006	-98	1720	69	5704	3.54	2.29	1.45	-1.40	0.69
K5	4546	208	615	41	1315	37	1265	2.62	1.59	1.23	3.85	5.24
K6	5767	290	3020	-21	2213	44	501	2.87	1.14	1.93	-0.40	0.54
K7/K6	2700	236	474	18	1428	54	1380	5.00	2.16	3.03	2.16	4.12
K7	3596	268	854	23	1521	74	2381	4.26	2.78	1.67	1.56	4.14
K8	5144	256	3376	-78	2100	65	4140	2.85	1.77	1.29	-1.33	0.24
K9/K8	5877	245	291	46	1900	37	4501	2.39	1.11	1.47	9.05	9.96
K9	1012	373	2812	-59	1701	16	2020	20.21	0.55	19.85	-1.19	-0.84
K10	3848	165	1004	80	2169	57	212	2.45	1.51	1.14	175.46	176.77
K11	6031	234	141	47	2247	50	883	2.22	1.28	1.14	161.48	162.56
K12	4564	254	99	12	2662	57	200	3.18	1.22	2.17	6.98	7.99
average	4346	242	1961	-22	1849	54	2140	4.35	1.72	2.83	-	2.22

Tab. 4.4.1: Measured and calculated values for seismic profile S1. Lighter color correlates with the more solid ones in matter of calculation process. F. ex., light green is calculated on based of bolder green column of Shelf-edge advance, etc. Trajectory and Foreset angle corrected used 0.2 correction number to get real angle before compaction and subsidence influence of relief of delta.

The values of Slope (foreset height) shows that Northern location has the highest in average number and descending towards to south. Rollover advance height has same value for N1, N2 than S1. The value for K1 is more likely the influence, and that is why the average is altered,

incorrect reading of rollover point. The rest of values show approximately the same development from rest of seismic profile measurement.

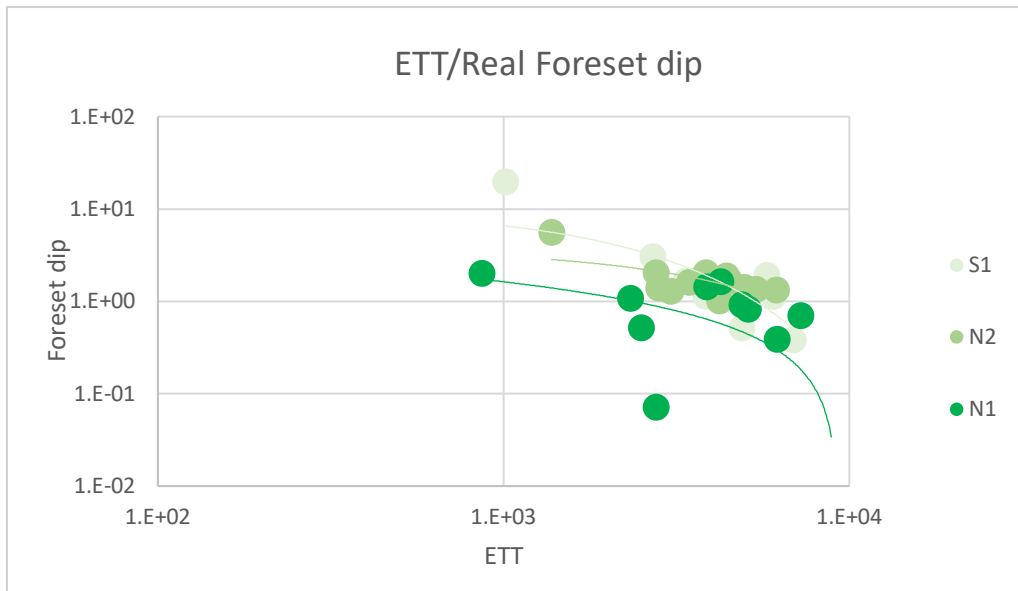
N2	Edge-to-toe (ETT)	Slope relief	Rollover advance		Shelf-edge advance		Toe advance	Ideal dip of foreset	Dip of topeset	Real dip of foreset corrected	Trajectory angle	Trajectory angle corrected
	[m]	[ms]	[m]	[ms]	[m]	[ms]	[m]	arctang [°]	arctang [°]	arctang [°]	arctang [°]	arctang [°]
K1	3047	220	2689	-72	1242	66	2054	4.14	3.06	1.28	-1.53	1.33
K2	1376	185	755	-7	1933	77	2541	7.67	2.28	5.59	-0.51	1.57
K3	4202	223	5202	-141	1476	57	3828	3.04	2.23	1.01	-1.56	0.47
K4	2808	137	1285	-29	1700	47	2423	2.80	1.59	1.40	-1.28	0.11
K5	4051	233	2181	-26	1348	50	2272	3.29	2.11	1.38	-0.69	1.22
K6	3448	196	4579	-75	1540	50	3907	3.25	1.84	1.60	-0.93	0.71
K7/K6	4419	222	1283	13	1710	36	1789	2.88	1.19	1.89	0.60	1.59
K7	3857	225	1099	13	1854	48	1213	3.33	1.50	2.04	0.68	1.98
K8	4516	232	2563	-46	1256	32	1383	2.95	1.47	1.68	-1.03	0.24
K9/K8	2754	155	487	42	1752	42	3076	3.22	1.38	2.04	4.93	6.11
K9	5360	258	2227	-20	1628	45	1799	2.76	1.60	1.36	-0.51	0.88
K10	4962	272	176	83	1389	46	1013	3.13	1.91	1.43	154.65	156.35
K11	6140	306	1177	72	2260	68	543	2.85	1.72	1.33	176.48	178.01
K12	6881	330	190	23	1666	71	200	2.75	2.42	0.53	6.76	8.98
avarage	3918	220	1977	-15	1622	51	2142	3.48	1.84	1.85	-	1.47

Tab. 4.4.2: Measured and calculated values for seismic profile N2. Lighter color correlates with the more solid ones in matter of calculation process. F. ex., light green is calculated on based of bolder green column od Shelf-edge advance, etc. Trajectory and Foreset angle corrected used 0.2 correction number to get real angle before compaction and subsidence influence of relief of delta.

Number in Real foreset angle show higher values, in relation to ETT. When the angle takes a steeper value, ETT shortens (graf. 4.4.1). As it is seen for K2 clinofom (fig. 4.4.2) with number 5.59 ° Real foreset angle vs 1376 m in ETT in comparison to other values in a whole clinofom set.

N1	Edge-to-toe (ETT)	Slope relief	Rollover advance		Shelf-edge advance		Toe advance	Ideal dip of foreset	Dip of topeset	Real dip of foreset corrected	Trajectory angle	Trajectory angle corrected
	[m]	[ms]	[m]	[ms]	[m]	[ms]	[m]	arctang [°]	arctang [°]	arctang [°]	arctang [°]	arctang [°]
K1	864	60	957	8	2004	76	3883	4.00	2.17	2.02	0.48	2.45
K2	3759	110	1930	-16	1822	73	687	1.68	2.28	-0.40	-0.49	1.60
K3	2507	89	3459	-36	1894	56	9845	2.03	1.71	0.52	-0.60	0.90
K4	8870	227	2941	-5	1720	69	179	1.47	2.29	-0.62	-0.10	1.99
K5	6176	192	3838	-73	1315	37	4937	1.78	1.59	0.39	-1.09	0.30
K6	7238	208	4017	-40	2213	44	467	1.64	1.14	0.70	-0.57	0.37
K7/K6	2759	98	2654	-46	1428	54	4779	2.04	2.16	0.07	-1.00	0.97
K7	4944	202	884	27	1521	74	1067	2.34	2.78	-0.24	1.75	4.34
K8	5110	213	4027	-85	2100	65	2802	2.39	1.77	0.82	-1.21	0.35
K9/K8	3865	159	938	17	1900	37	1328	2.36	1.11	1.45	1.02	1.93
K9	4252	148	3068	-24	1701	16	1173	1.99	0.55	1.64	-0.44	-0.09
K10	2325	97	2447	102	2169	57	98	2.39	1.51	1.08	177.61	178.92
K11	4892	172	213	-11	2247	50	204	2.01	1.28	0.93	-2.93	-1.85
K12	2532	125	108	30	2662	57	200	2.82	1.22	1.80	15.63	16.65
avarage	4428	152	2413	-14	1849	54	2419	2.16	1.72	0.64	-	1.37

Tab. 4.4.3: Measured and calculated values for seismic profile N1. Lighter color correlates with the more solid ones in matter of calculation process. F. ex., light green is calculated on based of bolder green column od Shelf-edge advance, etc. Trajectory and Foreset angle corrected used 0.2 correction number to get real angle before compaction and subsidence influence of relief of delta.



Graph 4.4.1: Showing the relation of ETT to Real foreset dip between Seismic lines (S1, N2 and N1). From North to south the trend shows decreasing trend, while foreset length (ETT) get gentle in trend at the southern part of delta geometry.

5. Discussion

The Draupne Formation is part of the Late Jurassic – Early Cretaceous depositional sequence in the North Sea, and is widely regarded as significant source rock (Norlex, NPD fact-page).

The shales of the Draupne Formation also often act as a seal due to their low permeability (Hansen et al. 2020). In this Chapter, we will discuss the clinoform analysis we performed and assess the ability of our formation to act as storage or sealing for CO₂.

Furthermore, we will discuss clinoform development, limitations of the analysis, controlling factors for contrasting the backstepping trend present in our prograding delta, and lastly we will discuss similarities to other clinoform developments, which are sand-storages in the northern Horda platform, such as Johansen Formation in Aurora (Sundal et al. 2015, Osmond et al. 2022) and Sognefjord Formation in Smeaheia fault block. where there is also studied presence of two caprocks. The primary one being the Draupne Formation and the secondary one being the Cromell Knoll Group (Mulrooney et al., 2020).

Subsequently, we address the implications of these findings for CO₂ storage and seal, highlighting the potential of the studied formations for carbon capture. The chapter concludes with recommendations for further research, setting a clear direction for future investigations to enhance our understanding of sedimentary systems, reservoir properties, and implications for CCS.

5.1. Evolution of depositional environment

Based on the study of Hansen et al. (2020), the Draupne Formation from South Viking Graben and its distant equivalent, Tau from Norwegian-Danish Basin and Hekkingen Formation in Barrents Sea, all appear to show good quality in organic matter. Hansen's paper shows that the Draupne Formation and its equivalents have good quality sealing properties. According to his study, each formation was deposited in marine environments following widespread rifting and transgression (Hansen et al. 2020, Johnson et al., 2022). The Draupne Formation mentioned in his paper and its equivalents (Tau and Hekkingen) seem to have more stable / undisturbed environment creating an organic shale-rich formation.

In contrast, according to our research, the Draupne Formation appear to have heterogeneous character (further discussion in the subchapter “5.2 - Clinoform analysis”) or nature although also deposited in marine environment., with more diverse environment conditions.

This discrepancy between the deposition environment assessment of the heterogeneous Draupne Formation clinoforms we observe versus the Draupne Formation shale with high content of organic matter, which appears to be a good seal, as observed in Hansen’s paper might be caused by varying depositional conditions and processes over time.

The Draupne Formation clinoforms, given their large size and complex geometry, likely formed under conditions of strong sediment supply from the Hardangerfjord delta. The spatial heterogeneity observed might be the result of changes in the sediment supply or shifts in the depositional environment over time, leading to variations in the clinoform geometry.

On the other hand, the deposition of the organic-rich shale within the Draupne Formation of Hansen’s paper would have likely occurred in a more stable, low-energy environment such as a deep, calm, marine setting.

Therefore, the seemingly contrasting characteristics of the Draupne Formation—heterogeneous clinoforms versus organic-rich shales—can be explained by the formation's dynamic depositional history. Changes in environmental conditions, such as sea-level fluctuations, variations in sediment supply, or shifts in depositional energy, could have led to the observed heterogeneity in our Draupne Formation. These factors underscore the importance of understanding the depositional environment and its evolution in interpreting the characteristics of a geological formation.

Horizons

Horizons between Top Statfjord and Top Sognefjord (fig. 4.1.3-5) remain debatable in this study area: according to Færseth et al.(1996) and Fazlikhani et al. (2017), one of the reflection horizons between Top Statfjord and Top Sognefjord is referred to as Brent Group. However, the Vestland Group is present in the southern part of the Norwegian North Sea (NPD Fact Page). According to well stratigraphic main groups examination (17/3-1, 17/4-1, 25/6-1, 26/4-1), it would fit better in our study location, but due to lack of penetration of our studied location, the horizon between Statfjord and Sognefjord stayed unidentified in our figures. Therefore it was identified as Middle Jurassic.

As we shift our focus to nearby regions such as the Ling Depression and South Viking Graben, the Draupne Formation directly overlays the Heather Formation, which is supported by the well strata examination (25/6-1, 17/4-1). Notably, the Hugin Formation sandstone is incorporated within the Heather Formation (Olsen et al. 2017). It can be assumed that the strong reflection horizon (fig. 3.3.1.1, 4.2.7-8) between the top of Sognefjord and bottom of Draupne is Heather but we kept the classification in this study as a sequence boundary since it is unclear and inconclusive.

Paleogeographic development:

Considering the source of the sediments, the transportation process, and the depositional environment, the lithological variations and thickness variations can indicate changes in depositional conditions over time.

Over time, the described region has seen significant geologic activity, including erosion, sediment transportation and deposition, and tectonic shifts. This has resulted in the formation of a complex delta system within the Viking Group, which has gone through stages of progradation and backstepping with continuous progradation. The Base Cretaceous Unconformity (BCU) represents an erosional event.

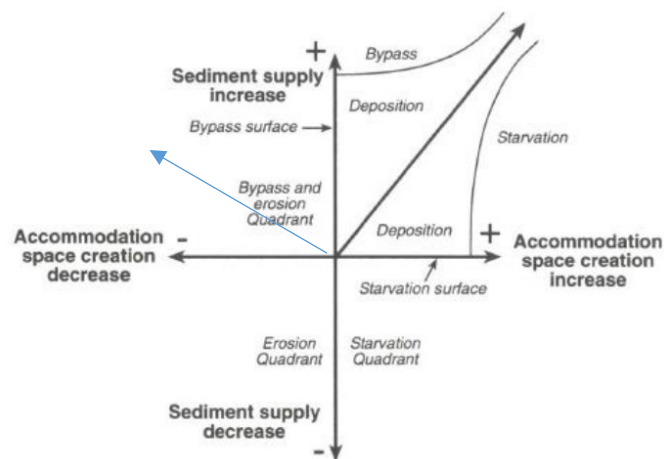


Fig. 5.1.1: Relationships between accommodation space and sediment supply in a coordinate system (Folkestad, A. & Steel, R. J. 2001)

Figure 5.1.1 can be taken as a description of the ratio of accommodation vs. sediment supply. In our clinoform system, the sediments prograde basin-ward (K1-K9) and aggregate (K10-K12). Our clinoforms fall in the quadrant with positive sediment supply and negative accommodation space which is demonstrated by the blue arrow in the picture.

5.2. Clinoform analysis

This chapter explores clinoforms, their limitations in analysis, changes in seismic facies patterns, and the impact of structural influences on their formation. We delve into the geometry and facies of clinoforms, discussing their thickness, lithology, and evolution in response to various factors like sediment supply, accommodation space and sea level changes. The correlation between clinoform thickness and geometric characteristics is also a subject of discussion.

5.2.1. Limitations and clinoform changing seismic facie pattern

By looking at the full size of shelf-edge prograding delta (further discussed in Chapter 5.3), it can be divided into sectors. Particularly the south sector has a structure and normal fault influence. The clinoform prograde over those elevated locations formed as a response to convergent movement in the later event of Late Cretaceous (sub-Hercynian event) (Biddle & Rudolph, 1988). Closer to the middle sector, the clinoforms are multi-faulted through the foreset, making the interpretation challenging. Despite this, the sector shows a nice pattern of progradation until K9 and becomes the easiest to detect. This location was the area from which the 3 most recognizable clinoform facies were recognized and taken as the reference pattern to be looking for in the other two sectors. The last area to be addressed falls in the northern sector of the delta profile. This part requires more time to determine with some level of clarity. And some inline seismic profile (HRTRE00 survey) must be interpreted to support the interpretation in crossline (W-E) direction. This very edge northern sector has not been considered in a regional map of a shelf-edge delta due to difficulty to recognize main clinoform. The seismic facies are significantly changed under recognition. Either the youngest has been preserved and it is those that should be followed or the oldest are not present and the oldest clinoforms are those to be followed. Mainly at the topsets the facies have changed into more condensed layering in vertical direction and in a more rugous, discontinuous pattern. This can be considered in further research for potential micro-trapping during migration of CO₂, which can result in a trap of the gas into a crest of this rugous folding spanning from Øygarden Fault Complex over 10km in the East-West direction.

5.2.2. Geometry and facies

The balance between the creation of accommodation space and the sediment supply can influence the shape and evolution of clinoforms (Mitchum et al., 1977; Burgess & Hovius, 1998; Helland-Hansen & Hampson, 2009). Progradation refers to the horizontal extension of sedimentary deposits in a particular direction, usually towards the basin or open water. Aggradation refers to the vertical accumulation of sediment, which contributes to the growth of depositional features. Shelf-edge clinoforms often display sigmoidal profiles, with oblique geometries present in cases of shelf-edge deltas and descending trajectories (Helland-Hansen & Hampson, 2009). The sedimentation on shelf-edge clinoforms is influenced by short-term progradation and long-term aggradation cycles. They exhibit lower progradation/aggradation ratios and higher progradation resistance ratios (fig. 5.1.1) compared to delta scale clinoforms (Patruno et al., 2015a, Patruno & Helland-Hansen, 2018; Helland-Hansen & Gjelberg, 2012). Further discussion is based on Anell & Midtkandal, (2015), Patruno & Helland-Hansen, (2018) paper. Considering influence and changes in deposition ratio (accommodation, starvation), sea level, slope gradient, and grain particles from the source (sediment composition), and sediment transport. Clinoforms can be described using three endmembers: oblique, tangential, and sigmoidal, corresponding to three types of curvature: Linear, Exponential, and Gaussian (Anell & Midtkandal, 2015). In the study, the delta system presents only the last two types of Exponential or Gaussian, which according to Anell & Midtkandal (2015) paper indicated by curved slopes influenced by changes in depositional ratio. Accommodation and sediment supply are fundamental in determining the geometries of clinoforms, need to be considered. In a system were identified Sigmoidal and Tangential shapes (fig. 4.2.5-7). The former suggests increasing accommodation and bigger supply of sediment, while the latter suggest developing during period of limited accommodation (Anell & Midtkandal, 2015). Mathematical modeling indicates that relative sea levels also influence the shape of clinoforms. Divergent sigmoidal clinoforms (fig. 4.2.5-7) were recognized in a clinoform set which indicate the stable sea level. Oblique type refers to falling sea level. K10, K8, K6 appear to be the case of sea level change. To the north there seems to be deviation. K8 and K6 fall in more likely sigmoidal chaotic. That could be altered by the influence of turbidities, clinoform collapse or diversity of grain particles apart from middle and southern part of delta lobe. The slope gradient is controlled by seabed relief (Anell & Midtkandal, 2015) and basin depth, with clinoforms in deep water developing steeper slopes than those in shallow water. Sediment composition also influences slope gradient, with coarser, less cohesive particles forming steeper slopes and muddy cohesive sediment forming gentler one types of clinoforms.

There is an interesting correlation between the thickness of clinoforms and their geometric characteristics. For example, the clinoforms exhibiting top-heavy geometry tended to have greater thicknesses, potentially attributable to increasing accommodation space. Similarly, the clinoforms with longer foreset and bottomset sections often demonstrated larger thicknesses, suggesting prolonged periods of stable sediment supply and sea-level conditions.

5.2.3. Controls

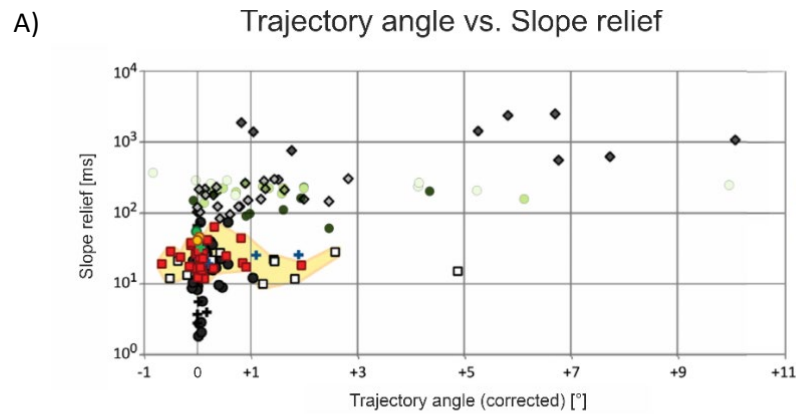
The clinoforms K1 to K9 shows a prograding, mostly descendent trend, while the last two clinoforms, K10 and K11 (K12 is partly eroded away at the foreset at most interpreted seismic profiles) in profile N2, S1 the trend has changed into backstepping, but the delta is still prograding. N1 has only one clinoform, K10 which has backstepping values. Furthermore, we will discuss what can cause the backstepping trend. One of the most common factors is the global sea-level rise, which can be caused by warm weather (melting down of icecaps). Another factor which is more likely is the influence of tectonic matter, for example, subsiding basin can result in increasing of accommodation space for depositing of sediments. Another strong factor lies within sediment supply change. There might be two cases of the change. The first is relocation of the delta supply sediment source, or secondly, backstepping of delta resulting in a decrease of sediment supply.

The gradient of thickness across the clinoforms provided further insights into their development. For instance, in some clinoform bodies, we observed a steeper gradient, suggesting a rapid increase in thickness over a short distance. This may be an indication of high sediment supply or rapid sea-level changes during the period of formation. On the contrary, a more gradual gradient was noted in other clinoform bodies, implying a slower and steadier increase in thickness, possibly due to a slower rate of sediment supply or stable sea-level conditions.

5.3. Similarities to Sognefjord and Johansen clinoform delta development

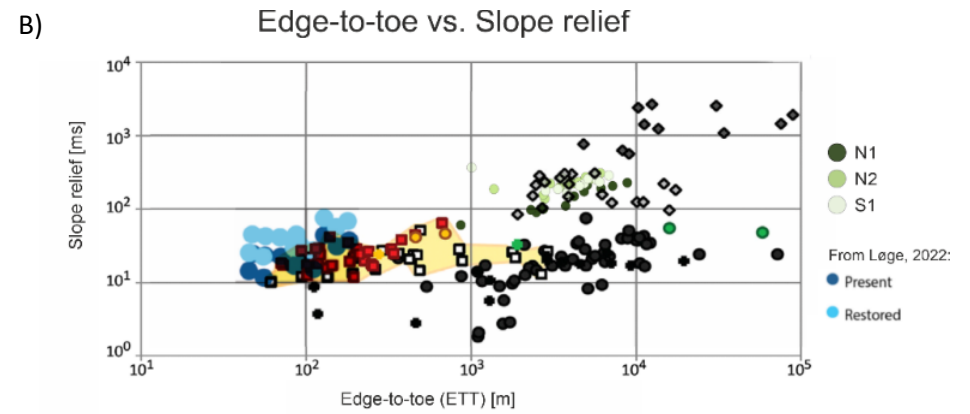
In this subchapter we will discuss the character of the Draupne Formation using data from Patruno et al. (2015a) and Løge (2022) in comparison with our measured and calculated clinoform parameters data. Patruno gives compiled data of the types of deltas including delta-scale (Sognefjord. Fig 5.3.1C), shelf-edge and marginal slope delta scale. Løge plotted her data of the Johanson Formation situated in the Horda platform (Aurora Fig 5.3.1C).

The Draupne unit in Stord basin is characterized by a prograding shelf-edge scale delta. The plotting data in the graphs (fig. 4.3.1A-B) supported our knowledge of type of delta. Our data in the graphs covers exact places correlated with ancient clinoform type (Patruno et al. 2015). After plotting the data in a graph 5.3.1C, our observation indicates tendency to coarser sand-prone deposition. The data places the Draupne Formation above the trend line, depicted by the yellow dashed line, suggesting an over-steepened angle, categorizing our delta as sand-prone. This contrasts with other studies of the Draupne Formation which classify its depositional content as being more consistent with a muddy rock type, suitable for serving as a seal rather than storage in the context of hydrocarbon reservoirs.



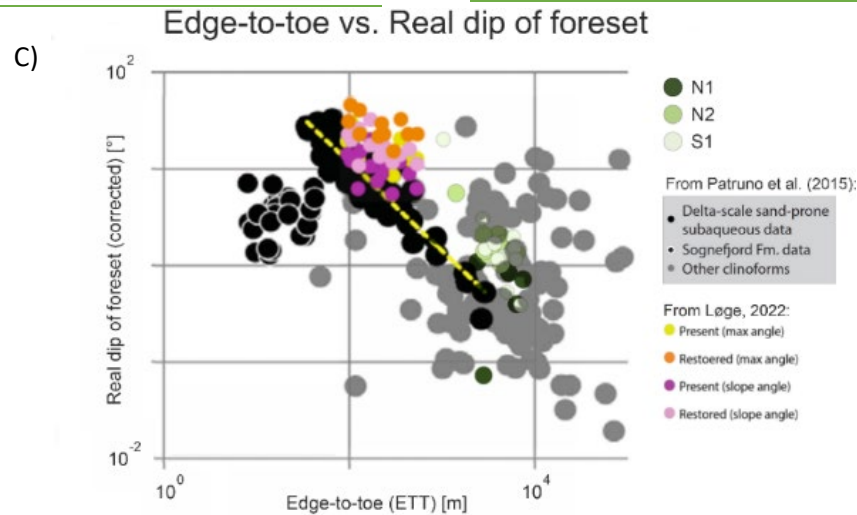
From Patruño et al. (2015):

- | | |
|--|---|
| ◆ Ancient to recent continental margin clinoforms | ◆ Ancient subaerial delta and shoreline clinoforms |
| ◆ Ancient to recent shelf prism clinoforms | ◆ Sognefjord Formation (Ancient delta-scale sand-prone subaqueous clinoforms) |
| □ Miocene to recent sand-prone subaqueous delta clinoforms | ◆ Blackhawk Formation (Ancient subaerial delta and shoreline clinoforms) |
| ◆ Quaternary muddy subaqueous delta clinoforms | ◆ Mancos Shale (Ancient muddy subaqueous delta clinoforms) |
| ◆ Quaternary subaerial delta and shoreline clinoforms (except small-scale steep Gilbert-type deltas) | ◆ Bridport Sand (Ancient delta-scale sand-prone subaqueous clinoforms) |
| | ◆ Down Cliff Clay (Ancient delta-scale sand-prone subaqueous clinoforms) |



From Patruño et al. (2015):

- | | |
|--|---|
| ◆ Ancient to recent continental margin clinoforms | ◆ Ancient subaerial delta and shoreline clinoforms |
| ◆ Ancient to recent shelf prism clinoforms | ◆ Sognefjord Formation (Ancient delta-scale sand-prone subaqueous clinoforms) |
| □ Miocene to recent sand-prone subaqueous delta clinoforms | ◆ Blackhawk Formation (Ancient subaerial delta and shoreline clinoforms) |
| ◆ Quaternary muddy subaqueous delta clinoforms | ◆ Mancos Shale (Ancient muddy subaqueous delta clinoforms) |
| ◆ Quaternary subaerial delta and shoreline clinoforms (except small-scale steep Gilbert-type deltas) | ◆ Bridport Sand (Ancient delta-scale sand-prone subaqueous clinoforms) |
| | ◆ Down Cliff Clay (Ancient delta-scale sand-prone subaqueous clinoforms) |



From Patruño et al. (2015):

- | |
|--|
| ◆ Delta-scale sand-prone subaqueous data |
| ◆ Sognefjord Fm. data |
| ◆ Other clinoforms |

From Løge, 2022:

- | |
|--------------------------|
| ◆ Present (max angle) |
| ◆ Restored (max angle) |
| ◆ Present (slope angle) |
| ◆ Restored (slope angle) |

Tab. 5.3.1: Three combined graphs A, B and C plotting our calculated data together with data from Patruño et al. (2015a) (graphs A, B, C) and Løge (2022) (graph C)

5.4. Implication for CO₂

The Sognefjord formation at Smaheia field, and Johanson Formation at Aurora, is regarded as a reliable storage rock for carbon capture and storage (CCS) purposes. The Draupne Formation is considered here as a primary storage, while also being evaluated for at the distant location as a caprock (Hansen et al., 2020; Johnson et al. 2022; Osmond et al., 2022).

Our comprehensive study of the clinoforms within the Draupne Formation provides important insights regarding CO₂ storage feasibility and migration risks within this geological setting.

The Draupne Formation benefits from a consistent sediment supply from the Hardangerfjord deltaic system, which has influenced its size and potential volume for CO₂ storage. Compared to the Sognefjord and Johansen formations, the clinoforms in the Draupne Formation are significantly larger, offering more accommodation space suitable for CCS operations. This larger size enhances its capacity to withstand CO₂ injection pressures, thereby improving storage prospects. However, the Draupne Formation presents challenges as a seal for CO₂ storage, unlike other regions with more effective seals. The formation tends to be sand-prone, promoting primary storage and migration. Consequently, evaluating the sealing properties of the overlying Cromer Knoll Group is essential. The surface map data suggests an eastward migration of CO₂ along the steepest surface gradient. The Øygarden Fault Complex, which spans the delta profile, has the potential to act as a barrier against CO₂ leakage, offering favorable conditions. Additionally, the thickness of the Cromer Knoll Group indicates it could serve as a reliable seal, minimizing leakage risks. The Draupne Formation exhibits heterogeneous deposition, as evidenced by variable and imbalanced clinoform geometry over time. This suggests the presence of diverse potential storage sites for CCS. A cyclical pattern is observed in the mid-section of the formation, characterized by repetitive variations in clinoform thickness. Tectonic activity, such as the Permo-Triassic rift, has influenced relief and the progradation of clinoforms, leading to variations in accommodation space. These variations may impact CO₂ capture efficiency and seal quality, warranting further investigation. In the Stord basin, regional variations in thickness and lithology are observed, including up to 700m thick shelf clinoforms. Accommodation space changes during the K9-K11 clinoform interval result in variable deposition. However, the delta prograde overall with the first eight clinoforms (K1-K8), featuring relatively short topsets and sediment accommodation at the foreset.

Cyclicality near the Upper rollover point is apparent in the middle sector of the delta profile until the backstepping trend of the last clinoform set (K9-K11). The partially eroded K12 clinoform frames the Draupne Formation succession. Despite backstepping in the K10-K11 interval, the delta continues to prograde.

The thickness of the Draupne Formation is a crucial factor in determining its capacity for CO₂ storage. A thicker reservoir provides more space to accommodate the injected CO₂. Evaluating the thickness variations across the region is essential to identify areas with optimal storage potential. The thickness of the seal or cap rock is an essential factor in determining the effectiveness of a geological storage site for carbon capture and storage (CCS) projects. The seal acts as a barrier preventing the upward migration of the injected CO₂. The necessary thickness of a seal can the pressure and volume of the injected CO₂ can influence the thickness of the seal needed. Higher pressures and volumes might require a thicker seal to prevent leakage. The physical properties of the seal itself, such as its permeability and capillary entry pressure, can determine the required thickness. Seals with lower permeability and higher capillary entry pressure can be effective even if they are thinner. The geometry of the reservoir and the seal, including factors like the dip of the layers and the presence of any faults or fractures, can impact the required seal thickness (Mondol et al, 2018, NPD fact page).

The storage capacity of the Draupne Formation depends on various factors, including its porosity and permeability. These properties influence the volume of CO₂ that can be effectively stored within the reservoir. Detailed characterization of the formation's lithology and petrophysical properties is necessary to estimate the storage capacity accurately.

Understanding the migration pathways of CO₂ within the Draupne Formation is vital for efficient and secure storage. The geometry of the underlying formations, as well as the presence of faults, influences the direction and extent of CO₂ migration. Evaluating these factors helps identify pathways and potential risks associated with CO₂ movement within the reservoir. In general rule the pathway follows steeper gradient and looking at the Surface map (Figure 4.1.2) of top Draupne Formation (The Viking Group alien with the top of Draupne) the CO₂ migration pathway go landward, perpendicular to contour.

The integrity of the Draupne Formation as a storage reservoir is important to consider. Any faults or fractures within the formation can compromise the containment of CO₂ and lead to leakage. A detailed analysis of the structural characteristics is necessary to assess the reservoir's integrity and identify areas with enhanced storage security. However, the overlying group (Cromer Knoll) thickness can serve as a sufficient seal in any possible attempt of leakage from Draupne Formation system due to multiple normal faulting, present at the central part of delta

profile or other factor leading to changes in reservoir conditions for storing and migration. Conducting thorough risk assessments considering factors such as caprock integrity and potential CO₂ migration paths further enhances the safety of storage operations.

5.5. Recommendation for further work

- Refinement of seal heterogeneity analysis: Regional mapping of the 3D extension of the prograding system, incorporating techniques such as seismic facies mapping, surface attribute analysis, and time-slice spectral decomposition in GADOTERIC, will enhance the analysis of seal heterogeneity. Additionally, targeting potential sites of sediment heterogeneity associated with missing or eroded sections of the Draupne Shale on footwalls will allow for a more comprehensive assessment of lithological variations. The results will contribute to the understanding of seal integrity and geo-mechanical behavior (source citation).. Measuring other geometric parameters: These include height, length, maximum vertical thickness, total advance of the rollover, thickness of the topset, the advance of the toe, and the dip of the slope. Calculation of clinoform volume bodies and estimation of the maximum thickness can yield better understanding of depositional environment and local changes within the delta profile.
- Petrophysical analysis of the Draupne Formation: A more detailed petrophysical analysis of the Draupne Formation is necessary to gain a better insight into its rock properties. This analysis should focus on detailed characterization of lithology and petrophysical properties, such as porosity and permeability. By accurately estimating the storage capacity, this assessment will aid in evaluating the potential of the Cretaceous compact units as potential seals, considering their favorable thickness (source citation).
- Further assessment of CO₂ storage potential: The assessment of CO₂ storage potential should expand to include detailed analysis of reservoir properties, such as porosity, permeability, and simulation of CO₂ migration and trapping mechanisms. These analyses will provide insights into the viability and effectiveness of the Draupne Formation as a storage site for CO₂ (source citation).

- High-resolution seismic studies: Conducting high-resolution seismic studies will enable more detailed imaging of the clinoforms within the Draupne Formation. This will enhance the interpretation by capturing smaller-scale features and variations within the clinoforms, allowing for a more accurate assessment of their geometry and sedimentary characteristics (source citation).
- By incorporating these elements into the master thesis chapter, a more comprehensive understanding of the Draupne Formation's CO₂ storage potential and its geological features can be achieved, contributing to the overall knowledge and research in the field.

6. Conclusion

Our in-depth study of the clinoforms within the Draupne Formation, particularly its calculated and measured parameters, has revealed crucial insights about the feasibility and risks associated with CO₂ storage and potential migration within this geological framework.

- Importantly, the Draupne Formation was fed by the Hardangerfjord deltaic system, providing a stable sediment supply over time that crucially contributes to its dimensions and impacts the potential volume for CO₂ storage.

- The Draupne Formation clinoforms are considerably larger than those in the Sognefjord and Johansen formations, affording more accommodation space suitable for CCS operations. The larger formation size directly correlates with the capacity to withstand the pressures associated with CO₂ injection, enhancing storage prospects.

- The Draupne Formation in the examined area presents a less than ideal seal for CO₂ storage, contrasting with other regions that have more homogenous and effective seals. As indicated by the "Edge-to-toe vs. Real dip of foreset" graph, the formation tends to be sand-prone, promoting primary storage and migration. This finding underscores the importance of evaluating the sealing character of Cromer Knoll Group, the units deposited above the Draupne Formation.

- The surface map data implies eastward CO₂ migration along the steepest surface gradient. The Øygarden Fault Complex, spanning across the delta profile, could potentially act as a barrier to CO₂ leakage, providing favorable conditions. Given the thickness of Cromer Knoll Group, it appears to offer a good seal, thus minimizing leakage risks.

- The Draupne Formation exhibits heterogeneous deposition, as shown by the variable and imbalanced clinoform geometry character which has been assessed and facies analysis over time. This suggests the presence of diverse potential storage sites for CCS.

- There appears to be a cyclical pattern in the formation's mid-section, as indicated by the repetitive variation of thicknesses between clinoforms. On the north and south, there seems to be a bigger influence of the tectonic activity on the relief the clinoforms prograde on,

driven by a past event (Permo-Triassic rift) and uplift and subsidence. These significant variations in accommodation space across the entire delta may have implications for CO₂ capture efficiency and seal quality, and thus warrant further exploration.

- The Stord basin shows regional variations in thickness and lithology, with up to 700ms thick shelf clinoforms. variable deposition due to changes in accommodation space, especially during the K9-K11 clinoform interval. Overall scale the delta prograde with first 8 clinoform (K1 - K8) with relatively short topsets with sediment accommodation at the foreset. In the middle sector of delta profile can be noted up the appearance of cyclicity in distance of Upper rollover point. The pattern occurs till the backstepping trend of last members of clinoform set (K9 – K11). K12 is framing Draupne Formation succession and is partly eroded at the foreset. Direction of prograding delta, despite the backstepping (K10 – K11), The delta is still prograding.

Reference list

- Amrizal, A., & Nordfjord, S. (2017). An integrated study of the Cretaceous sequence stratigraphic development in the Northern Stord Basin, North Sea. *European Association of Geoscientists & Engineers*. <https://doi.org/10.3997/2214-4609.201701531>
- Anell, I., & Midtkandal, I. (2015). A morphoclimatic classification of clinofolds. *Journal of Sedimentary Research*, 85(5), 538-556.
- Anell, I., & Midtkandal, I. (2015). The quantifiable clinofold – types, shapes and geometric relationships in the Plio-Pleistocene Giant Foresets Formation, Taranaki Basin, New Zealand. *Bulletin of the Royal Society of New Zealand*, 50(2), 139-150. <https://doi.org/10.1111/bre.12149>
- Anell, I., Thybo, H., & Artemieva, I. (2009). Cenozoic uplift and subsidence in the North Atlantic region: Geological evidence revisited. *Tectonophysics*, 474(1-2), 78–105. <https://doi.org/10.1016/j.tecto.2009.04.006>
- Anell, I., Thybo, H., & Stratford, W. (2010). Relating Cenozoic North Sea sediments to topography in southern Norway: The interplay between tectonics and climate. *Earth and Planetary Science Letters*, 300, 19–32. <https://doi.org/10.1016/j.epsl.2010.09.009>
- Baig, I., Faleide, J. I., Mondol, N. H., & Jahren, J. (2019). Burial and exhumation history controls on shale compaction and thermal maturity along the Norwegian North Sea basin margin areas. *Marine and Petroleum Geology*, 104, 61-85. <https://doi.org/10.1016/j.marpetgeo.2019.03.010>
- Basset, M. G. (2003). Sub-Devonian geology. In D. Evans, C. Graham, A. Armour, & P. Bathurst (Eds.), *The Millennium Atlas: Petroleum geology of the central and northern North Sea* (pp. 61-63). The Geological Society of London.
- Biddle, K. T., & Rudolph, K. W. (1988). Early Tertiary structural inversion in the Stord Basin, Norwegian North Sea. *Journal of the Geological Society, London*, 145, 603-611. <https://doi.org/10.1144/gsjgs.145.4.0603>
- Brown, A. R. (1999). *Interpretation of three-dimensional seismic data* (5th ed., Vol. 42). American Association of Petroleum Geologists. <https://doi.org/10.1306/M4271346>
- Burchfiel, B. C., Stewart, J. H., & Davis, G. H. (1972). Fault patterns and basin structure of the northern Tetons. *Geological Society of America Bulletin*, 83(7), 2165-2194.
- Burgess, P. M., & Hovius, N. (1998). Rates of delta progradation during highstands: Consequences for shelf bypass and deep water sedimentation. *Journal of the Geological Society London*, 155(2), 217-222. <https://doi.org/10.1144/gsjgs.155.2.0217>
- Bøe, R., Fossen, H., & Smelror, M. (2010). Mesozoic sediments and structures onshore Norway and in the coastal zone. *Norges Geologiske Undersøkelse Bulletin*, 450, 15-32. https://www.ngu.no/upload/Publikasjoner/Bulletin/Bulletin450_15-32.pdf
- Cameron, T. D. J., Crosby, A., Balson, P. S., Jeffery, D. H., Lott, G. K., Bulat, J., & Harrison, D. J. (1992). United Kingdom offshore regional report: The geology of the southern North Sea. HMSO for the British Geological Survey.

- Catuneanu, O. (2006). Principles of sequence stratigraphy. Elsevier.
- Catuneanu, O., Abreu, V., Bhattacharya, J. P., Blum, M. D., Dalrymple, R. W., Eriksson, P. G., ... & Willis, B. J. (2008). Towards the standardization of sequence stratigraphy. *Earth-Science Reviews*, 92(1-2), 1-33.
- Catuneanu, O., Abreu, V., Bhattacharya, J.P., Blum, M.D., Dalrymple, R.W., Eriksson, P.G., et al., (2009). Towards the standardization of sequence stratigraphy. *Earth-Science Reviews*, 92, 1–33.
- Catuneanu, O., Galloway, W. E., Kendall, C. G. St. C., Miall, A. D., Posamentier, H. W., Strasser, A., & Tucker, M. E. (2011). Sequence Stratigraphy: Methodology and Nomenclature. *Newsletters on Stratigraphy*, 44(3), 173-245. <https://doi.org/10.1127/0078-0421/2011/0011>
- Coe, A. L., & Hesselbo, S. P. (2003). Development of the diagenetic concretionary fabric in mudrocks: evidence from the Kimmeridge Clay Formation (Upper Jurassic), England. *Journal of Sedimentary Research*, 73(6), 1054-1065.
- Chew, D. M., & Strachan, R. A. (2014). The Laurentian Caledonides of Scotland and Ireland. *Geological Society London Special Publications*. <https://doi.org/10.1144/SP390.16>
- Cook, P. J. (1999). Sustainability and nonrenewable resources. *Environmental Geosciences*, 6(4), 185–190. <https://doi.org/10.1046/j.1526-0984.1999.64004.x>
- Deegan, C. E., & Scull, B. J. (1977). A standard lithostratigraphic nomenclature for the Central and Northern North Sea (Report 77/25). Institute of Geological Sciences, Oljedirektoratet, Bulletin 1.
- Doré, A. G. (1995). The influence of tectonics on Mesozoic sedimentation at the rifted continental margin of the northern North Sea. In R. J. Steel, V. L. Felt, E. P. Johannessen, & C. Mathieu (Eds.), *Sequence Stratigraphy on the Northwest European Margin* (pp. 163-205). Norwegian Petroleum Society (NPF), Special Publication 5.
- Doré, A. G., Lundin, E. R., Jensen, L. N., Birkeland, O., Eliassen, P. E., & Fichler, C. (1999). Principal tectonic events in the evolution of the northwest European Atlantic margin. In A. J. Fleet & S. A. R. Boldy (Eds.), *Petroleum Geology of Northwest Europe*. <https://doi.org/10.1144/0050041>
- Dreyer, T., Whitaker, M., Dexter, J., Flesche, H., & Larsen, E. (2005). From spit system to tide-dominated delta: Integrated reservoir model of the Upper Jurassic Sognefjord Formation on the Troll West Field. Geological Society, London, Petroleum Geology Conference Series, 6(1), 423. <https://doi.org/10.1144/0060423>
- Evans, S., & Braathen, A. (2022). Evaluating CO₂ storage potential in an under-explored basin: Stord Basin, Northern North Sea. *European Association of Geoscientists & Engineers*, 2022, 1 – 5. <https://doi.org/10.3997/2214-4609.202210712>
- Evans, D., Graham, C., & Arthur, P. (Eds.). (2003). *The Millennium Atlas: Petroleum Geology of the Central and Northern North Sea*. Geological Society of London. <https://doi.org/10.1017/S0016756803218124>

- Faleide, J. I., Vågnes, E., & Gudlaugsson, S. T. (1993). Late Mesozoic-Cenozoic evolution of the south-western Barents Sea in a regional rift-shear tectonic setting. *Marine and Petroleum Geology*, 10(3), 186-214. [https://doi.org/10.1016/0264-8172\(93\)90104-Z](https://doi.org/10.1016/0264-8172(93)90104-Z)
- Faleide, T. S., Braathen, A., Lecomte, I., Mulrooney, M. J., Midtkandal, I., Bugge, A. J., & Planke, S. (2021). Impacts of seismic resolution on fault interpretation: Insights from seismic modelling. *Tectonophysics*, 816. <https://doi.org/10.1016/j.tecto.2021.229008>
- Faleide, J. I., Kyrkjebø, R., Kjennerud, T., Gabrielsen, R. H., Jordt, H., Fanavoll, S., & Bjerkebæk, E. (2015). Tectonostratigraphy of the greater Barents Sea: Implications for petroleum systems. In Geological Society, London (Vol. 67, No. 1, pp. 61-74). *Petroleum Geology of the Barents Sea*.
- Fazlikhani, H., Fossen, H., Gawthorpe, G., Faleide, J. I., & Bell, R. B. (2017). Basement structure and its influence on the structural configuration of the northern North Sea rift. *Tectonics*, American Geophysical Union. <https://doi.org/10.1002/2017TC004514>
- Fazlikhani, H., Faleide, J. I., Jahren, J., Mondol, N. H., & Marcussen, Ø. (2017). Sedimentological analysis and reservoir characterization of a multi-darcy, billion barrel oil field – The Upper Jurassic shallow marine sandstones of the Johan Sverdrup field, North Sea, Norway. *Marine and Petroleum Geology*, 84, 102-134. <https://doi.org/10.1016/j.marpetgeo.2017.03.029>
- Folkestad, A., & Steel, R. J. (2001). The alluvial cyclicity in Hornelen basin (Devonian Western Norway) revisited: A multiparameter sedimentary analysis and stratigraphic implications. *Norwegian Petroleum Society Special Publications*, 10, 39-50. [https://doi.org/10.1016/S0928-8937\(01\)80007-2](https://doi.org/10.1016/S0928-8937(01)80007-2)
- Fossen, H. (1992). The role of extensional tectonics in the Caledonides of south Norway. *Journal of Structural Geology*, 14, 1033-1046. [https://doi.org/10.1016/0191-8141\(92\)90034-T](https://doi.org/10.1016/0191-8141(92)90034-T)
- Fossen, H., & Rykkeli, D. E. (1992). Postcollisional extension of the Caledonide orogen in Scandinavia: Structural expressions and tectonic significance. *Geology*, 20, 737-740. [https://doi.org/10.1130/0091-7613\(1992\)020<0737:PEOTCO>2.3.CO;2](https://doi.org/10.1130/0091-7613(1992)020<0737:PEOTCO>2.3.CO;2)
- Fossen, H., Odinsen, T., Færseth, R.B., & Gabrielsen, R.H.(2000). Detachments and low-angle faults in the northern North Sea rift system. *Geological Society London Special Publications*. <https://doi.org/10.1144/GSL.SP.2000.167.01.06>
- Fossen, H., & Hurich, C. A. (2005). The Hardangerfjord Shear Zone in SW Norway and the North Sea: A large-scale low-angle shear zone in the Caledonian crust. *Journal of the Geological Society*, 162, 675-687.
- Færseth, R. B., Gabrielsen, R. H., & Hurich, C. A. (1995). Influence of basement in structuring of the North Sea basin, offshore southwest Norway. *Norsk Geologisk Tidsskrift*, 75, 105-119. https://foreninger.uio.no/ngf/ngt/pdfs/NGT_75_2&3_105-119.pdf
- Færseth, R. B. (1996). Interaction of Permo-Triassic and Jurassic extensional fault-blocks during the development of the northern North Sea. *Journal of the Geological Society of London*, 153, 931-944. <https://doi.org/10.1144/gsjgs.153.6.0931>
- Gabrielsen, R. H., Færseth, R. B., Steel, R. J., Idil, S., & Kløvjan, O. S. (1990). Architectural styles of basin fill in the northern Viking Graben. In D. J. Blundell & A. D. Gibbs (Eds.), *Tectonic Evolution of the North Sea Rifts* (pp. 158–179). Clarendon Press.

- Gabrielsen, R., Kyrkjebo, R., Faleide, J. I., Fjeldskaar, W., & Kjennerud, T. (2001). The Cretaceous post-rift basin configuration of the Northern North Sea. *Petroleum Geoscience*, 7(2), 137-154. <https://doi.org/10.1144/petgeo.7.2.137>
- Glennie, K. W. (1998). Lower Permian - Rotliegend. In K. W. Glennie (Ed.), *Petroleum Geology of the North Sea: Basic Concepts and Recent Advances* (4th ed., pp. 137-173). Blackwell. <https://doi.org/10.1002/9781444313413.ch5>
- Gradstein, F. M., Hammer, O., & Anthonissen, E. (2005). *Norwegian Offshore Stratigraphic Lexicon*. Museum of Natural History, Geological Department University of Oslo.
- Gradstein, F. M., Anthonissen, E., Brunstad, H., Charnock, M., Hammer, O., Hellem, T., & Lervik, K. S. (2010). Norwegian Offshore Stratigraphic Lexicon (NORLEX). *Newsletters on Stratigraphy*, 44, 73-86.
- Gradstein, F. M., Ogg, J. G., Smith, A. G., et al. (2004). *A Geologic Time Scale 2004*. Cambridge University Press.
- Gradstein, F. M., Ogg, J. G., & Smith, A. G. (2012). *A Geologic Time Scale 2004*. Cambridge University Press. <https://doi.org/10.1017/CBO9780511536045>
- Helland-Hansen, W. (1995). Sequence stratigraphy theory: Remarks and recommendations. *Norwegian Petroleum Society Special Publications*, 5, 13-21. [https://doi.org/10.1016/S0928-8937\(06\)80060-3](https://doi.org/10.1016/S0928-8937(06)80060-3)
- Helland-Hansen, W., & Hampson, G. J. (2009). Trajectory analysis: Concepts and applications. *Basin Research*, 21(4), 454-483. <https://doi.org/10.1111/j.1365-2117.2009.00425.x>
- Helland-Hansen, W., & Gjelberg, H. (2012). Towards a hierarchical classification of clinoforms. *AAPG Search and Discovery Article #90142*
- Ikelle, L. T., & Amundsen, L. (2005). Introduction to Petroleum Seismology. *Society of Exploration Geophysicists*. <https://doi.org/10.1190/1.9781560801702>
- IPCC. (2005). IPCC Special Report on Carbon Dioxide Capture and Storage. Prepared by Working Group III of the Intergovernmental Panel on Climate Change [Metz, B., O. Davidson, H. C. de Coninck, M. Loos, and L. A. Meyer (eds.)]. Cambridge University Press, Cambridge, United Kingdom and New York, NY, USA, 442 pp. https://www.ipcc.ch/site/assets/uploads/2018/03/srcss_wholereport-1.pdf
- Isaksen, D., & Tonstad, K. (Eds.). (1989). A revised Cretaceous and Tertiary lithostratigraphic nomenclature for the Norwegian North Sea. *NPD-Bulletin No. 5*. <https://www.npd.no/globalassets/1-npd/publikasjoner/npd-bulletins/npd-bulletin-5-1989.pdf>
- Jarsve, E., Maast, T., Gabrielsen, R., Faleide, J. I., Nystuen, J. P., & Sassier, C. (2014). Seismic stratigraphic subdivision of the Triassic succession in the Central North Sea; integrating seismic reflection and well data. *Journal of the Geological Society*, 171(3), 353-374. <https://doi.org/10.1144/jgs2013-056>
- Jackson, C., Kane, K., & Larsen, E. (2010). Structural evolution of minibasins on the Utsira High, Northern North Sea; implications for Jurassic sediment dispersal and reservoir distribution. *Petroleum Geoscience*, 16, 105-120. <https://doi.org/10.1144/1354-079309-011>
- Johannessen, E. P., & Steel, R. J. (2005). Shelf-margin clinoforms and prediction of deepwater sands. *Basin Research*, 17(4), 521-550. <https://doi.org/10.1111/j.1365-2117.2005.00278.x>

- Johnson, H., Richards, P. C., Long, D., & Graham, C. C. (2012). The geology of the UK Hatton-Rockall Margin. *Marine and Petroleum Geology*, 38, 41-57.
- Johnson, J. R., Hansen, J. A., Rahman, M. J., Renard, F., & Mondol, N. H. (2022). Mapping the maturity of organic-rich shale with combined geochemical and geophysical data, Draupne Formation, Norwegian Continental Shelf. *Marine and Petroleum Geology*, 138, 105525. <https://doi.org/10.1016/j.marpetgeo.2022.105525>
- Kearey, P., Brooks, M., & Hill, I. (2002). *An Introduction to Geophysical Exploration*. Wiley.
- Krivenko, N. (2014). Seismic interpretation at the Horda Platform, North Sea. Detailed characterization of Sognefjord Formation.
- Lervik, K-S. (2006). Triassic lithostratigraphy of the northern North Sea basin. *Norwegian Journal of Geology*, 86, 93–116. https://foreninger.uio.no/ngf/ngt/pdfs/NJG_86_093-116.pdf
- Lervik, K-S. (2021). Triassic depositional systems of the northern North Sea – an alternative interpretation from cores. *Norwegian Journal of Geology*, 101, 202110. <https://dx.doi.org/10.17850/njg101-2-5>
- Løge, M. B. (2022). Reservoir characterization and sedimentological interpretations at the Aurora CO₂ storage site: Seismic facies analysis and clinofom decompaction [Master's thesis, University of Oslo]. DUO – Digitale Utgivelser ved UiO. <http://www.duo.uio.no/>
- Lundin, E. (2002). Atlantic – Arctic seafloor spreading history. In E. A. Eide (Ed.), *BATLAS – Mid Norway plate reconstructions atlas with global and Atlantic perspectives* (pp.40-47). Geological Survey of Norway.
- Mitchum, R. M. J., Vail, P. R., & Thompson, S. I. (1977). Seismic stratigraphy and global changes in sea-level, part 2: The depositional sequence as the basic unit for stratigraphic analysis. In C. Payton (Ed.), *Seismic Stratigraphy: Application to Hydrocarbon Exploration* (Vol. 26, pp. 53–62). AAPG Mem. <https://doi.org/10.1306/M26490>
- Mitchum, R. M., Vail, P. R., & Sangree, J. B. (1977). Seismic stratigraphy and global changes of sea level, part 6: stratigraphic interpretation of seismic reflection patterns in depositional sequences. In *Seismic Stratigraphy—Applications to Hydrocarbon Exploration* (Vol. 26, pp. 117-133). American Association of Petroleum Geologists.
- Mondol, N. H., Fawad, M., & Park, J. (2018). Petrophysical analysis and rock physics diagnostics of Sognefjord Formation in the Smeaheia area, northern North Sea. In Fifth CO₂ Geological Storage Workshop (pp. 1-5). European Association of Geoscientists & Engineers. <https://doi.org/10.3997/2214-4609.201802951>
- Mulrooney, M. J., Osmond, J., Skurtveit, E., Wu, L., & Braathen, A. (2018). Smeaheia, a potential northern North Sea CO₂ storage site: Structural description and de-risking strategies. In Fifth CO₂ Geological Storage Workshop (pp. 1-5). European Association of Geoscientists & Engineers. <https://doi.org/10.3997/2214-4609.201802957>
- Nanda, N. C. (2016). *Seismic data interpretation and evaluation for hydrocarbon exploration and production*. Springer. <https://doi.org/10.1007/978-3-319-26491-2>

- National Energy Technology Laboratory. (n.d.). Carbon Storage FAQs. Retrieved [Jun 2023], from <https://www.netl.doe.gov/carbon-management/carbon-storage/faqs/carbon-storage-faqs>
- Nordgulen, Ø., & Andresen, A. (2008). The Precambrian. In I. B. Ramberg et al. (Eds.), *The Making of a Land; Geology of Norway* (pp. 62–120). Geological Society of Norway.
- NPD-Factpages. (2023). Norwegian Petroleum Directorate (Oljedirektoratet). <http://factpages.npd.no>
- Nøttvedt, A., Gabrielsen, R. H., & Steel, R. J. (1995). Tectonostratigraphy and sedimentary architecture of rift basins, with reference to the northern North Sea. *Marine and Petroleum Geology*, 12, 881-901. [https://doi.org/10.1016/0264-8172\(95\)98853-W](https://doi.org/10.1016/0264-8172(95)98853-W)
- Olsen, H., et al.(n.d.). Sedimentological analysis and reservoir characterization of a multi-darcy billion-barrel oil field: The Upper Jurassic shallow marine sandstones of the Johan Sverdrup field North Sea Norway. <https://doi.org/10.1016/j.marpetgeo.2017.03.029>
- Osagiede, E. E., Rotevatn, A., Gawthorpe, R., Kristensen, T. B., Jackson, C. A.-L., & Marsh, N. (2020). Pre-existing intra-basement shear zones influence growth and geometry of non-colinear normal faults, western Utsira High–Heimdal Terrace, North Sea. *Journal of Structural Geology*, 130, 103908. <https://doi.org/10.1016/j.jsg.2019.103908>
- Osmond, J. L., Mulrooney, M. J., Holden, N., Skurtveit, E., Faleide, J. I., & Braathen, A. (2022). Structural traps and seals for expanding CO₂ storage in the northern Horda platform, North Sea. *AAPG Bulletin*, 106(9), 1711-1752. <https://doi.org/10.1306/0322221110>
- Patrino, S., Hampson, G. J., Jackson, C. A.-L., & Dreyer, T. (2015). Clinoform geometry, geomorphology, facies character and stratigraphic architecture of a sand-rich subaqueous delta: Jurassic Sognefjord Formation, offshore Norway. *Sedimentology*, 62, 350–388. <https://doi.org/10.1111/sed.12153>.
- Patrino, S., Hampson, G. J., & Jackson, C. A.-L. (2015). Quantitative characterisation of deltaic and subaqueous clinoforms. *Earth-Science Reviews*, 142, 79-119. <https://doi.org/10.1016/j.earscirev.2015.01.004>
- Patrino, S., Kombrink, H., & Archer, S. G. (2021). Cross-border stratigraphy of the Northern, Central and Southern North Sea: A comparative tectono-stratigraphic megasequence synthesis. Geological Society London Special Publications. <https://doi.org/10.1144/SP494-2020-228>
- Partington, M. A., Mitchener, B. C., Milton, N. J., & Fraser, A. J. (1993). Genetic sequence stratigraphy for the North Sea late Jurassic and early Cretaceous: Distribution and prediction of Kimmeridgian to late Ryazanian reservoirs in the North Sea and adjacent areas. In *Petroleum Geology of Northwest Europe: Proceedings of the 4th Conference* (pp. 347-370). <https://doi.org/10.1144/0040347>
- Pellegrini, M., Gómez-Ortiz, D., & García-Castellanos, D. (2020). Clinoforms and clinothems: Fundamental elements of basin infill. *Basin Research*, 32(2), 191-214. <https://doi.org/10.1111/bre.12446>
- Phillips, T., Jackson, C. A.-L., Bell, R., Duffy, O. B., & Fossen, H. (2016). Reactivation of intra basement structures during rifting: A case study from offshore southern Norway. *Journal of Structural Geology*, 91, 54–73. <https://doi.org/10.1016/j.jsg.2016.08.008>

- Posamentier, H.W., & Vail, P.R. (1988). Eustatic controls on clastic deposition II – Sequence and Systems Tract Models. In C.K. Wilgus et al. (Eds.), *Sea-Level Changes: An Integrated Approach* (pp. 125-154). SEPM Special Publication 42. <https://doi.org/10.2110/pec.88.01.0125>
- Quiquerez, A., & Dromart, G. (2006). Sedimentary dynamics of ancient coastal deposits: Use of a new method of erosion quantification and application to the Urgonian limestone, south-east basin, France. *Sedimentology*, 53(1), 105-123.
- Reading, H. G., & Levell, B. K. (1996). Controls on the sedimentary record. In *Sedimentary Environments: Processes, Facies and Stratigraphy* (3rd ed.). Blackwell Science Ltd.
- Riber, L., Dypvik, H., & Sørli, R. (2015). Altered basement rocks on the Utsira High and its surroundings, Norwegian North Sea. *Norwegian Journal of Geology*, 95(1), 57–89. <https://doi.org/10.17850/njg95-1-04>
- Rodosta, T., Bromhal, G., & Damiani, D. (2017). U.S. DOE/NETL Carbon Storage Program: Advancing Science and Technology to Support Commercial Deployment. *Energy Procedia*, 114, 5933-5947. <https://doi.org/10.1016/j.egypro.2017.03.1730>
- Sangree, J. B., & Widmier, J. M. (1977). Seismic stratigraphy and global changes of sea level, Part 9: Seismic interpretation of clastic depositional facies. In C. E. Payton (Ed.), *Seismic stratigraphy-applications to hydrocarbon exploration* (Vol. 26, pp. 165-184). American Association of Petroleum Geologists Memoir. <https://doi.org/10.1306/M26490C11>
- Sheriff, R. E. (2006). Factors affecting seismic amplitude. *Geophysical Prospecting*, 23, 125-138. <https://doi.org/10.1111/j.1365-2478.1975.tb00685.x>
- Shanley, K. W., & McCabe, P. J. (1994). Perspectives on the sequence stratigraphy of continental strata. *AAPG Bulletin*, 78(4), 544-568. <https://doi.org/10.1306/BDF9258-1718-11D7-8645000102C1865D>
- Steel, R.J., & Olsen, T. (2002). Clinoforms, clinoform trajectory and deepwater sands. In J.M. Armentrout & N.C. Rosen (Eds.), *Sequence Stratigraphic Models for Exploration and Production: Evolving Methodology, Emerging Models and Application Histories* (pp. 367-381). *GCS-SEPM Special Publication*.
- Stewart, S. A. (2007). Salt tectonics in the North Sea Basin: A structural style template for seismic interpreters. In A. C. Ries, R. W. H. Butler, & R. H. Graham (Eds.), *Deformation of the Continental Crust: The Legacy of Mike Coward* (pp. 361-396). Geological Society, London, Special Publications, 272.
- Sundal, A., Nystuen, J. P., Rørvik, K.-L., Dypvik, H., & Aagaard, P. (2016). The Lower Jurassic Johansen Formation, northern North Sea – Depositional model and reservoir characterization for CO₂ storage. *Marine and Petroleum Geology*, 77, 1376-1401. <https://doi.org/10.1016/j.marpetgeo.2016.01.021>
- Surlyk, F. (2003). The Jurassic of East Greenland: A sedimentary record of thermal subsidence, onset and culmination of rifting. *Geological Survey of Denmark and Greenland Bulletin*, 1, 659-722. <https://doi.org/10.34194/geusb.v1.4674>
- Sørensen, S., & Tangen, O. H. (1995). Exploration trends in marginal basins from Skagerrak to Stord. *Norwegian Petroleum Society Special Publications*, 4, 97-114. [https://doi.org/10.1016/S0928-8937\(06\)80039-1](https://doi.org/10.1016/S0928-8937(06)80039-1)

- Underhill, J. R., & Partington, M. A. (1993). Jurassic thermal doming and deflation in the North Sea: Implications of the sequence stratigraphic evidence. Geological Society, London, Petroleum Geology Conference Series, 4, 337-345. <https://doi.org/10.1144/0040337>
- Underhill, J. R., & Partington, M. A. (2002). Jurassic thermal doming and deflation in the North Sea: Implications of the sequence stratigraphic evidence. In A.G Doré et al.(Eds.), Exhumation of the North Atlantic Margin: Timing, Mechanisms and Implications for Petroleum Exploration (pp. 337-345). Geological Society, London, Special Publications, 196.
- Uroza, C., & Steel, R. J. (2008). A highstand shelf-margin delta system from the Eocene of West Spitsbergen, Norway. *Sedimentary Geology*, 203(3-4), 229-245. <https://doi.org/10.1016/j.sedgeo.2007.12.003>
- Vigran, J. O., Mangerud, G., Mørk, A., Worsley, D., & Hochuli, P. A. (2014). Palynology and geology of the Triassic succession of Svalbard and the Barents Sea. Geological Survey of Norway, Special publication, 14.
- Van Wagoner, J. C., Posamentier, H. W., Mitchum, R. M., Vail, P. R., Sarg, J. F., Loutit, T. S., & Hardenbol, J. (1988). An Overview of the Fundamentals of Sequence Stratigraphy and Key Definitions. Exxon Production Research Company, Houston, Texas. <https://doi.org/10.2110/pec.88.01.0039>
- Vail, P. R. (1987). Seismic stratigraphy interpretation procedure. *Atlas of Seismic Stratigraphy* (Vol. 1, pp. 1-10). American Association of Petroleum Geologists.
- Vail, P.R., Audemard, F., Bowman, S.A., Eisner, P.N., Perez-Cruz, C. (1991). The stratigraphic signatures of tectonics, eustasy and sedimentology – an overview. In G. Einsele, W. Ricken & A. Seilacher (Eds.), *Cycles and Events in Stratigraphy* (pp. 617–659). Springer.
- Veeken, P. C. H. (2007). The Seismic Reflection Method and Some of Its Constraints . In K. Helbig & S. Treitel (Eds.), *Seismic Stratigraphy, Basin Analysis and Reservoir Characterisation* : Vol. Volume 37 (First edition, pp. 7–74). Elsevier.
- Vollset, J., & Doré, A. G. (Eds.). (1984). A revised Triassic and Jurassic lithostratigraphic nomenclature for the Norwegian North Sea (NPD-Bulletin No. 3). Oljedirektoratet.
- Whipp, P. S., Jackson, C. A. L., Gawthorpe, R. L., Dreyer, T., & Quinn, D. (2014). Normal fault array evolution above a reactivated rift fabric; a subsurface example from the northern Horda Platform, Norwegian North Sea. *Basin Research*, 26(4), 523–549. <https://doi.org/10.1111/bre.12050>
- Würtzen, C. L., Faleide, J. I., Nystuen, J. P., Anell, I. M., & Midtkandal, I. (2021). Syn- to post-rift alluvial basin fill: Seismic stratigraphic analysis of Permian-Triassic deposition in the Horda Platform, Norway. *Basin Research*, 34(2). <https://doi.org/10.1111/bre.12644>
- Yilmaz, O. (2001). *Seismic data analysis*. Society of Exploration Geophysicists.
- Zachariah, A.-J., Gawthorpe, R., Dreyer, T., & Corfield, S. (2009). Controls on early post-rift physiography and stratigraphy, lower to mid-Cretaceous, North Viking Graben, Norwegian North Sea. *Basin Research*, 21(2), 189-208. <https://doi.org/10.1111/j.1365-2117.2008.00371.x>

- Zanella, E., & Coward, M. P. (2003). Structural framework. In D. Evans, C. Graham, & A. Armour (Eds.), *The Millennium Atlas: Petroleum Geology of the Central and Northern North Sea* (pp. 45-59). The Geological Society of London.
- Ziegler, P. A. (1982). *Geological Atlas of Western and Central Europe* (pp. 130-150). Geological Society Publishing House.
- Ziegler, P. A. (1990). *Geological Atlas of Western and Central Europe*. 2nd Edition, Shell Internationale Petroleum Mij. B.V. and Geological Society, London, 239 p.
- Ziegler, P. A. (1992). North Sea rift system, *Tectonophysics*, 208, 55–75. [https://doi.org/10.1016/0040-1951\(92\)90336-5](https://doi.org/10.1016/0040-1951(92)90336-5)
- Zoeppritz, K. (1919). On reflection and transmission of seismic waves by surfaces of discontinuity, *Nachrichten von der Königlichen Gesellschaft der Wissenschaften zu Göttingen, Mathematisch-physikalische Klasse*, 66–84.
- Schlumberger. (n.d.). Seismic velocity. Schlumberger Oilfield Glossary. https://glossary.slb.com/en/terms/s/seismic_velocity
- National Energy Technology Laboratory. (n.d.). Carbon storage FAQs. U.S. Department of Energy. <https://www.netl.doe.gov/carbon-management/carbon-storage/faqs/carbon-storage-faqs>